Phytochemical screening, cytotoxicity and anticancer activity of Lobostemon fruticosus extracts on human lung cancer cell line

---

MSc Dissertation

Ms Lungile Melly Ndlovu

0607223P

March 2015

A dissertation submitted to the Faculty of Science, University of Witwatersrand, Johannesburg, in fulfilment of the requirements for the degree of Master of Science.

Research Output

.

Poster presentation: Elucidating the cytotoxic effects of taxol, camptothecin and *Lobostemon fruticosus* extracts on non-small cell lung cancer (NSCLC) (2014). The Post Graduate Cross Faculty Symposium. University of the Witwatersrand, Johannesburg, South Africa.

Declaration

I declare that this dissertation is my own, unaided work. It is being submitted for the degree of Master of Science in the University of the Witwatersrand, Johannesburg. It has not been submitted for any other degree or examination at any other University.

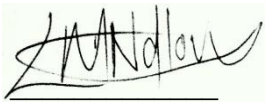

Lungile Melly Ndlovu

___18th____ day of___March_____, 2015

Dedication

I dedicate this work to my Lord God and to my family; Sanah Grace Ndlovu, my loving and ever praying mother. My dearest father, Abednigo Ndlovu, to my awesome older brothers Vusi, Mandla and twin brother Lunga Ndlovu.

ABSTRACT

Lung cancer is currently the most deadly form of cancer due to the fact that metastasis occurs in the lymph nodes making it difficult to remove by surgical means. Chemotherapy has been the most successful method of treatment, although it has been harmful to human health as a consequence of non-specific cytotoxicity. There has been, therefore, a growing interest in cancer research to develop alternative cancer treatments, which are less toxic. Currently plant-derived drugs are perceived to be more effective as they display both cytotoxic activity and are less harmful to overall human health. Thus the aim of the study was to determine the cytotoxic effects of the plant *Lobostemon fruticosus* on A549 cells. The IC_{50} of the methanol and butanol extracts of *L. fruticosus* were obtained at 40 µg/ml and 50 µg/ml, respectively. DNA fragmentation was observed after 48 hour exposure to treatments, indicating that the plant extracts induced apoptosis. Cell cycle analysis indicated that the plant extracts inhibited cell cycle progression at the sub-G_0 phase, which indicated that the cells had undergone apoptosis. RT-PCR showed that the expression of p53 was down-regulated; however, p21 and Bax were up-regulated in all treatments. LC-MS identified that the compounds from the plant extracts are known apoptotic inducers. The results lead to the conclusion that the extracts of *L. fruticosus*, induce cell death in A549 cells. The plant extracts induced a p53-independent apoptotic mechanism, which was mediated by Bax and p21.

Key words: *Lobostemon fruticosus,* camptothecin, taxol, Non-small cell lung cancer (NSCLC)

“Ah, great it is to believe the dream as we stand in youth by the starry stream; but a greater thing is to fight life through and say at the end, the dream is true.”

Edwin Markham

ACKNOWLEDGMENTS

I owe a debt of gratitude to my supervisor Dr Lesetja R. Motadi, for constantly challenging me intellectually, for his guidance and for believing in me throughout this research process. I would like to thank my co-supervisor, Ms Mpho S. Choene, for her assistance and input with my research and my advisor Dr Boitelo Letsolo for her constant inspiration and motivation.

I thank my parents Grace and Abedingo Ndlovu for their patience and encouragement throughout my life and their unwavering support with every decision I made; and my siblings Vusi, Mandla and Lunga Ndlovu, for blessing me with the gift of the unconditional love that one can only get from family.

I would also, like to give my best shout out to my friends Teboho, Rorisang, Jonathan, Neo, Morakane and Wilson for the pep-talks and extraordinary moments that we've shared. You have helped me through my darkest times and shown me the true treasure of friendship.

To my awesome colleagues and my fellow trouble makers, Pontsho, Malangu, Sindiswa, Philemon, and Vinny, who have made my time in the lab both phenomenal and thought-provoking.

I would also like to that the National Research foundation (NRF) and TATA- Africa for funding my studies.

Above all I would like to thank my Lord God, my Saviour Jesus Christ and my constant companion the Holy Spirit for the grace that saw me through when no hope was found and for the strength to overcome every obstacle. I say EBENZA for you have been with me until now. I thank you ELOHIM my creator and I praise you ADONAI my Lord.

Table of Contents

Research Output i

Declaration ii

Dedication iii

ABSTRACT iv

Acknowledgments vi

List of abbreviations xi

Chapter One: Introduction and Literature Review 1

1.1. Medicinal plants and their use in traditional medicine 1

1.1.1. *Lobostemon fruticosus* 2

1.2. Cancer 3

1.2.1. Cancer 3

1.2.2. Lung cancer 4

1.3. Cell cycle 7

1.3.1. Loss of cell cycle control in cancer cells 8

1.4. Apoptosis 9

1.4.1. The intrinsic pathway 10

1.4.2. Extrinsic Pathway 11

1.4.3. Apoptotic genes and proteins 12

1.5. Aim and Objectives 14

1.5.1. Aim 14

1.5.2. Objectives 14

Chapter Two: Materials and Methods 15

2.1. Materials 15

2.2. Methods 15

2.2.1. Cell culturing 15

2.2.2. Plant collection and preparation 15

2.2.3. MTT-Assay 16

2.2.4. xCELLigence ™ 17

2.2.5. DNA fragmentation 18

2.2.6. Flow cytometry: Apoptosis 19

2.2.7. Cell cycle analysis 19

2.2.8. RNA- extraction and reverse transcription 20
2.2.9. Real-Time Polymerase chain reaction (RT-PCR) 22
2.2.10. Liquid Chromatography- Mass Spectrometry 25
2.2.11. Statistical analysis 27
Chapter Three: Results 28
3.1. MTT assay 28
3.2. The xCELLligence system 29
3.3. DNA fragmentation 30
3.4. Flow Cytometry 31
3.5. Cell cycle analysis 34
3.6. Real Time polymerase chain reaction (RT-PCR 36
3.7. Liquid chromatography- Mass spectrometry (LC-MS) 40
3.7.1. Methanol extract profile of *Lobostemon fruticosus* 40
3.7.2. Butanol extract profile of *Lobostemon fruticosus* 50
Chapter Four: Discussion and conclusion 61
4.1. Discussion 61
4.2. Conclusion 68
Chapter Five: References 70
Appendix A 84
Appendix B 85

List of figures

Figure 1: A schematic diagram of the cell cycle 8
Figure 2: Diagram description of p53 activation 13
Figure 3: Percentage of cell death of treated A549 cells. 29
Figure 4: Real time analysis of cell growth of treated A549 cells. 30
Figure 5: The 1% agarose gel for DNA fragmentation of A549 gDNA. 31
Figure 6: Scatter graph of A549 cells 33
Figure 7: Histogram profiles of A549 cells 35
Figure 8: Relative expression of apoptotic genes vs Gadph in A549 cells. 37
Figure 9: Non-targeted LC-MS chromatographic profiles of methanol extract of *L. fruticosus* 41
Figure 10: LC-MS chromatographic profile 2-hydroxylamino-4,6-dinitrotouene. 42
Figure 11: LC-MS chromatographic profile 4-hydroxycoumarin. 43
Figure 12: LC-MS chromatographic profile for Sarpagine. 44
Figure 13: LC-MS chromatographic profiles of 7-O-methelylvitexin 2"-O-β-L-rhamnoside. 46
Figure 14: LC-MS chromatographic profile of 7-O-β-D-glucosylapigenin. 47
Figure 15: LC-MS chromatographic profile of hypoglycin B. 48
Figure 16: LC-MS chromatographic profile of Ricinoleate. 49
Figure 17: Non-targeted LC-MS chromatographic profiles of butanol extract of *L. fruticosus* 51
Figure 18: LC-MS chromatographic profiles of Justidin B 52
Figure 19: LC-MS chromatographic profiles of Tropine. 53
Figure 20: LC-MS chromatographic profiles unknown. 54
Figure 21: LC-MS chromatographic profiles Flavocommelin 55
Figure 22: LC-MS chromatographic profiles Fisetin 56
Figure 23: LC-MS chromatographic profiles unknown 57
Figure 24: LC-MS chromatographic profiles unknown 58
Figure 25: LC-MS chromatographic profiles Nodakenin 59

List of tables

Table 1: Reverse transcriptase cocktail mixture 21
Table 2: Reverse transcription protocol 22
Table 3: Components of qRT-PCR mix 24
Table 4: Type of LC-MS analysis 27
Table 5: Statistcal analysis of box plot of CPT 38
Table 6: Statistcal analysis of box plot of TXL 38
Table 7: Statistcal analysis of box plot of methanol extract 39
Table 8: Statistcal analysis of box plot of butanol extract 39
Table 9: List of compound found in methanol exctracts and their function 50
Table 10: List of compound found in butanol exctracts and their function 60

List of abbreviations

A549	Human lung carcinoma cell line
AIF	Apoptosis inducing factor
APAF-1	Apoptotic protease activating factor
BAD	Bcl-2 associated death promoter
BAK	Bcl-2 homologous antagonist killer
BAX	Bcl-2 associated X protein
BCL-2	B-cell leukaemia 2
BCL-X	B-cell leukaemia extra large
BH3	Bcl-2 homology 3 domain
BP	Base pair
cd	Cell death
CDK	Cyclin-dependent kinase
cDNA	Complementary DNA
CI	Cell index
CPT	Camptothecin
DIABLO	Direct IAP binding protein
DISC	Death-inducing signalling complex
DMEM	Dulbecco's modified eagle media
DMSO	Dimethyl sulfoxide
DNA	Deoxyribonucleic acid

E2F	Eukaryotic transcription factor 2
EDTA	Ethylenediamine tetraacetic acid
FACS	Fluorescence-activated cell sorter
FADD	Fass-associated death domain
FBS	Foetal bovine serum
FITC	Flourescein-isothiocynate
GAPDH	Glyceraldehyde 3-phosphate dehydrogenase
IAP	Inhibitor of apoptosis proteins
kb	Kilobases
LC-MS	Liquid chromatography-mass spectrometry
MDM-2	Murine double minute 2
MOMP	Mitochondrial outer membrane permeabilisation
MPF	M-phase promoting factor
mRNA	Messenger RNA
MTT	3-(4, 5-Dimethylthiazolyl-2)-2, 5-diphenyltetrazolium bromide
Mw	Molecular weight
NADH	Nicotinamide adenine dinucleotide
NADPH	Nicotinamide adenine dinucleotide phosphate
NSCLC	Non-small cell lung cancer
Omi/HtrA2	Omi/high temperature requirement protein A
p21/WAF1/CIP1	CDK inhibitor 1 or CDK inhibitor protein 1
p53/Tp53	Protein 53/ Tumour-suppressor protein 53
PBS	Phosphate buffered saline

PI	Propidium iodide
PCR	Polymerase chain reaction
Q-TOF	Quadrupole-Time of flight
RNA	Ribonucleic acid
RT	Retention time
RTCA	Real time cell analyser
RT-PCR	Real time PCR
ROS	Reactive oxygen species
SD	Standard deviation
Smac	Second mitochondria-derived activator caspase
TNF	Tumour necrosis factor
TRAIL	TNF-related apoptosis induced ligand
V	Volts
WHO	World health organisation

Chapter One: Introduction and Literature Review

1.1. Medicinal plants and their use in traditional medicine

Medicinal plants have been used throughout human history. The chemical compounds produced in plants, known as secondary metabolites, have been known to play an important role in their biological functions. Plants use secondary metabolites as a defence mechanism against predation from insects and herbivores. Furthermore, these compounds are known to be an effective defence against fungal infections (Desai *et al*., 2008). These properties have been manipulated for centuries through various methods of extraction and used as medicine for many communities around the world (Rahmatullah and Biswas, 2012) . The use of plants as traditional medicine remains a prevalent practice to date in many rural communities devoid of access to modern medicine (Fabricant and Farnsworth, 2001). These communities continue to thrive due to the extensive knowledge of medicinal properties of the various medicinal plants used by traditional healers, many of which are still being discovered by modern medicine. In various countries, plants from numerous families have been used to treat various ailments that affect the community (Amira *et al*., 2012). For example, *Phylolocca dodencandra* was used to treat and control the prevalence of schistosomiasis as the plant was commonly known to be an effective molluscicide (Lemma, 1971). There has been a notable increase in the use of medicinal plants for commercial purposes these past three decades (Cai *et al*., 2004; Amira *et al*., 2012). In agricultural practices, medicinal plants have been used for several centuries for maintenance and conservation of livestock health, such as the use of *Polokowskia tabacco* to treat intestinal disorder in cows (Amira *et al*., 2012).

Phytochemicals, such as phenolics, are organic compounds that are naturally found in plants and are non-nutritive bioactive substances that have been linked with the anti-cancer properties in a variety of plant based foods (Tapsell *et al*., 2006). Furthermore, these

compounds have various anti-inflammatory and anti-oxidant properties that aid in reducing the damage caused by free and active oxygen within the system (Amira *et al*., 2012). This is mainly due to the fact that plants contain various compounds including flavonoids and phenyl propanoids, which are effective anti-oxidants (Cai *et al*., 2004).

1.1.1. *Lobostemon fruticosus*

Lobostemon fruticosus is a plant that is indigenous to South Africa and commonly referred to as pyjama bush (English), agdaegeneesbos and douwurmbos (Afrikaans) (Levyns, 1934). It is a member of the *Boraginaceae* family otherwise referred to as the 'forget-me-nots' (Hilger and Böhle, 2000). The shrub which can reach heights of 1 m and is characterised with densely hairy branches, oval-shaped leaves and long (25 mm) funnel-shaped flowers that often appear in a variety of colours, ranging from purple to white, which is a known characteristic of plants found in the *Boraginacaeae* family (Levyns, 1934; Hilger and Böhle, 2000). *Lobostemon Fruticosus* is widely distributed along Namaqualand, the Cape Peninsula and Worcester, and was used as a popular old Cape remedy shrub by the Khoisan, the settlers and Malays (Levyns 1934). The leaves were used as a tea to cure ringworms, the lotion was applied to wounds and a lotion was made from a mixture with *Meliathus comosus* and *Galenia africana* was used to cure syphilis (www.plantsafrica.com). The plant was believed to cure any ailment within eight days, hence the name agtedaegeneebos. However, little is known about the chemistry of this plant. Well known members of the family contain napthoquinone derivatives, pyrrolizidine alkaloids, cyclitols, phenolic acids, tannins and ureide allatonins (found in the comfrey root) (www.plantsafrica.com). Some of the extracts that were mentioned above, such as napthoquinone derivatives and saponins, are known to have cytotoxic effects in cancer cells (Huang and Zou, 2011; Cui *et al*., 2011).

1.2. Cancer

1.2.1. Cancer

Cancer is a genetic disease that results in uncontrolled cell division. It is brought about by mutations in genes that cause an increase in the rate of cell proliferation and a decrease in apoptosis (Erenpreisa and Cragg, 2007). Throughout the ages researchers have been able to identify environmental, chemical and physiological factors (or carcinogens) that lead to cancer formation within the human body (Meng *et al*., 2012; Wogan *et al*., 2004). These carcinogens were directly linked to an increase in tumour incidences in animals and humans (Ames, 1983; Ames and Gold, 1990) . The process with which cancer is formed as a result of carcinogens (called carcinogenesis), results from either genetic mutation or epigenetic changes. The cancer cells gain a selective advantage and undergo clonal expansions as a result of pro-oncogenes.(Ames and Gold, 1990; Henderson and Feigelson, 2000).

Many physiological processes, such as metabolism may produce highly reactive oxygen species (ROS) and other endogenous carcinogens, which can lead to oxidative destruction of biomolecules (catabolism) (Yager, 2000). A large production of these ROS by-products could result in the development of degenerative diseases such as atherosclerosis, cancer and diabetes in humans (Halliwell and Cross, 1994; Cai *et al*., 2004) . The secondary metabolites such as phenolic compounds, tannins, quinines and vitamins found in plants have antioxidant properties and they reduce the high incidence of free radicals and ROS within the body (Cai *et al*., 2004; Campbell *et al*., 2005). There have not been a lot of studies done to investigate the effects of *Lobostemon fruticosus* on cancer cells; therefore, it would be interesting to investigate whether this medicinal plant has any cytotoxic effects on lung cancer cells.

1.2.2. Lung cancer

Lung cancer is among the most frequently reported cases of cancer worldwide, with a 13-15% occurrence of all known cancers being reported daily (WHO, 2009). Lung cancer is also the most deadly form of cancer as it has been observed to be resistant to most therapeutic treatments and it demonstrates metastasis within lymph nodes (Burris, 2009; Benlloch *et al*., 2009). Over the past two decades there has been an increase in the number of lung cancer incidences and its mortality rate has also increased (Weill *et al*., 2000).

In South Africa, lung cancer is the second leading cancer in males and the 6th leading form of cancer in women (Groenewald *et al*., 2007). Sixty percent of the leading causes of cancer are related to smoking, this form of cancer affects secondary smokers or passive smokers as well as primary smokers (Sitas *et al*., 2004; Groenewald *et al*., 2007). Other known causes are industrial and domestic air pollution. Most lung cancers start of on the cells lining the interior passage of the lung and are referred to as bronchogenic carcinomas (Kellermann *et al*., 1973; Engels, 2008). HIV/AIDS has also been listed as a causative agent for lung cancer together with various other forms of cancer (Engels, 2008).

Lung cancer incidences were once recorded to be low in developing countries as compared to developed countries like the United States of America and United Kingdom (Alberg and Samet, 2003). This was mainly due to the higher rates of cigarette smoking and due to industrial wastes omitted near the cities in developed countries. However, with a change in people's life styles, in developing countries, and the more industries being built to boost the economy of developing countries, the incidence of lung cancer has increased drastically. Nearly 90% of most non-small cell lung cancer (NSCLC) occurrences are believed to be caused by cigarette smoking and about 10% is a result of industrial toxic products such as asbestos and radon gases (Engels, 2008). These cases were investigated as the use of tobacco

has always been prevalent in developing countries and there was still a very low incidence of lung cancer cases in developing countries (Mzileni *et al*., 1999). However, research has shown that the introduction of various chemicals in cigarettes, meant to make them more addictive, have contributed to the development of lung cancer in regular smokers (Winkler *et al*., 2013).

Changes in modern lifestyle over the years have permitted youth to start smoking at earlier stages of their lives and some children are being subjected to secondary smoke inhalation as young as two years (Lam *et al*., 2004). Moreover, there has been an increase in the number of women who smoke as a result of these lifestyle changes. These factors have also contributed to the increase in lung cancer incidences in developing countries such as those in African and Asia (Lam *et al*., 2004).

There has been a very low survival rate in patients with lung cancer; the low prognosis is due to the fact that patients are rapidly diagnosed with lung cancer in the late stages when the symptoms begin to present themselves. This is due to the limited forms of lung cancer screening tests (Parkin and Moss, 2000). Furthermore, patients diagnosed with lung cancer at the late stage rarely live longer than five years after diagnosis (Benlloch *et al*., 2009). Therefore, there have been various attempts to try and cure late stage lung cancer (Kelly *et al*., 2001).

Currently, there are three known approaches to lung cancer treatment, namely, surgical resection, radiotherapy and chemotherapy (Ettinger *et al*., 2010). Surgery offers the best chance of curing NSCLC in patients with advanced lung cancer. However, only a limited amount of patients are suitable for surgical resection and therefore a large amount of affected patients opt for non-surgical approaches (Ettinger *et al*., 2010). Radiotherapy is a non-surgical approach that has been used as an alternative to surgical resection, however, there

has only been a report of only 10% of lung cancer patients who have been cured after radiotherapy (Jassem, 2007; Klastersky and Awada, 2012). As a result some patients also have used chemotherapy as the next non-surgical alternative, however, this option has been the cause of an overall deterioration in patient health (Ettinger *et al*., 2010). Chemotherapeutic drugs are non-specific and seem to affect both healthy and cancerous cells within the patient. Furthermore, there have been reports of an increased resistance to current therapies on patients with advanced lung cancer cells (Sechler *et al*., 2013). Therefore, there is currently an urgent need to develop a better alternative in lung cancer treatments.

A tumour that is localised within a specific area, a lump, can be treated with high energy radiation which can damage the DNA of the cancerous cells (Shipley *et al*., 1999). This is due to the fact that DNA from cancerous cells lacks the ability to repair damages as opposed to that in normal cells (Mathews *et al*., 2000; Kerr *et al*., 1994). However, metastatic or malignant tumours are treated with chemotherapeutic drugs, which are toxic to actively dividing cells. These drugs are administered to the circulatory system and interfere with the cell cycle (Arap *et al*., 1998). These drugs do, however, interfere indiscriminately with normal cells as well as cancerous cells and may result in various unpleasant side effects (Arap *et al*., 1998).

The body also has a way of dealing with unwanted proliferation. Once DNA has been damaged three possible outcomes may occur; the damaged DNA could be efficiently repaired leading to normal cellular function, DNA could be irreparably damaged leading to a mutation or systematic cell death (apoptosis) (Kerr *et al*., 1994). It has been discovered that the genes that are affected during the formation of cancer play a significant role in cellular development, immune response and various other biological processes (Huang *et al*., 1988). Cancer causing genes, or oncogenes, arises from genetic changes from normal pro-oncogenes that are involved in cell growth and division. This change arises as a result of various genetic

errors in the proto-oncogenes, namely translocation, amplification and point mutations (Zhang *et al*., 2010). These errors result in changes in the gene product which lead to the production of protein that is defective and resistant to degradation and thus result in abnormalities within the cell cycle and result in cancer formation (Campbell *et al*., 2005).

Furthermore, these mutations can affect tumour suppressor genes, which produce proteins that prevent uncontrolled cell growth (Greenblatt *et al*., 1994; Sager, 1989). These tumour suppressor proteins repair damaged DNA, control anchorage to cell matrix and are components of the cell signalling pathway which regulate the cell cycle in normal cells (Sager, 1989). An example of this could be the production of p53 protein which is actively involved in the repair of damaged DNA. If the damaged DNA is irreparable the p53 protein activates pro-apoptotic genes. The product proteins of the pro-apoptotic genes induce apoptotic cell death(Campbell *et al*., 2005).

1.3. Cell cycle

Cell division occurs sequentially within a eukaryotic system. There are stop and go signals that trigger the period of cell division and its senescence (Erenpreisa and Cragg, 2007). The cell cycle can be distinguished by the interphase and the mitotic phase (Campbell *et al*., 2005). The interphase, referred to as the longer phase of the cell cycle, accounts for nearly 90% of the entire cycle. It is divided into various sub phases, namely, the G_0 phase (stage at which cell growth is stunted), G_1 phase (first gap phase) also referred to as the restriction point with which cell growth is either allowed or entered into the G_0 phase (Hartwell and Weinert, 1989; Campbell *et al*., 2005). The S phase is the stage at which DNA synthesis occurs and finally the G_2 phase (second gap phase) that precedes the mitotic phase of the cell cycle.

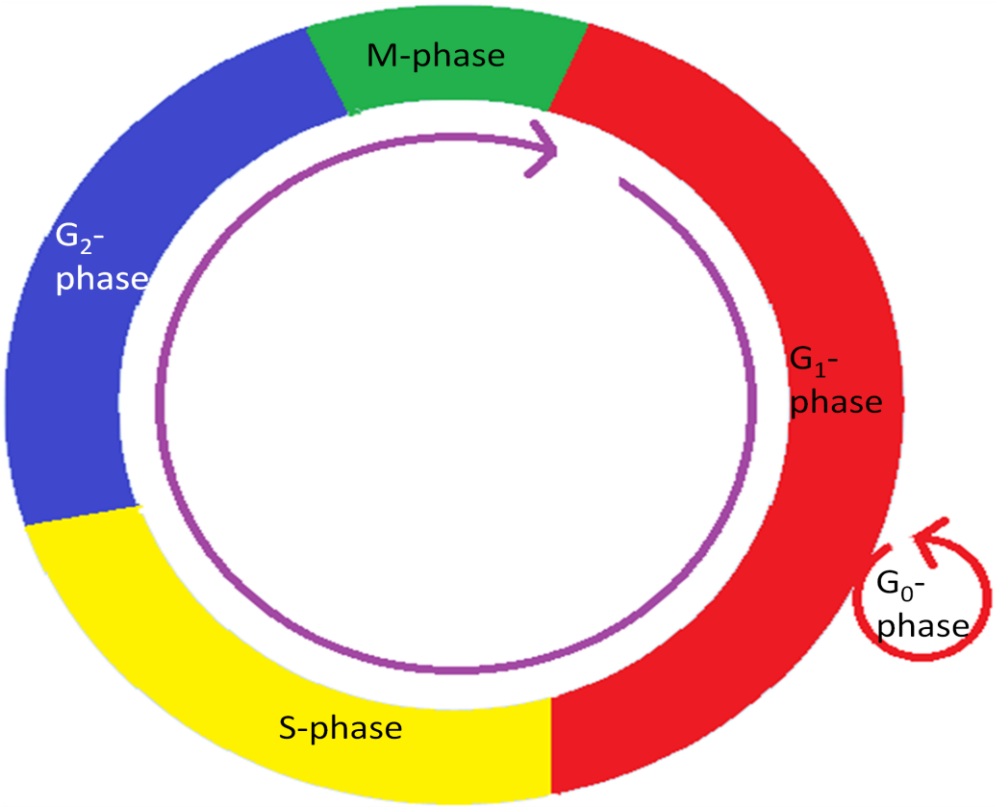

Figure 1. A schematic diagram of the cell cycle, displaying the various phases of the cycle namely the G_0, G_1, G_2, S and M phases.

1.3.1. Loss of cell cycle control in cancer cells

Cancer cells do not respond systematically to the body's regular control system because of their uncontrollable proliferation and concurrent invasion of other tissue (Sherr, 1996). This may be due to their apparent independence to the presence of growth factors or rather due to an abnormality that may occur in the signal pathways responsible for conveying growth factor signals to the cell cycle control system (Campbell *et al*., 2005). Furthermore, this uncontrollable proliferation could be as a result of an abnormal cell cycle control system (Hartwell and Kastan, 1994). Various studies have shown that abnormal cells could stop proliferating at random check points. However, there has been little evidence of this occurrence in cancer cells (Kastan *et al*., 1995). Tumour cells are found to have an unusual

number of chromosomes and secrete signal molecules that cause rapid and unhindered cell growth (Lengauer *et al*., 1998).

1.4. Apoptosis

Apoptosis, also known as programmed cell death, is the most vastly investigated topic in modern cell biology (Wong, 2011). Not to be confused with necrosis, in which cell death is brought about as a result of strenuous conditions affecting the cells surroundings. Apoptosis occurs as a result of the cell actively participating in the process of cell death due to specific stimuli in the cell's environment (Nanji and Hiller-Sturmhofel, 1997; Kroemer, 1999). The process of apoptosis is fundamental in natural cell death of the cell with damaged DNA after radiation exposure, and in pathological processes brought about anticancer drugs (Wong, 2011). The changes in cellular morphology, induced by apoptosis, appears similarly in almost all the eukaryotic cells as it affects both the nucleus and the cytoplasm of the cell (Hacker, 2000). However, the time it takes to complete the process of cell death varies from cell to cell based on the stimuli and the pathways that lead to apoptosis (Hacker, 2000).

To understand the conditions that affect apoptosis in cancerous cells, one must have a knowledge of the mechanism of apoptosis (Hacker, 2000). This understanding is essential when designing drugs that target specific apoptotic pathways and the genes involved (Wong, 2011). The molecules that play a central role in this process are caspases, also known as cystein-aspartic proteases, which when activated cleave various proteins that either become activated or deactivated in order to carry out a cascade of reactions that will eventually result in apoptosis (Favaloro *et al*., 2012; Wong, 2011). Researchers have identified three main pathways that are involved in apoptosis, namely the intrinsic and extrinsic pathways which are well known and eventually lead to a common pathway (see Figure 1) (Favaloro *et al*.,

2012). The third pathway occurs in the endoplasmic reticulum, although very little is known about this current pathway (Wong, 2011) and thus it will not be discussed further.

1.4.1. The intrinsic pathway

The intrinsic pathway, also referred to as the mitochondrial pathway, is initiated within the cell and the initial processes in this pathway utilise mitochondrial proteins (Favaloro *et al*., 2012). These proteins leak out of the mitochondrial membrane to promote apoptosis, as a result of the specific signals that were elicited. Cytochrome c, a protein involved in electron transfer inside healthy mitochondrial organelles, acts as a death factor outside the mitochondria. This process is triggered by internal conditions within the cell, such as DNA damage, hypoxia and severe oxidative stress (Wong, 2011). The BCL-2 family are important in regulating the intrinsic pathway (Gross *et al*., 1999). The members of this protein family are divided into the pro-apoptotic and anti-apoptotic groups. Proteins such as Bcl-2, Bcl-X and Bcl-W are characterised as anti-apoptotic; whereas Bax, Bak and Bad proteins are pro-apoptotic (Korsmeyer, 1999). The proteins that are anti-apoptotic inhibit the secretion of cytochrome-c from mitochondria, and those that are pro-apoptotic trigger the release of cytochrome-c (Gross *et al*., 1999). Mitochondrial outer membrane permeabilisation (MOMP), otherwise known as mitochondrial leakage, occurs as a result of stress brought about by pro-apoptotic proteins that directly affect the mitochondrial membrane (Wong, 2011). These proteins bind to the mitochondrial membrane causing the formation of pores (Korsmeyer, 1999). Upon release cytocrome-c binds to an apoptotic protease activating factor (APAF-1) and inactive caspase 9 (Procaspase 9), to form a large apoptosome complex. Caspase 9 is then activated upon autocatalysis. In addition, either the Smac/DIABLO or the Omi/HtrA2 promoters will bind to inhibitor of apoptosis proteins (IAP) (Favaloro *et al*., 2012). AIP's inhibit the activation of caspases in non-apoptotic conditions. However, the

binding of these specific promoters can often disrupt the interaction between AIP and caspases. This leads to caspases activation, which initiates apoptosis (Korsmeyer, 1999).

1.4.2. Extrinsic Pathway

The extrinsic pathway, often referred to as the death receptor pathway, is activated by death receptors upon ligand binding. Most death receptors are from the TNF/NGF family (Kerr *et al*., 1994). Popular death TNFR1 and Fas (CD95) interact with specific extracellular ligands called TNF and Fas ligand respectively (Wong, 2011). Upon ligand binding these trans-membranal receptors recruit adapter proteins called TNF receptor-associated death domain (TRADD), Fas-associated death domain (FADD) specific for either one of the receptors, together with inactive caspase 8 (Procaspase 8) (Favaloro *et al*., 2012) The newly formed ligand-receptor-adapter protein complex (now referred to as the death-induced signal complex (DISC)), activates caspases 8, which initiates apoptosis (Favaloro *et al*., 2012; Fulda and Debatin, 2004).

As mention earlier, both the intrinsic and extrinsic pathway reach convergent apoptotic pathway. Caspase 9 is the upstream caspases for the intrinsic pathway whereas caspase 8 is for the extrinsic pathway. Both these caspase are therefore referred to as the initiator caspase in their respective pathways (Fulda and Debatin, 2004). These two pathways converge at caspase 3 activation, a process facilitated by the activation of both caspase 9 and 8 for the intrinsic and extrinsic pathways respectively (Favaloro *et al*., 2012). Once active caspases 3, which is the most common executioner caspase, activates the caspase-activated deoxyribonuclease, an enzyme responsible for the disruption of nuclear apoptosis (Baud and Karin, 2001; Fulda and Debatin, 2004). Furthermore caspase 3 cleaves and subsequently activates other caspases which are responsible for the several cellular proteins, namely, DNA repair protein kinases, and several other proteins that are involved in cellular integrity (Favaloro *et al*., 2012). These protein degradations affect the cell cycle, signalling pathways

and the cellular cytoskeleton, resulting morphological changes in cellular structure, indicative of apoptosis (Fulda and Debatin, 2004).

1.4.3. Apoptotic genes and proteins

a) P53 tumour-suppressor gene and its protein product

The p53 (TP53) gene is the most common tumour-suppressor gene. TP53 has a molecular weight of 53 kDa, which is indicative of its name (Campbell *et al*., 2005). TP53 plays a crucial role in the inhibition of cell proliferation, it functions as a transcriptional factor that promotes the synthesis of cell cycle-inhibiting proteins (Thor *et al*., 1992). TP53 has variety of cellular functions which include, DNA repair, thus preventing the formation of cancer causing mutations, and playing a role in cell signalling pathways that inhibit the cell cycle (Ryan *et al*., 2001). The protein is activated by various physiological stressors, such as DNA damage; upon activation, p53 activates other genes such as the p21 gene (Komarova *et al*., 2000). P21 binds to cyclin-dependent kinases (cdk's), thereby halting the cell cycle and allowing the DNA repair process (Komarova *et al*., 2000). However, in the case where DNA is irreparable, TP53 will activate pro-apoptotic genes, such as Bax, that induce apoptosis (Campbell *et al*., 2005).

Among all the human cancer cases recorded more than 50% were found to be as a result of a defective p53 gene (Wong, 2011). Studies have shown that mutations in this particular gene were common in cancer (Sigal and Rotter, 2000). These findings showed the crucial role p53 plays in regulating the cell cycle and apoptosis. Cyclin dependent kinases play a direct role in controlling the cell cycle. Part of the regulation of the cell cycle is achieved by the inactivation and hyper-phosphorylation of negative regulators of the cell cycle such as retinoblastoma tumour suppressor (Rb) proteins. Upon gene stress the accumulation of p53 induces a cell cycle arrest at G_1 phase, where DNA can be repaired before replication occurs

in the S-phase. The accumulation of p53 up-regulates the expression of p21 proteins. The p21 protein also known as WAF1 protein inhibits cdks by forming a p21-cdk-cyclin complex (Cdk2/A complex). This leads to the accumulation of hypo-phosphorylated Rb proteins. Rb is required to regulate the E2F transcriptional factor, however upon hypo-phosphorylation, Rb can no longer activate E2F thus resulting in G_1 arrest (Figure 2).

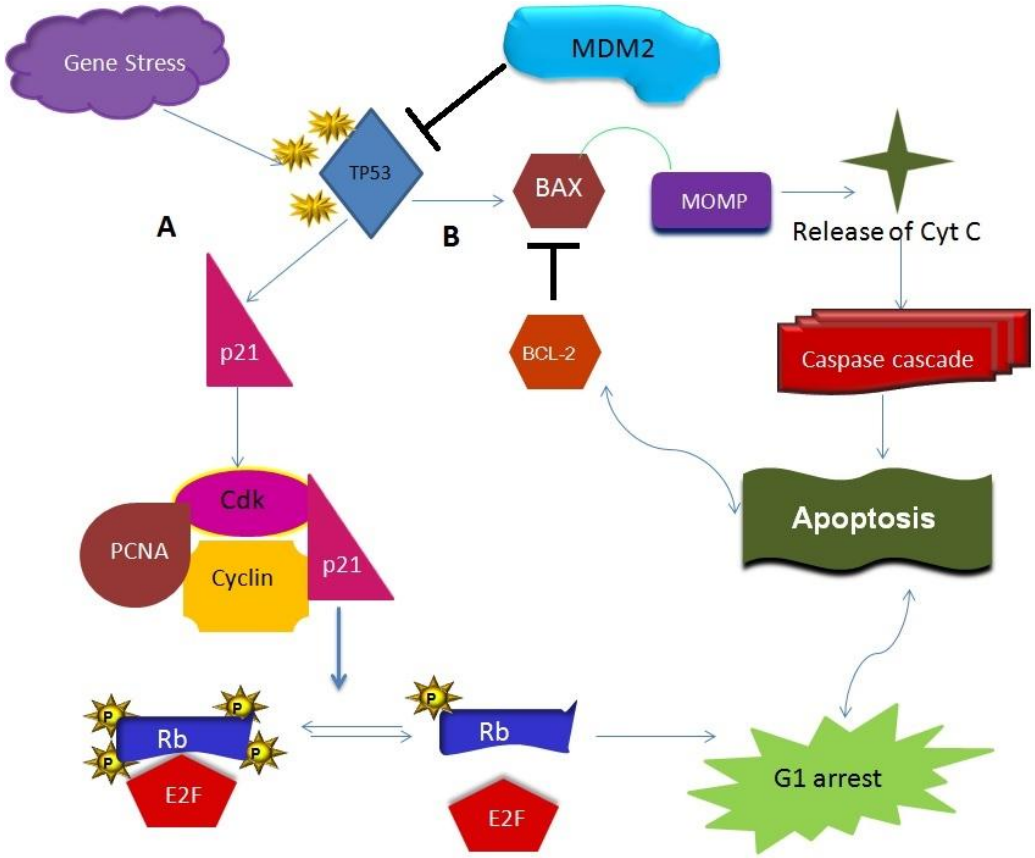

Figure 2. Diagram description of p53 activation and up regulation of genes involved with cell cycle arrest (p21) and pro-apoptotic genes (BAX) and the subsequent genes involved in inhibiting p53 (MDM2) and anti-apoptotic genes (BCL-2).

b) <u>The BCL-2 genes and apoptosis</u>

Members of the Bcl-2 gene family, together with their protein products play an important role in apoptosis and are functional mostly with the intrinsic pathway. This Bcl-2 gene was the first member to be identified and were called B-cell lymphomas (Gross *et al.*, 1999). The protein product of the pro-apoptotic and the anti-apoptotic proteins exert extreme pressure by

initially permeating the mitochondrial membrane through either cellular intermembrane channels or through cellular pores (Korsmeyer, 1999). TP53 targets Bax to signal apoptosis. Bax is translocated into the mitochondria and these results in mitochondrial outer membrane permearbilisation, which leads to the subsequent release of cytochrome c into the cytosol, thus activating a caspase cascade that will result in apoptosis (Figure 2). Genes such as TP53 play a functional role in the induction of apoptosis, therefore TP53 and other related genes (Bax, p21 and Bcl-2) and their functions will be examined in this study.

From the process of cell cycle analysis and apoptosis, it is clear that defects in the two processes hold the key to a successful cancer drug target. While on the other hand medicinal plants and phytochemicals provide an opening to target these two processes. The use of traditional medicine is a growing approach for non-surgical treatments in all forms of lung cancer.

1.5. Aim and Objectives

1.5.1. Aim

The aim of the project is to identify specific extracts of the South African medicinal plant, *Lobostemon fruticosus*, which display direct anti-cancer activity and cytotoxicity on human lung cancer cells.

1.5.2. Objectives

- To monitor the changes in cell proliferation of non-small cell lung cancer (A549) cell line following treatment with crude plant extract of *Lobostemon fruticosus*
- Determine whether these extracts induce apoptosis as a mode of cell death
- Observe whether these plant extracts affect the apoptotic genes
- To identify the compounds in *Lobostemon fruticosus* that might be responsible for cell death

Chapter Two: Materials and Methods

2.1. Materials

A549 non-small lung cancer cell line was purchased at ATCC (USA). The *Lobostemon fruticosus* plant was collected in Hermanus (Western Cape, South Africa). The A549 cells were cultured in small culture flasks containing Dulbecco's modified eagle media (DMEM with L-glutamine, Sigma, USA) which was supplemented with 10% (v/v) foetal bovine serum (FBS, Sigma) and 1% (v/v) penicillin/streptomycin (Sigma). The cells were incubated at 37 °C and 5% CO_2. Trypsin-EDTA and MTT (3-(4, 5-dimethylthiazolyl-2)-2, 5-diphenyl-tetrazolium bromide) were purchased at Sigma- Aldrich (USA).

2.2. Methods

2.2.1. Cell culturing

The A549 cell line was passaged/subcultured regularly (between two and three days) in a 25 cm^2 culture flask. Cells were maintained in DMEM/MEM media, supplemented with 10% (v/v) foetal bovine serum and 1% (v/v) penicillin/streptomycin. The cells were kept in sterile conditions in an incubator maintained at constant 37 °C temperature with 5% CO_2. All the cells were allowed to reach 70-80% confluence prior to treatments or harvesting.

2.2.2. Plant collection and preparation

Lobostemon fruticosus was collected in the Fernkloof nursery, located in Hermanus in the Western Cape (South Africa). *Lobostemon fruticosus* was air dried at room temperature for 3 weeks. The whole plant was ground into fine powder. Ten grams of the crude plant was dissolved in 100 ml methanol and 100 ml butanol each and allowed to shake at room temperature at 150 rpm over night. The methanol and butanol extracts were then filtered using Whatman paper and allowed to dry in the incubator. Final weight of the dried extract,

289.6 mg methanol and 96.2 mg butanol, were dissolved in 1 ml DMSO to the final concentration of 289.6 mg/ml and 96.2 mg/ml for methanol and butanol, respectively. The dissolved extracts were stored in -20 °C.

2.2.3. MTT-Assay

Principle

Measurement of cell viability and proliferation form the basis for numerous *in vitro* assays of a cell population's response to external factors. The reduction of tetrazolium salts is now widely accepted as a reliable way to examine cell proliferation (Mosmann, 1983). MTT (3-(4, 5-dimethylthiazolyl-2)-2, 5-diphenyltetrazolium bromide) also referred to as tetrazolium, is yellow in colour, this compound is reduced, during cell proliferation, by metabolically active cells into formazan which appears purple (Mosmann, 1983). Along with various other reactions, the most well notable reason for this occurrence is due, in part, to the active dehydrogenase enzymes that produce NADH and NADPH. The crystalline formazan is solubilised with DMSO or other detergents and quantified spectrophotometrically (Mosmann, 1983).

Technique

Cells were seeded, at a density of 5000 cells/ 90 µl media each; cell density was determined by means of a haemocytometer. The cells were incubated at 37 °C, 5% CO_2 overnight to allow cells to adhere to the plates and grow. The cells were then treated with two treatment controls, camptothecin (CPT) (0.25-5 µM) and (10-200 nM) taxol (TXL); then with methanol and butanol extracts at increasing concentrations (1-100 µg/ml). DMSO, methanol and butanol were used as controls to the final concentration 0.001% (v/v). The assay had a non-treatment control, and a blank with only media. The treated cells were incubated for 24 hours (h) prior to addition of MTT. A 5 µg/ml MTT stock solution was dissolved in PBS and

filtered, 10 µl of the dissolved MTT was added onto each well and incubated for 4 h. Upon formation of formazan crystals, 90 µl of DMSO was added in each well to dissolve the purple crystals. The plate was read at 570 nm wavelength using the Thermo Scientific™ Multiskan Go reader. Cell death was calculated

$$\%\ Cell\ viabilty = \frac{OD\ (treated) - OD\ (blank)}{OD\ (untreated) - OD\ (blank)} \times 100 \qquad \text{eq. 1}$$

$$\%Cell\ death = 100 - \%\ Cell\ viability \qquad \text{eq. 2}$$

The IC_{50} was determined as 50% cell viability.

2.2.4. xCELLigence ™

Principle

The xCELLigence ™ system monitors cellular events in real-time, as it measures the electrical impedance (resistance) within the interdigitated microelectrodes located below the xCELLigence tissue culture plates (Roche xCELLigence™ manual). The use of impedance measurements has improved upon the use of conventional endpoint assays in that it provides more accurate quantitative assays, not only of the cell count and health but also cellular adhesion, viability and morphology (Urcan *et al*., 2010). The xCELLigence system is used to obtain dynamic real time data , to continuously monitors the state of the cells throughout the entire experiment, can measure the short-term and long-term cellular changes, and can analyse real-time cellular effects as it occurs in its natural environment- this is due to the non-toxic analysis of the tissue culture (Urcan *et al*., 2010).

Technique

Cells were seeded at 5×10^3 per well and cultured in the chamber of the E-16 plates overnight (37 °C, 5% CO_2) to allow cells to adhere to the plates and grow. The Cells were

then treated with 0.5 µM CPT and 50 nM taxol; then with 35 µg/ml and 45 µg/ml methanolic and 50 µg/ml butanolic extracts of *L. fruticosus*, and control solution of 0.01% (v/v) DMSO, methanol and butanol respectively. Cells were then allowed to grow over a period of 72 h.

2.2.5. DNA fragmentation

Principle

Apoptotic cell death can be characterised by observing specific morphological and biochemical changes that distinguish it from other forms of cell death, such as necrosis (Nanji and Hiller-Sturmhofel, 1997). One of these specific features is DNA fragmentation (Basnakian and James, 1994). Cells undergoing apoptosis release endonucleases, enzymes that catalyse the hydrolysis of phosphodiester bonds found within a polynucleotide chain. DNA is cleaved by the endonuclease enzyme into nucleosomal units (oligomers) that are about 180 bp in size (Basnakian and James, 1994). The fragmented DNA is resolved on an agarose gel to verify if apoptosis had actually occurred. This method is referred to as DNA laddering assay. During apoptosis, the activity of the endonuclease, called caspase-activated DNase (CAD), is catalysed by caspase-3, which cleaves the inhibitor of caspase-activated DNase (ICAD) (Liu *et al*., 1997).

Technique

Cells that were 70-80% confluent (6×10^6) were treated and incubated for 24 h (CPT and TXL) and 48 h (all treatments including DNase control). Detached cells were harvested by centrifugation (2054 × g, 5 min, 25 °C). Furthermore, adherent cells were trypsinised for 2 min, washed with DMEM and harvested by centrifugation (2054 × g, 5 min, 25 °C). gDNA was extracted using Quick-gDNA™ miniprep (Zymo Research). The gDNA was run in 1% Agarose gel (1× Tris-Borate-EDTA buffer) at 90 V. The agarose gel was then analyzed using the Gel-Doc viewer.

2.2.6. Flow cytometry: Apoptosis

Principle

Flow cytometry is a technique that is used for the analysis of multiple parameters of individual cells within heterogeneous populations (Mandy *et al*., 1995). This method is used in various techniques, namely cell counting, immunophenotyping, green fluorescent protein (GFP) expression as well as ploidy analysis. When conducing this technique, a large number of cells (1000 cells/sec) pass through a laser beam, as these cells pass through the beam a light that emerges between the cells is then captured for analysis (Jayat and Ratinaud, 1993). This data can be analysed using flow cytometry software (BD Accuri), which can report on the cellular characteristics of each of the cells. These characteristics are namely the size, phenotype, health and complexity of the cell (Jayat and Ratinaud, 1993).

Technique

Cells were treated and incubated for 24 h. Detached cells were harvested by centrifugation (2054 × g, 5 min, 25 °C). Furthermore, adherent cells were trypsinised for two min and rinsed and harvested by centrifugation (2054 × g, 5 min, 25 °C). Harvested cells were re-suspended with 500 µl 1× Annexin V Binding buffer. The cells were then subjected to 5 µl Annexin V-FITC and 5 µl propidium iodide and incubated for 5 min at room temperature in the dark. Cells were then analysed using BD Accuri™ Flow cytometer.

2.2.7. Cell Cycle analysis

Principle

Cell cycle analysis studies the DNA content found in pre-fixed cells by means of flow cytometry. The technique aims to identify the stage of DNA development within the pre-

mitotic phases of the cell cycle. Propidium iodide is the fluorescent stain that is used to bind to DNA and indicate the cell cycle phase that DNA population is found.

Technique

Cells were allowed to grow to 70%- 80% confluence. This was followed by treatments of the cells with 50 nm taxol, 0.5 µM camptothecin, 50 µg/ml of methanol and 50 µg/ml butanol extracts for 48 h prior to fixing. The treated cells were then washed with 1× PBS twice upon the removal of media and trypinised for two min with Trypisn-EDTA. DMEM media was then added onto trypsinised cells then the cells were harvested by centrifugation (2054 × g, 3 min, 25 °C). Cells were resusupended in 30 µl of ice cold 1 ×PBS and 70 µl of 100% ethanol which was pre-chilled at -20 °C. Cells were kept at -20 °C until they were required further experimental procedures. On the day of analysis the fixed cells were stained with FxCycle™ PI/RNAse staining solution (Life Technologies) and analyzed by flow cytometry and analyzed with the BD accuri™.

2.2.8. RNA-extraction and reverse transcription

Principle

In order to study the specific gene expression of target genes within cells, it is essential that a reliable extraction of total non-degraded RNA be conducted (Burgmann *et al*., 2003). The most important aspect of RNA extraction is to prevent RNA degradation. Most protocols employ RNase inhibitors such as denaturants, namely sodium-dodecyl sulfate (SDS) or β-mercaptoethanol, to reduce the loss of RNA or prevent RNA degradation during extraction.

Technique

RNA was extracted using NucleoSpin® RNA II extraction kit (Macere-Nagel). Contaminating DNA was removed by adding RNase free DNase directly on to the

NucloclеoSpin® silica membrane contaminated with DNA. Furthermore, the RNA was subjected to repeated washes with two buffers that remove salts, metabolites and any residual cellular component. The purified RNA was eluted with RNase-free water and immediately stored at -70 ℃ to ensure RNA stability (NucloclеoSpin® protocol). The RNA integrity was confirmed by means of a denaturation gel and the A260/A280 ratio was < 1.7. Extracted RNA was reversed transcribed to cDNA using Takara Bio Inc. PrimeScript™ RT reagent Kit (Perfect Real Time) using the protocol in Table 1.

Table 1. Reverse transcriptase cocktail mixture

Content	**Volume (µl)**
5X PrimeScript Buffer	2
PrimeScript RT Enzyme Mix I	0.5
Oligo dT Primer	0.5
Oligo dT Primer	0.5
dH_2O	5.5
RNA sample	1
Total	**10**

The Labnet multigene thermocycler was used with the following conditions:

Table 2. Reverse transcription PCR protocol

	Temperature (°C)	Time (Min)
1	35	15
1	85	0.167
1 Cycle	4	∞

2.2.9. Real-Time Polymerase chain reaction (RT-PCR)

Principle

Real-time PCR (RT-PCR) uses the same principle of amplification as that of basic PCR. However, this method of PCR monitors product formation and amplification in real time. This is made possible by the use of the real-time PCR machine which contains specific detectors, which detect the fluorescent markers that are stimulated during amplification of DNA in each cycle (Bustin *et al*., 2005).

Technique

Reverse transcribed cDNA was amplified by PCR using the following primers

a) **GADPH**:

Forward – 5′-TGT AGT TGA GGT CAA TGA AGG G- 3′,

Reverse – 5′-ACA TGC CTC AGA CAC CAT G- 3′;

b) **p21**:

Forward – 5′ -GAG ACT AAG GCA GAA GAT GTA GAC- 3′,

Reverse – 5′ - GCA GAC CAG CAT GAC AGA T- 3′

c) **P53**:

Forward – 5′ -GAC GCT AGG ATC TGA CTG C- 3′,

Reverse – 5′ -GAC ACG CTT CCC TGG ATT G -3′.

d) **MDM2**

Forward – 5′-GTG CAT TTC CAA TAG TCA CCT AA- 3′,

Reverse – 5′-AGA AGG ACA AGA ACT CTC AGA TG- 3′;

e) **BAX**:

Forward – 5′ –AAA GAT GGT CAC GGT CCA AC- 3′,

Reverse – 5′ – CAA ACT GGT GCT CAA GGC- 3′

f) **BCL-2**:

Forward – 5′ -AGC CAG GAG AAA TCAAAC AGA G- 3′,

Reverse – 5′ -GAT GAC TGA GTA CCT GAA CCG -3′.

The Luminaris HiGreen™ qPCR mastermix (Life Science) was prepared to a final cocktail mix of 10 µl (Table 3).

Table 3: components of qRT-PCR mix

Components	Volume (µl)
2 ×Luminaris HiGreen™ qPCR mastermix	5
Fwd + Rvs	1
cDNA	1
Nuclease free water (make up to 10 µl)	3
Total	**10**

The Roche light cycler 480 was used to amplify and record PCR amplification:

Initial denaturation step: 95 °C for 10 min

Denaturation step: 95°C for 15 sec

Annealing step: 60 °C for 30 sec

Extension step: 72 °C for 30 sec

40 Cycles

Samples data was calculated and analysed using REST 2009 software, a tool developed for the analysis of gene expression data from quantitative PCR (qPCR). This is done by computing the gene expression ratio from crossing point (CP) values of the target genes versus those of the control (GAPDH). Each gene from the different treatments was plotted using similar genes from the untreated cells as a reference.

2.2.10. Liquid Chromatography- Mass Spectrometry

Principle

Liquid chromatography-mass spectrometry (LC-MS) combines two analytical techniques, namely high performance liquid chromatography (HPLC) and mass spectrometry (MS). Individually, these techniques are very efficient, however combining the two creates an efficient and much more powerful analytical tool (Korfmacher, 2005). HPLC separates compounds found in a mixture by their physical or chemical properties, which include the size, charge of specific affinity of that particular compound (Wisniewski, 1992). Chromatographic techniques are characterised by the presence of the mobile and stationary phase. The stationary phase contains specific compounds (silica or sephadex) that usually retard analytes found in the mobile phase. The mobile phase carries the mixture of analytes through the stationary phase, where the analytes will then be separated based on their chemical or physical properties (Wisniewski, 1992). The analyte will then get separated at different times and can then be collected and analysed individually. The length of the stationary phase will determine the time and purity of the analyte upon analysis, this means that the longer the stationary phase (column) the longer it will take for analytes to separate, thus ensuring that the compound in pure. Analytes with similar properties and size can be thoroughly distinguished in longer columns. Short columns however, ensure that analytes are separated at a faster rate but the purity of the analyte cannot always be ensured, thus, the type of column used is determined by the type of chromatographic data that is desired.

Once the analytes have been separated they enter into the photodiode array (PDA), which contains a light source (such as tungsten) which scans compound at different wavelengths (Korfmacher, 2005). As the separated compound enters the PDA the light shines through the compound and as the compound absorbs the light, there will be a peak at specific wavelength, this is due to the fact that each compound has a unique absorbance (Korfmacher, 2005). The

point of maximum absorbance (λ_{max}) vs absorbance is part of the PDA display that can be used to determine the compound of interest. Another part of the PDA display is absorbance versus time, which indicates when the compound was eluted from the column (Korfmacher, 2005). The information on the PDA displays can give a clear understanding of the compound of interest. HPLC can be very effective in determining known compounds in an analyte mixture, however, if the analytes have various unknown compounds it could be difficult to analyse them. The combination of HPLC with MS does ensure that an unknown compound can be identified (Korfmacher, 2005). After PDA analysis, the analyte travels through an interface to the MS. When the analyte reaches the MS it immediately interacts with the electron spray ioniser (ESI), which vaporises the analyte and subsequently ionises the vaporised analyte, with either a negative or positive charge. Upon ionisation the analyte then enters the quadrupole, which is made up of four charged rods that keep changing their charge rapidly (1000/sec) between negative and positive charges. The charged analytes encounter the charged rod and are either deflected or they pass through the quadropole. Deflected analytes get lost within the quadrupole chamber and those that pass through the quadrupole hit the detector. At the precise moment of impact the detector then record the quadrupole charge. The mass of the analyte is determined by the quadrupole charge and the time of impact between the compound and the detector. A light compound will have a lower charge recorded as opposed to the heavier compound and light compound will travel at a faster speed than a much heavier compound (Korfmacher, 2005). Once the analyte is detected, data showing various ions and their various intensities will be computed. By combing the data found in MS and that of the PDA, unknown compound can then be identified from literature of from various MS libraries.

Technique

The samples of both the methanol and butanol extracts were sent to the University of Fort Hare for LC-MS. Sample preparation was conducted using the following:

Table 4. Type of LC-MS analysis

Mass Spectrometer	**TripleTOF 5600**
Config Table Version	01
Firmware Version	M402001 B4T0301 M3L2002 B3T0300
Component Name	Hybrid Quadrupole-TOF LC-MS/MS Mass Spectrometer
Component ID	Triple TOF 5600
Manufacturer	AB Sciex Instruments
Model	1032150/AD
Serial Number	AY22261112
Source Housing	DuoSpray Ion Source

Unknown compounds were determined from MS library Mass Bank www.**mass**bank.jp

2.2.11. Statistical analysis

The results of each of the experimental procedures, performed either in triplicate or duplicates, are the expression of the mean and standard deviation of the mean. Degrees of statistical significance of data sets (duplicate or triplicate) were determined using Student's t-test. This was conducted under the inference that p-values ≤ 0.05 were significant.

Chapter Three: Results

3.1. MTT assay

The cell viabilty assay was conducted to assess the effects of cell growth of A549 cells that were treated with increasing concentrations of the following cytotoxic compounds camptothecin (0.25- 15 µM) and taxol (10-500 nM) in comparison to those of the methanol and butanol extracts of the medicinal plant *Lobostemon fruticosus*. A549 cells were treated over a 24 hour period and the cytotoxic effects of these treatments were calculated againts the untreated A549 cells.

The research findings indicated that each of the treatments induced various degrees of cell death (cd) at increasing concentrations. Each of the treatments achieved an IC_{50} at various concentrations. Camptothecin-induced 50.5% cd at 1 µM, taxol induced, 50.9% cd at 50 nM. The methanol and butanol extracts of *L. fruticosus* induced 41.3% cd at 40 µg/ml, and 49.6% cd at 50 µg/ml , respectively (Figure 3). The negative control DMSO induced 1.4% cd at 0.001% (v/v). The results show that at higher concentrations, cells treated with methanol extracts (50 and 100 µg/ml) showed a significant decrease in cell death. This indicated that the extracts of *L. fruticosus* did reveal levels of cell toxicity at relatively low concentrations (Figure 3).

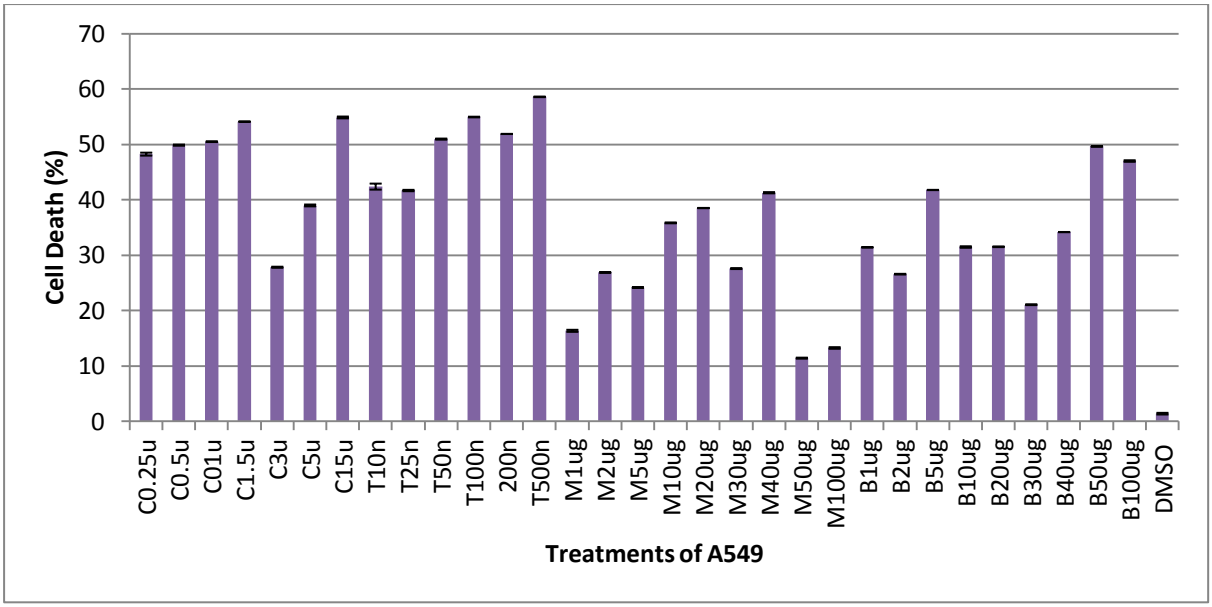

Figure 3: Percentage of cell death of treated A549 cells. Cells were treated with increasing concentrations of CPT (C 0.25-15 µM), TXL (T 1-500 nM), methanol and butanol extracts of *L. Fruticosus* (M and B 1-100 µg/ml *rsp*). The control DMSO was prepared a to the final concentration of 0.001% (v/v).

3.2. The xCELLigence system

The xCELLigence system was used to observe cell growth and stability (cell adherence) at real time. To achieve this cells were seeded on E-plate 16 to monitor cell impedence and viablity in a non-invasive and non-fixative environment. The changes in the cells' electrical impedence were detected and expressed as the cell index. Seeded cells were allowed to attach for 22 h prior to cell treatment (arrow, Figure 4). The assessment of cellular proliferation was conducted using A549 cell line. The growth curve analysis was conducted over a period of ± 72 h (3 days) upon cell treatment, at a seeding density of 5000 cells/cm^2. The experiment was conducted in duplicates. Negative controls of DMSO (0.001%, v/v), methanol and butanol (0.0001%, v/v) were included in order to observe whether the mode of cell death was exerted as a result of the treatments or of the the solvents they were extracted and dissolved in.

Cell index increased continuously for all treated and untreated cells, however the data shows that after a period of 29 h cells treated with CPT began to show a decline in cell index, indicating that cytotoxicity of CPT took effect after 29 h of exposure to the cells (Figure 4). The results also indicated that the negative controls did not affect cell growth of the A549 cells. The cells treated with TXL showed a continuous increase in cell growth, however, after 54 h of treatment, there was a change in the pattern of cell growth, which seems to suggest that the cells began responding to the inhibitory effects of TXL. There seemed to be no difference in the pattern or degree of cell growth of both the methanol extracts and the butanol extract.

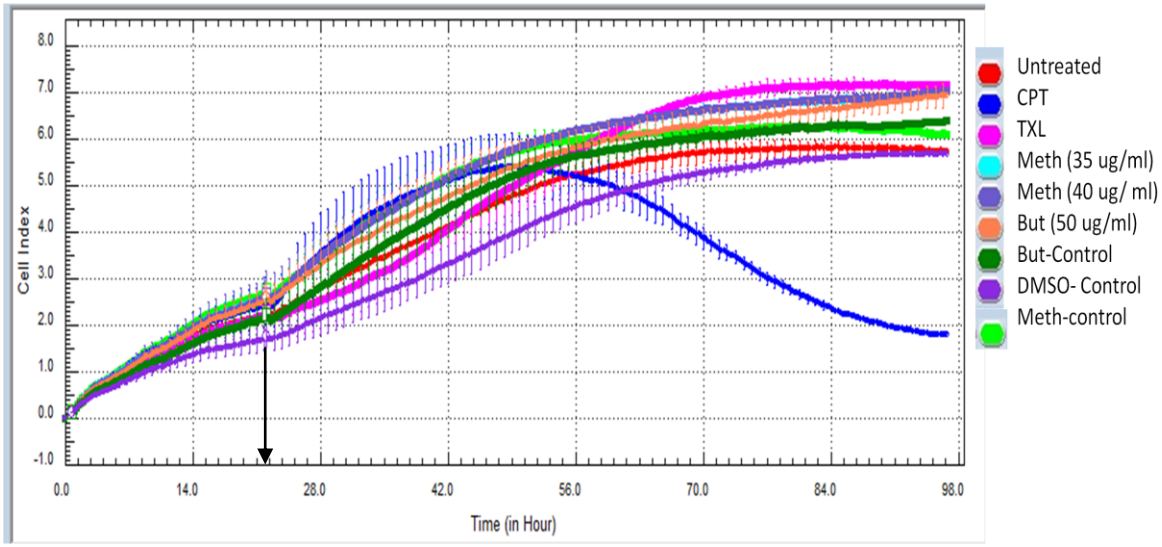

Figure 4: Real time analysis of cell growth of treated A549 cells. Cell growth of untreated and treated A549 cells was analysed using xCELLigence system. Cells were seeded and incubated for 24 h prior to treatment (indicated by the arrow).

3.3. DNA fragmentation

DNA fragmentation profiles were identified by significant smearing on the electrophoretogram. The gDNA of treated cells was examined in relation to the gDNA of the untreated cells (Figure 5). The treatments were conducted in 24 h for 0.5 µM CPT (C1),

15 nM T and 50 nM TXL (T1 and T2 respectively) prior to DNA extraction, 1 µl of DNase (D) was added on to 10 µl of gDNA of untreated cells as a positive control (Figure 5A). Cells were also treated for 48 h with 0.5 µM CPT (C2), 50 nM TXL (T3), 40µg/ml methanol (M) and 50 µg/ml butanol extracts of *L. fruticosus* (Figure 5B). These finding indicate that DNA fragmentation in both the methanolic and the butanolic plant extracts of *L. fruticosus* showed DNA fragmentation began after two days, this was also indicated with CPT and TXL after 48 h treatments as compared to the 24 h treatments. Degrees of fragmentation were expressed in comparison to those of the positive control.

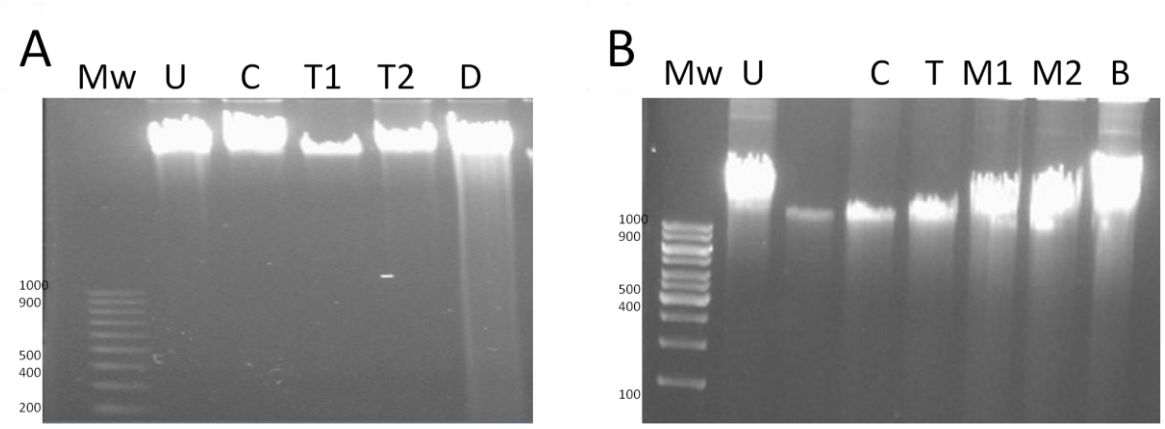

Figure 5: The electrophoretograms for DNA fragmentation of A549 gDNA (A and B). Mw is molecular weight marker (100 bp), U is untreated, C is 0.5 µM camptothecin treatment, T1 is 15 nM and T2 is 50 nM taxol, M1 is 35 µM methanol extract, M2 is 45 µM methanol extract and 50 µM butanol extract. A control of DNase treated gDNA (D) was used.

3.4. Flow Cytometry

Cells that were treated with camptothecin, taxol, and the extracts of *L. fruticosus* were analysed, using a flow cytometer, to measure the degree of apoptotic activity after treatment over a 24 hour period. The scatter graph was set up with four quadrants, namely Q1-LL which represented viable cells (Annexin-V and Pi negative), Q1-UL which represents dead cells, these were either necrotic cells or a cell death (Pi positive), Q1-UR which represents

cells that underwent late apoptosis (Annexin-V and Pi positive) and cells that underwent the early stages of apoptosis were represented by the Q1-LR quadrant (Annexin-V positive). The data of cell death recorded in the UR and LR quadrants were added together in order to sum up the total percentage of apoptotic cells that were observed during the assay. The level of apoptosis are as follows: 6% (untreated cells), 7.4% (CPT), 27.8% (TXL), 17.6 % (methanol extract) and 21.9% (butanol extract). The data was collected in duplicates (n = 2) and standard deviation was calculated from the mean (mean±SD), the varying degrees of apoptosis were plotted on a bar graph (Figure 6F). The data was statistically analysed using Student's t-test and high degree of significance was observed.

The analysis of untreated A549 cells indicated that 87.9% of cells located in the Q1-LL quadrant, remained viable; 12.1% of cell death was observed with 6.1% in the UL quadrant, 4.4% in the UR quadrant and 1.6% were found in the LR quadrant (Figure 6A). Cells that were treated with CPT indicated that 63.1% of cells located in the LL quadrant remained viable; 36.2% cell death was also observed with 29.5% cells in the UL quadrant, 6.7% in the UR quadrant, and 0.7% in the LR quadrant (Figure 6B). In Figure 6B, data indicated that 72.0% of cells treated with TXL remained viable (LL quadrant); 28.0% cell death was recorded with 0.2% in the UL quadrant, 2.4% in the UR quadrant and 25.4% in the LR quadrant (Figure 6C). Cells treated with methanol extract of the *L. fruticosus* plant (Figure 6D) displayed 71.1% viable cells in the LL quadrant; 28.9% cell death was also observed with 12.0% in the UL quadrant, 14.4% in the UR quadrant and 2.5% in the LR quadrant. The cells that were treated with butanol extracts of the *L. fruticosus* plant recorded 63.1% of viable cells in the LL quadrant; 36.8% cell death was observed with 15.8% cell in UL quadrant, 17.5% cell death in the UR quadrant and 3.5% in the LR quadrant (Figure 6E).

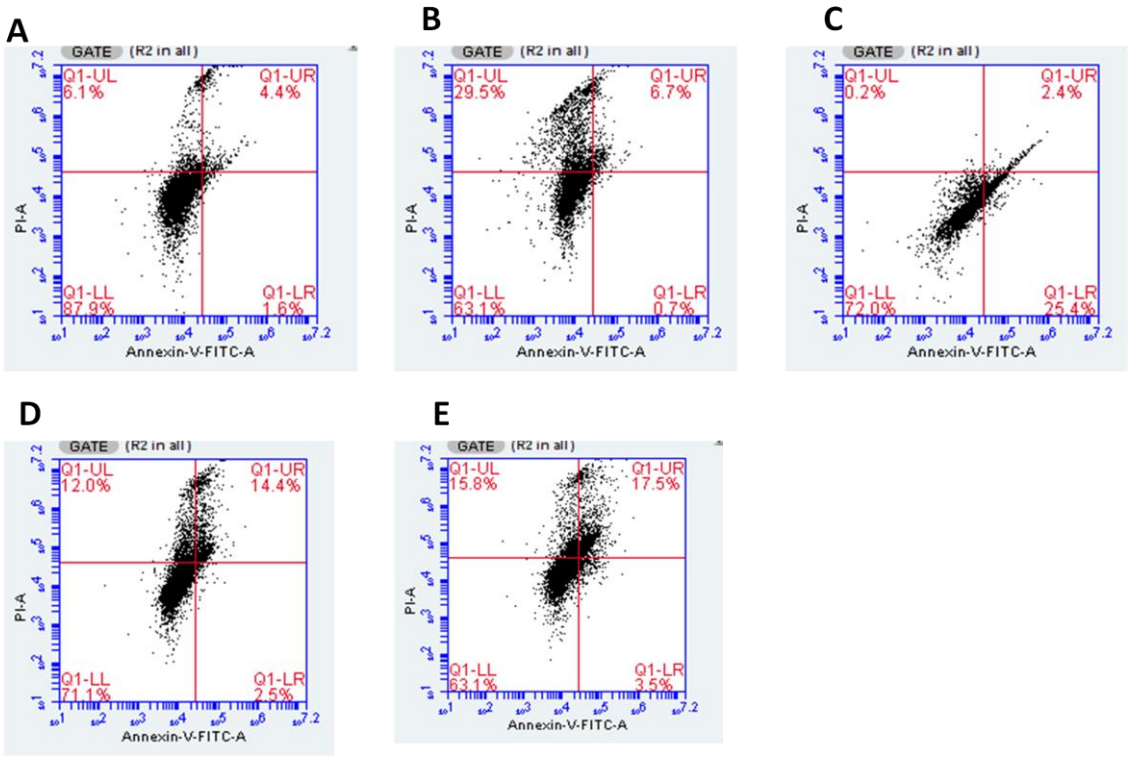

F

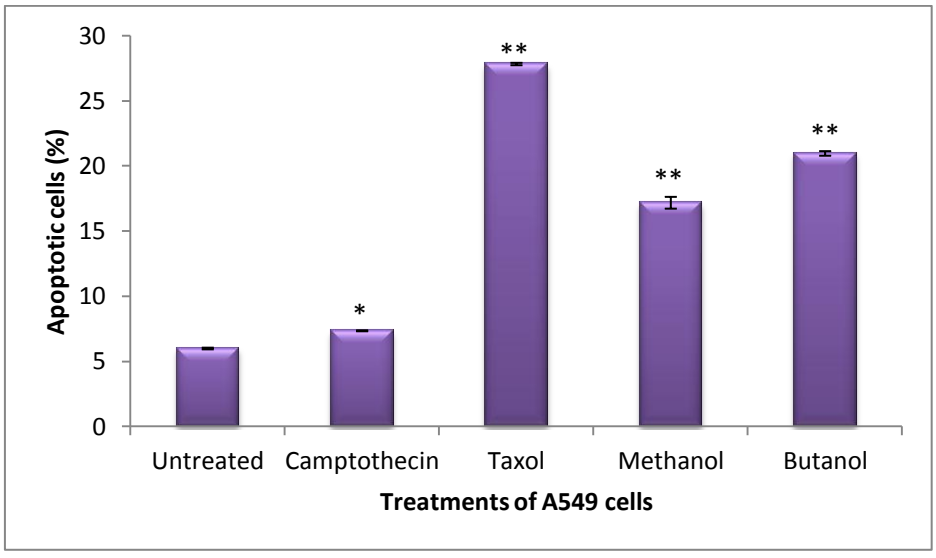

Figure 6: Scatter graph of A549 cells depicting stages of viable cells (LL), cell death (UL), early (LR) and late (UR) stages of apoptosis (A-E). Statistical representation of apoptotic cells after treatment in comparison with untreated cells (F). Plots A-E show results of apoptotic studies of untreated cells of A549 together with cells treated with camptothecin, taxol, methanol and butanol plant extracts, respectively. *Findings were very significantly different ($p \leq 0.01$), **Findings were extremely significantly different ($p \leq 0.001$).

3.5. Cell Cycle analysis

The changes in cell cycle of A549 cells were monitored using a flow cytometer, propidium iodide was the stain used to detect the cells' DNA ploidy at different stages of the cell cycle. The histograms of cell cycle analysis illustrate cell progression and inhibition from G_0/G_1 to the S and G_2/M phase of cell cycle (Figure 7). Cells were treated for 48 h, fixed with 70% ethanol and stained with a DNA staining chemical; propidium iodide for DNA based cell cycle distribution analysis. The untreated cells (A) displays some degree of cell cycle progression, however CPT (B) and TXL (C) display an inhibition of cell progression at the S phase and the plant extracts display inhibition at G_0/G_1 followed by subsequent cell death. The data was collected in triplicates (n = 3) and standard deviation was calculated from the mean (mean ± SD), the changes in cell cycle distribution were plotted on a bar graph (Figure 7F). The population of cells at each stage of cell cycle were statistically analysed using Student's t-test and high degree of significance was observed.

The cell cycle distributions of treated cells were compared to those of untreated cells, which displayed 88.9% cells at G_0/G_1; 6.6% cells at S, 1.6% cells at G_2/M and 2.9% at sub-G_0 (apoptotic) phase (Figure 7A). Cells that were treated with CPT displayed a distribution of 60.1% cells at G_0/G_1, 1.2% cells at S-phase, 0.2% cells at G_2/M phase and 38.6% cells at sub-G_0 phase (Figure 7B). Cells treated with TXL displayed a distribution of 4.8% cells at G_0/G_1 phase; 0.4% cells at S phase, 0% at G_2/M phase and 94.8% at sub-G_0 phase (Figure 7C). The cells that were exposed to methanol extracts of *L. fruticosus* resulted in 0.1% cells at G_0/G_1 phase; 0% cells at both the S and G_2/M phases and 99.9% cells at the sub-G0 phase (Figure 7D). Cells that were treated with butanol extracts of *L. fruticosus* resulted in 1.3% cell at the G_0/G_1 phase; 0% for cells at both S and G_2/M phases and 98.7% cell at the sub-G_0 phase (Figure 7E).

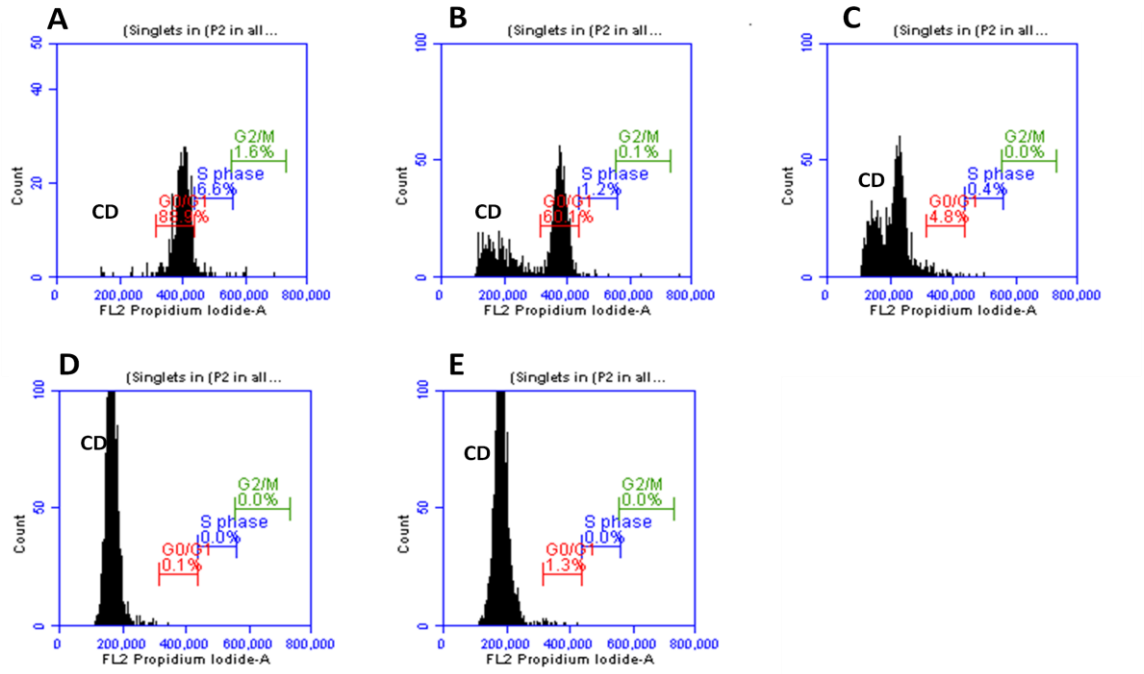

F

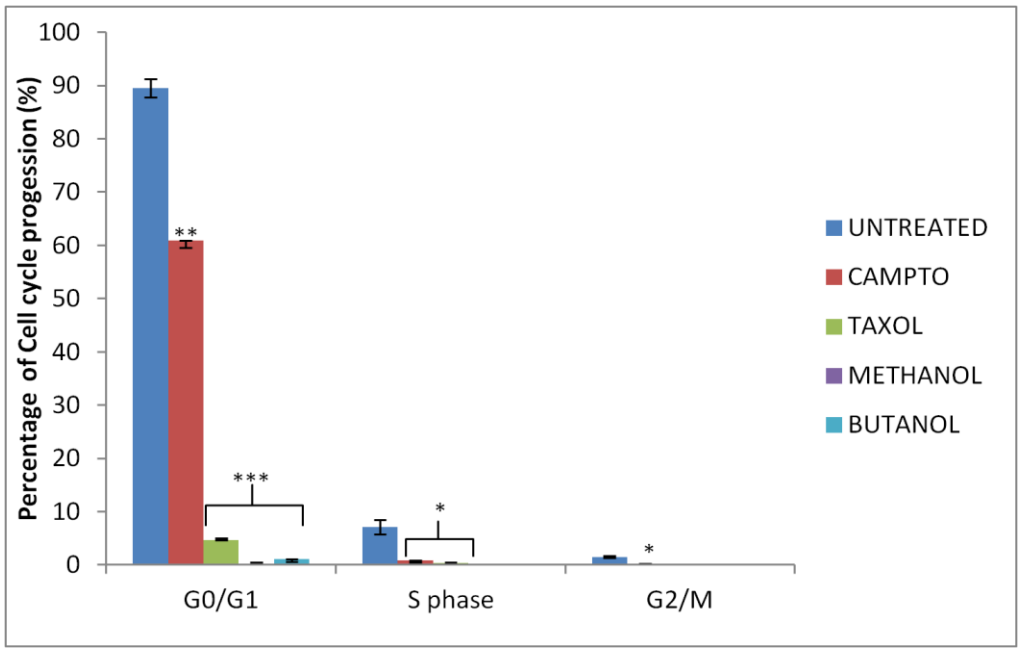

Figure 7: Histogram profiles of A549 cells depicting stages of cell cycle development and degree of cell death (cd) before and after treatments. The untreated cells (A) CPT (B) and TXL(C) methanol (D) and butanol (E) extracts of *L. fruticosus*. The population of cells at each stage of cell cycle were statistically analysed (F).*Significantly different ($p \leq 0.05$) **finding were very significantly different ($p \leq 0.01$), ***finding were extremely significantly different ($p \leq 0.001$).

3.6. Real Time polymerase chain reaction (RT-PCR)

The relative expression of target genes was obtained using GAPDH as the reference gene. The measure of gene expression was normalised with the expression ratio set at 1. This means that the mean expression points set below 1 signify down regulation of the target gene, those set above 1 signify the up regulation of the target gene and those that are found directly at one or significantly close to the ratio signify that no changes in gene expression had occurred after treatments. The data is presented in the form of box plots (Figure 8 A-D). The 1% agarose gel was used to verify these findings (Figure 8E).

The data receive was extrapolated using the Rest 2009 program to statistically construct the expression of the crossing point (CP) values. Results for the treatments were plotted using the genes from the untreated cells as a reference (Figure 8 A-D) and statistical data was constructed from the tables below.

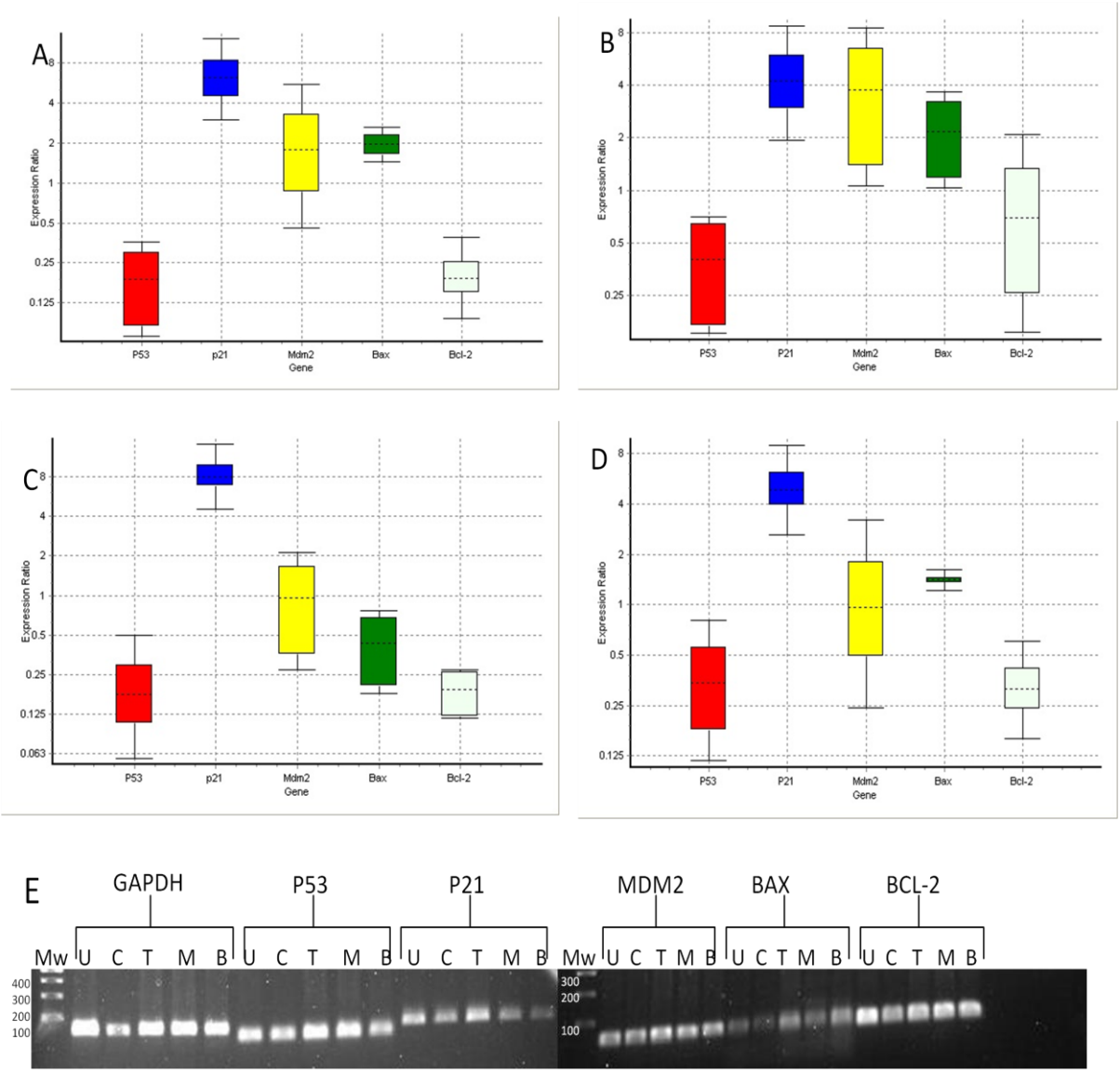

Figure 8: Relative expression of apoptotic genes vs. GAPDH in A549 cells. Cells were treated with CPT (A), TXL (B), Methanol (C) and Butanol (D) extracts of *L. fruticosus* over a 48 hour period. Genes from untreated cells were used as a reference and the electrophoretogram (E) was conducted to view degree of gene expression. The apoptotic genes were expressed from untreated cells (U), CPT treated cells (C), TXL treated cells (T), cells treated with methanol (M) and butanol (B) extracts.

The data was extrapolated using the Rest 2009 programme to statistically construct the expression of the crossing point (CP) values. Results for the treatments were plotted (Figure 8 A-D) and statistical data was constructed from tables below (Tables 5-8). Insignificant data was depicted with N/S; the *p*-value was displayed as P(H1), the reaction efficiency was 0.9.

The results from the CPT treatment indicated that p53 was down (expression mean of 0.158); p21 was up (mean of 6.052) and Mdm2 showed no significant (N/S) changes (mean of 1.593). Bax was up (mean of 1.943) and Bcl-2 was down (mean of 0.192) (Table 5).

Table 5: Statistical analysis of box plot of CPT

Gene	Type	Expression	Std. Error	95% C.I.	P(H1)	Result
Gapdh	REF	1.000				
P53	TRG	0.158	0.078 - 0.325	0.071 - 0.353	0.000	DOWN
P21	TRG	6.052	3.956 - 9.881	3.148 - 11.854	0.000	UP
Mdm2	TRG	1.593	0.707 - 4.136	0.496 - 5.327	1.000	N/S
Bax	TRG	1.943	1.556 - 2.441	1.460 - 2.591	0.000	UP
Bcl-2	TRG	0.192	0.131 - 0.305	0.100 - 0.374	0.000	DOWN

The results from TXL treatment indicated that after cells treated for 48 h indicated that p53 was down (expression mean of 0.329); p21 was up (mean of 4.091) and Mdm2 was up (mean of 2.987). Bax was up (mean of 1.943) and Bcl-2 displayed no significant (N/S) changes in expression (mean of 0.568) (Table 6).

Table 6: Statistical analysis of box plot of TXL

Gene	Type	Expression	Std. Error	95% C.I.	P(H1)	Result
Gapdh	REF	1.000				
P53	TRG	0.329	0.162 - 0.672	0.155 - 0.702	0.000	DOWN
P21	TRG	4.091	2.557 - 6.987	2.034 - 8.382	0.000	UP
Mdm2	TRG	2.987	1.264 - 7.264	1.092 - 8.241	0.000	UP
Bax	TRG	1.943	1.115 - 3.408	1.046 - 3.617	0.000	UP
Bcl-2	TRG	0.568	0.220 - 1.616	0.166 - 2.006	0.661	N/S

The results from cells treated with Methanol extract of *L. fruticosus* indicated that p53 was down (expression mean of 0.168); p21 was up (mean of 8.001) and Mdm2 displayed no significant (N/S) changes in gene expression (mean of 0.764). Bax was down (mean of 0.371) and Bcl-2 was down (mean of 0.661) (Table 7).

Table 7: Statistical analysis of box plot of methanol extract

Gene	Type	Expression	Std. Error	95% C.I.	P(H1)	Result
Gapdh	REF	1.000				
P53	TRG	0.168	0.087 - 0.372	0.062 - 0.477	0.000	DOWN
P21	TRG	8.001	5.928 - 11.526	4.716 - 13.828	0.000	UP
Mdm2	TRG	0.764	0.323 - 1.853	0.281 - 2.089	0.834	N/S
Bax	TRG	0.371	0.193 - 0.716	0.181 - 0.760	0.000	DOWN
Bcl-2	TRG	0.178	0.118 - 0.268	0.117 - 0.270	0.000	DOWN

The results from cells treated with the butanol extract of *L. fruticosus* indicated that p53 was down (mean of 0.308); p21 was up (mean of 4.85) and Mdm2 displayed no significant (N/S)changes in expression (mean of 0.88). Bax was up (mean of 1.410) and Bcl-2 was down (mean of 0.311) (Table 8).

Table 8: Statistical analysis of box plot of butanol extract

Gene	Type	Expression	Std. Error	95% C.I.	P(H1)	Result
Gapdh	REF	1.000				
P53	TRG	0.308	0.155 - 0.654	0.123 - 0.785	0.000	DOWN
P21	TRG	4.850	3.457 - 7.261	2.751 - 8.711	0.000	UP
Mdm2	TRG	0.880	0.396 - 2.325	0.266 - 3.059	0.830	N/S
Bax	TRG	1.410	1.304 - 1.531	1.233 - 1.613	0.000	UP
Bcl-2	TRG	0.311	0.211 - 0.490	0.168 - 0.588	0.000	DOWN

3.7. Liquid chromatography- Mass spectrometry (LC-MS)

3.7.1. Methanol extract of *Lobostemon fruticosus*

The experiment utilised an untargeted method of profiling extracts of *L. fruticosus,* by applying the quadropole-time-of-flight liquid chromatography- mass spectrometry tandem (Q-TOF LC-MS/MS). This would ensure that a broad spectra of peaks from various molecules, each with a unique mass-to-charge ratio (m/z), would be detected from the sample (Figure 9) (Zhu *et al*., 2013). The figures below (Figures 10-16) are profiles of compounds identified from LC-MS of the methanol extracts of *L. fruticosus*. The mass of these compounds were identified by determining the charge that the quadrupoles were at upon molecular impact and the compound's retention time (RT). The list of compounds found in the methanol extract was then tabulated below (Table 9).

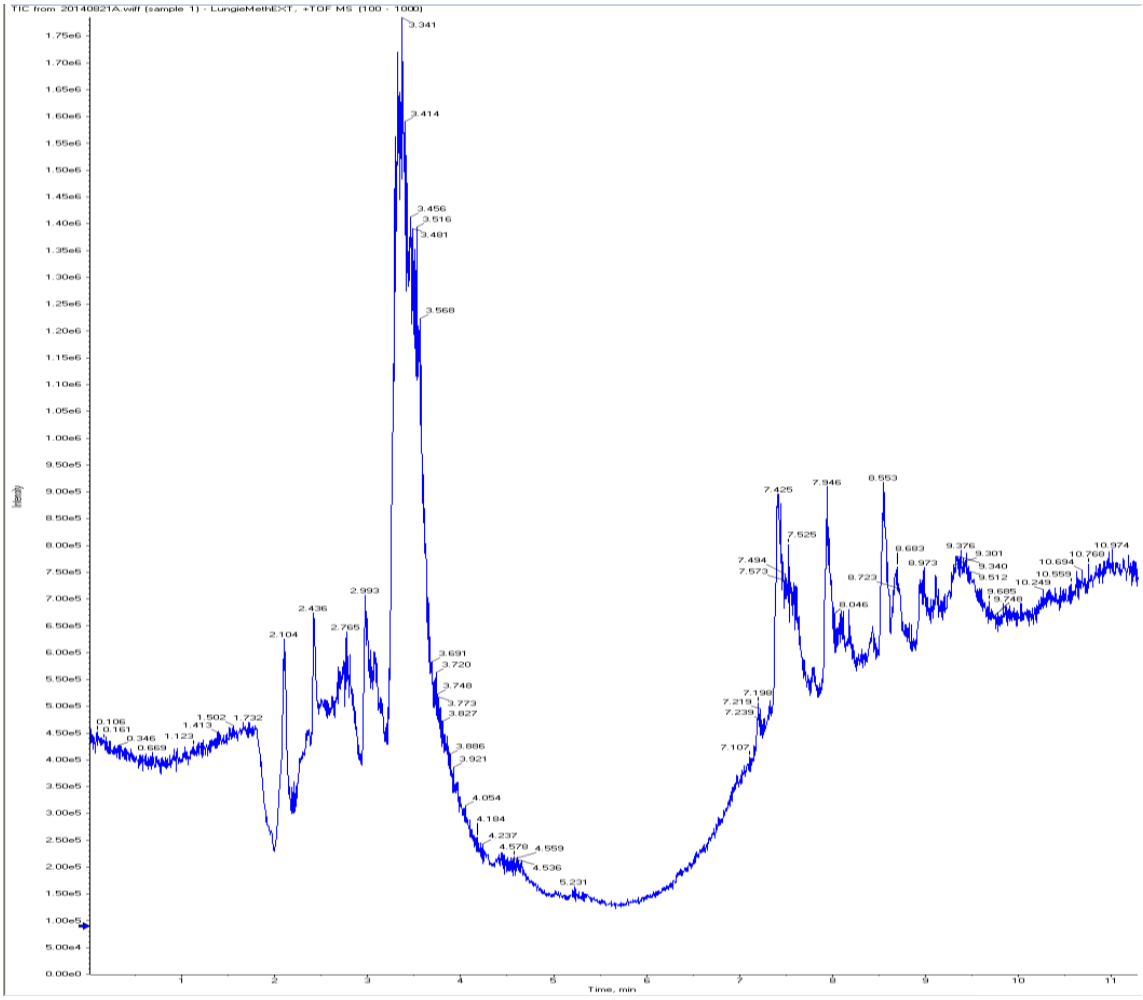

Figure 9: Non-targeted LC-MS chromatographic profiles of the methanol extracts of *Lobostemon fruticosus.*

1. 2-Hydroxylamino-4 ,6-dinitrotluene

2-Hydroxylamino-4 ,6-dinitrotluene ($C_7H_7N_3O_5$) was one of the compounds identified in the methanol extract of *L. fruticosus*. The mass spectrum was observed at 10.27 min (Figure 10A), with mass-to-charge ratio (m/z) peaks highlighted at 376.0991 and 377.1027 m/z for the protiated compound ($M+H^+$) and its isotopic species (M+1) respectively (Figure 10B). The compound belongs to the toluene family and its molecular mass is 213.15 Da.

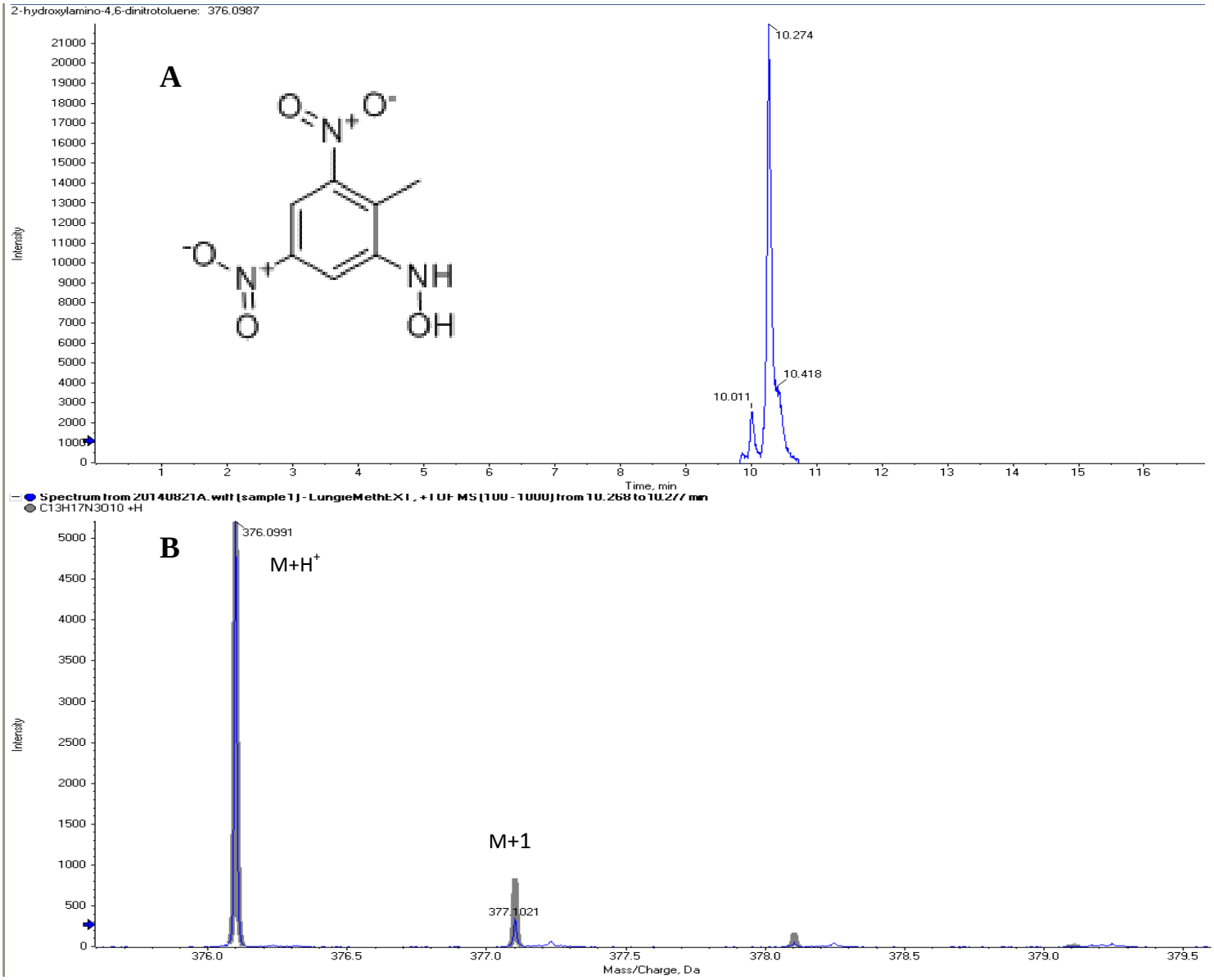

Figure10: LC-MS chromatographic profile 2-hydroxylamino-4,6-dinitrotouene. Spectrum at 10.27 min with the compound structure (A) displaying highlighted peaks at 376.0991 and 377.1027 m/z (B).

2. 4-Hydroxycoumarin

4- Hydroxycoumarin ($C_9H_6O_3$) was another compound identified in the methanol extract of *L. fruticosus*. The sample was similar to that of Figure 10 with a mass spectrum was found at 10.27 mins (Figure 11A), with mass-to-charge ratio (m/z) peaks highlighted at 376.0991 and 377.1027 m/z for the protiated compound ($M+H^+$) and its isotopic species (M+1) respectively (Figure 11B). The compound belongs to the coumarin family and its molecular mass is 162.14 Da.

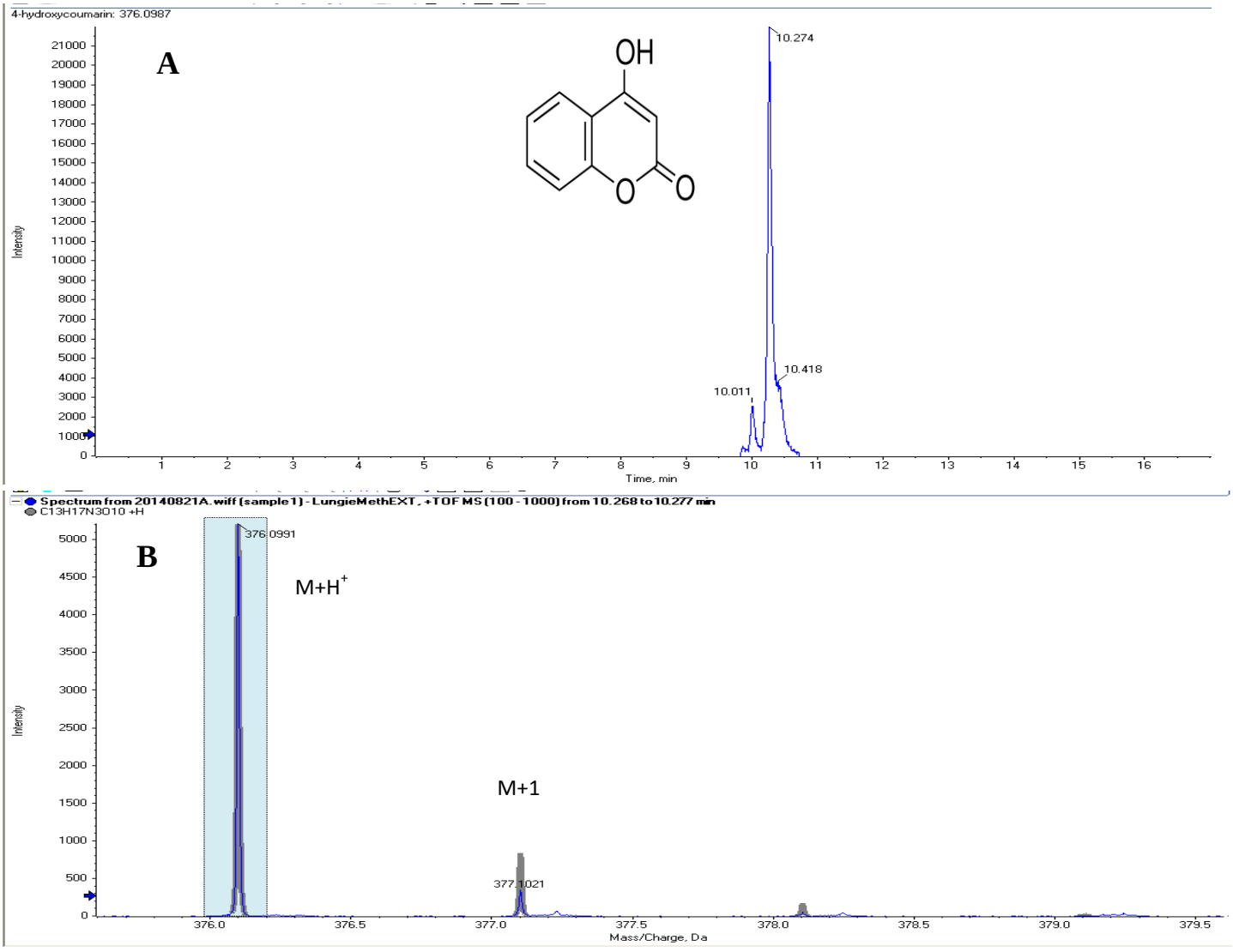

Figure 11: LC-MS chromatographic profile 4-hydroxycoumarin. Spectrum at 10.27 min with the compound structure (A) displaying highlighted peaks at 376.0991 and 377.1027 m/z (B).

3. Sarpagine

Sarpagine ($C_{19}H_{22}N_2O_2$) was identified in the methanol extract of *L. fruticosus*. The compound's mass spectrum was found at 10.27 min (Figure 12A), with mass-to-charge ratio (m/z) peaks highlighted at 209.0808 and 211.1306 m/z for the protiated compound ($M+H^+$) and its isotopic species (M+2) respectively (Figure 12B). The compound belongs to a group of indole alkaloids of the Alkaloid family and its molecular mass is 310.39 Da.

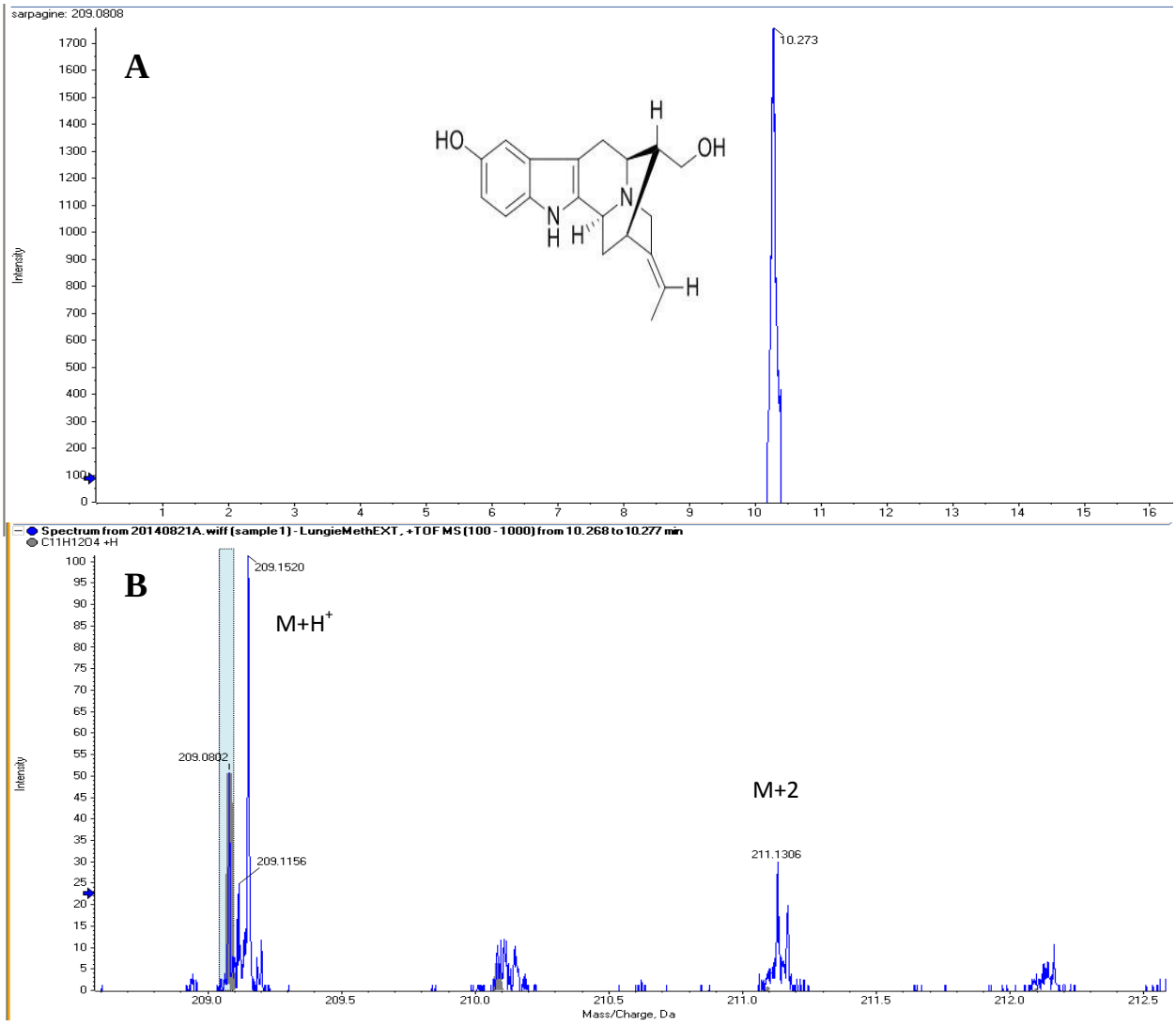

Figure 12: LC-MS chromatographic profile for Sarpagine. Spectrum at 10.27 min with the compound structure (A) displaying highlighted peaks at 209.0808 and 211.1306 m/z (B).

4. 7-O-methylvitexin 2''-O-β-rhamnoside

7-O-methylvitexin 2''-O-β-rhamnoside ($C_{28}H_{32}O_{14}$) is another compound that was identified in the methanol extract of *L. fruticosus*. The compound has a mass spectrum found at 10.311 min (Figure 13A), with peaks highlighted at 221.19 m/z f for the protiated compound ($M+H^+$) and 222.1912 and 223.1315 for its isotopic species (M+1 and M+2 respectively) respectively (Figure 13B). The compound belongs to a group of glycoxyflavones of the flavonoid family and its molecular mass is 592.1792 Da.

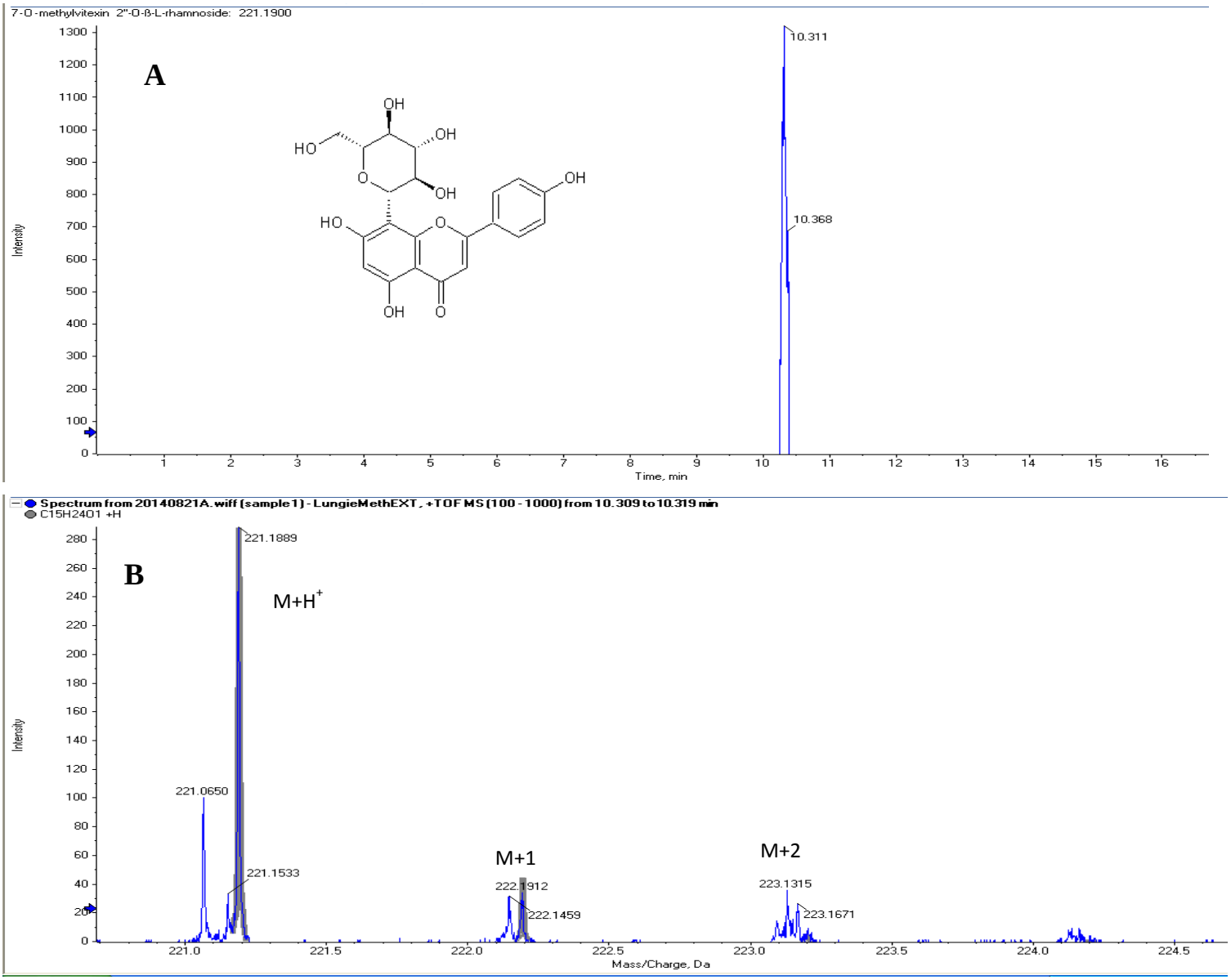

Figure 13: LC-MS chromatographic profiles of 7-O-methelylvitexin 2"-O-β-L-rhamnoside. Spectrum at 10.31 min with the compound structure (A) displaying highlighted peaks at 221.1899, 222.1912 and 223.1315 m/z (B).

5. 7-O-β-D-glucosylapigenin

7-O-β-D-glucosylapigenin ($C_{21}H_{20}O_{10}$) was identified in the methanol extract of *L. fruticosus*. The compound has a mass spectrum found at 2.106 min (Figure 14A), with peaks highlighted at 221.19 m/z f for the protiated compound ($M+H^+$) and various dysregulated peaks (Figure 14B). The compound belongs to a group of glycoxyflavones of the flavonoid family and its molecular mass is 432.28 Da.

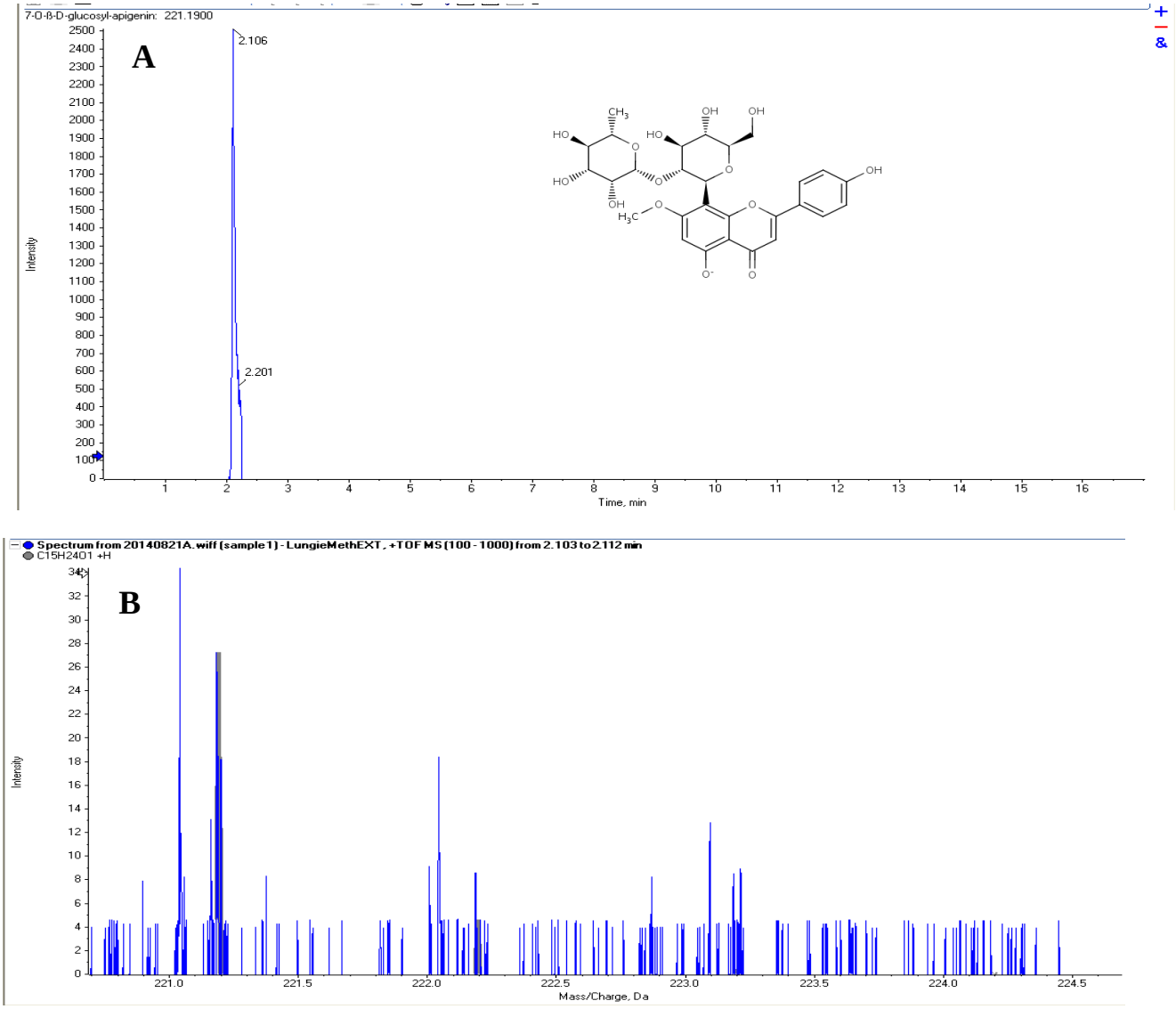

Figure 14: LC-MS chromatographic profile of 7-O-β-D-glucosylapigenin. Peak 221.1899 at 2.11 min Spectrum at 2.11 min with the compound structure (A) displaying highlighted peaks at 221.183 m/z (B).

6. Hypoglycin B

Hypoglycin B ($C_{12}H_{18}N_2O_5$) was identified in the methanol extract of *L. fruticosus* . The compound has a mass spectrum found at 2.95 min (Figure 15A), with peaks highlighted at 157.08 m/z f for the protiated compound ($M+H^+$) and 158.0,159.0 and 160.08 for its isotopic species (M+1, M+2 and M+3 respectively) (Figure 15B). The compound has a molecular mass is 270.28 Da.

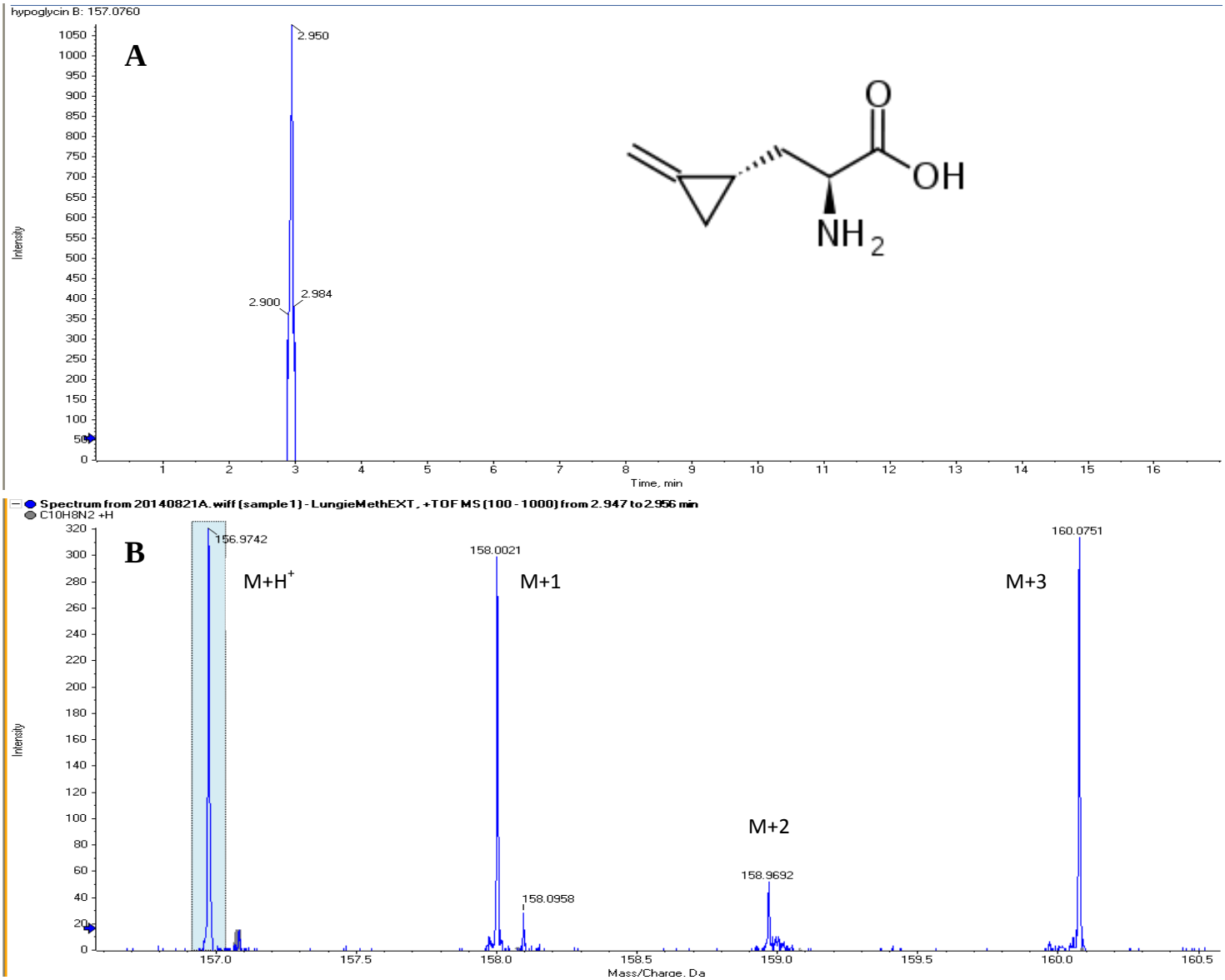

Figure 15: LC-MS chromatographic profile of hypoglycin B. Peak 157.0823 at 2.95 min Spectrum at 2.95 min with the compound structure (A) displaying highlighted peaks at 157.08, 158.0, 159.0 and 160.08 m/z (B).

7. Ricinoleate

Ricinoleate ($C_{18}H_{33}O_3$) is another compound that was identified in the methanol extract of *L. fruticosus*. The compound has a mass spectrum found at 10.97 min (Figure 16A), with peaks highlighted at 309.13356 m/z f for the protiated compound ($M+H^+$) and 310.235, 311.2201 and 312.2263 for its isotopic species (M+1,M+2 and M+3 respectively) (Figure 16B). The compound belongs to a group of unsaturated fatty acids its molecular mass is 298.461 Da.

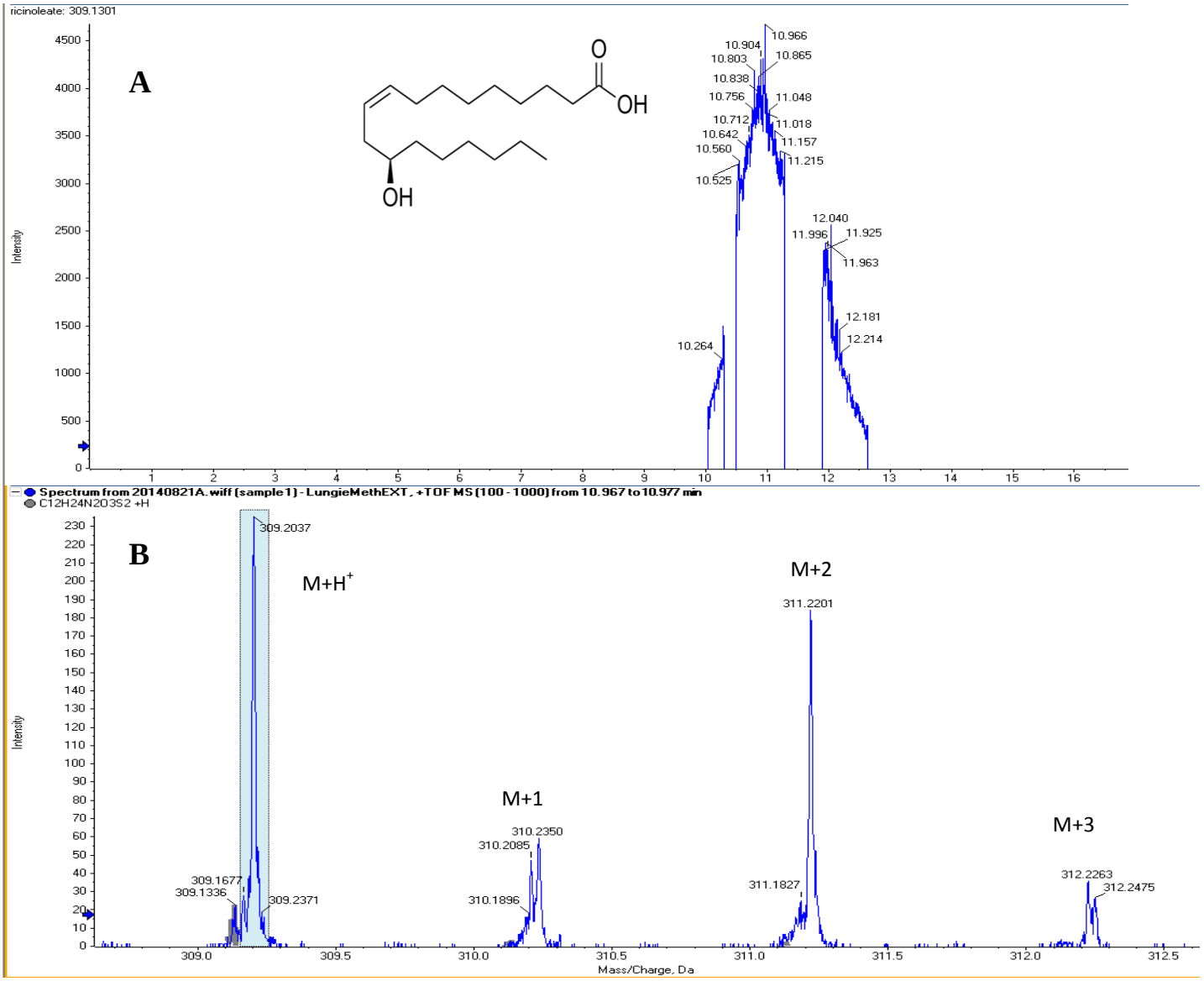

Figure 16: LC-MS chromatographic profile of Ricinoleate. Peak 309.13356 at 10.97 Spectrum at 10.97 min with the compound structure (A) displaying highlighted peaks at 309.13356 ,310.235, 311.2201 and 312.2263 m/z (B)

Table 9. **List of compound found in methanol extracts and their function**

Compound	Function	Reference
2-hydroxylamino-4,6-dinitrotoluene	Unknown	
4-hydroxycoumarin	Anti-tumour Anticancer	(Jung *et al*., 2004, Stanchev *et al*., 2008)
Sarpagine	Induce apoptosis	(Feng *et al*., 2013)
7-methylvitexin-2"-O-β-L-rhamnoside	Anti-inflammatory	(Knogge and Weissenbock, 1984, Panthong *et al*., 1994)
7-O-β-D-glucosylapigenin	Anti-inflammatory	(Arango *et al*., 2013, Panthong *et al*., 1994)
Hypoglycin B	N/A	
Ricinoleate	Anti-inflammatory	(Vieira *et al*., 2000)

3.7.2. Butanol extract profile of *Lobostemon fruticosus*

The figures below (Figures 17-25) are chromatographic profiles of compounds identified from LC-MS of the butanol extracts of *L. fruticosus* The experiment uses similar application as those described in Figure 10. The figures below (Figures 18-25) are profiles of compounds identified from LC-MS of the butanol extracts of *L. fruticosus* and were identified by their mass/charge ratio (Da) and their relative intensities from the mass spectrometry library, Mass Bank the compounds were then tabulated below (Table 10).

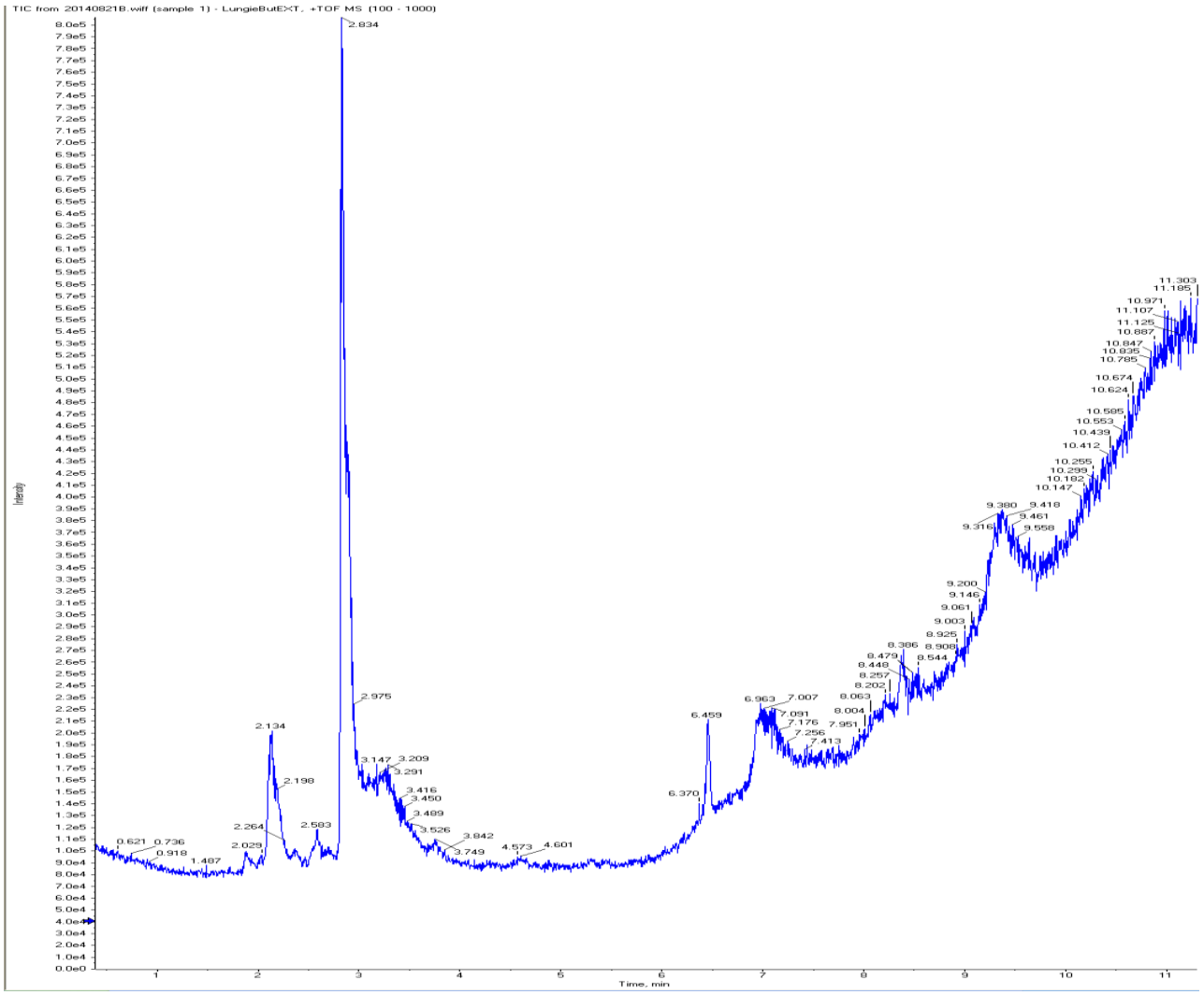

Figure 17: Non-targeted LC-MS chromatographic profiles of the butanol extracts of *Lobostemon fruticosus.*

1. Justicidin B

Justicidin ($C_{21}H_6O_6$) a compound that was identified in the butanol extract of *L. fruticosus* MassBank. The compound has a mass spectrum found at 2.11 min (Figure 18A), with peaks highlighted at 365.1048 m/z for the protiated compound ($M+H^+$) and 366.1083for its isotopic species (M+1) (Figure 18B). The compound belongs to a group of aryl naphthalene lignans and its molecular mass is 364.348 Da.

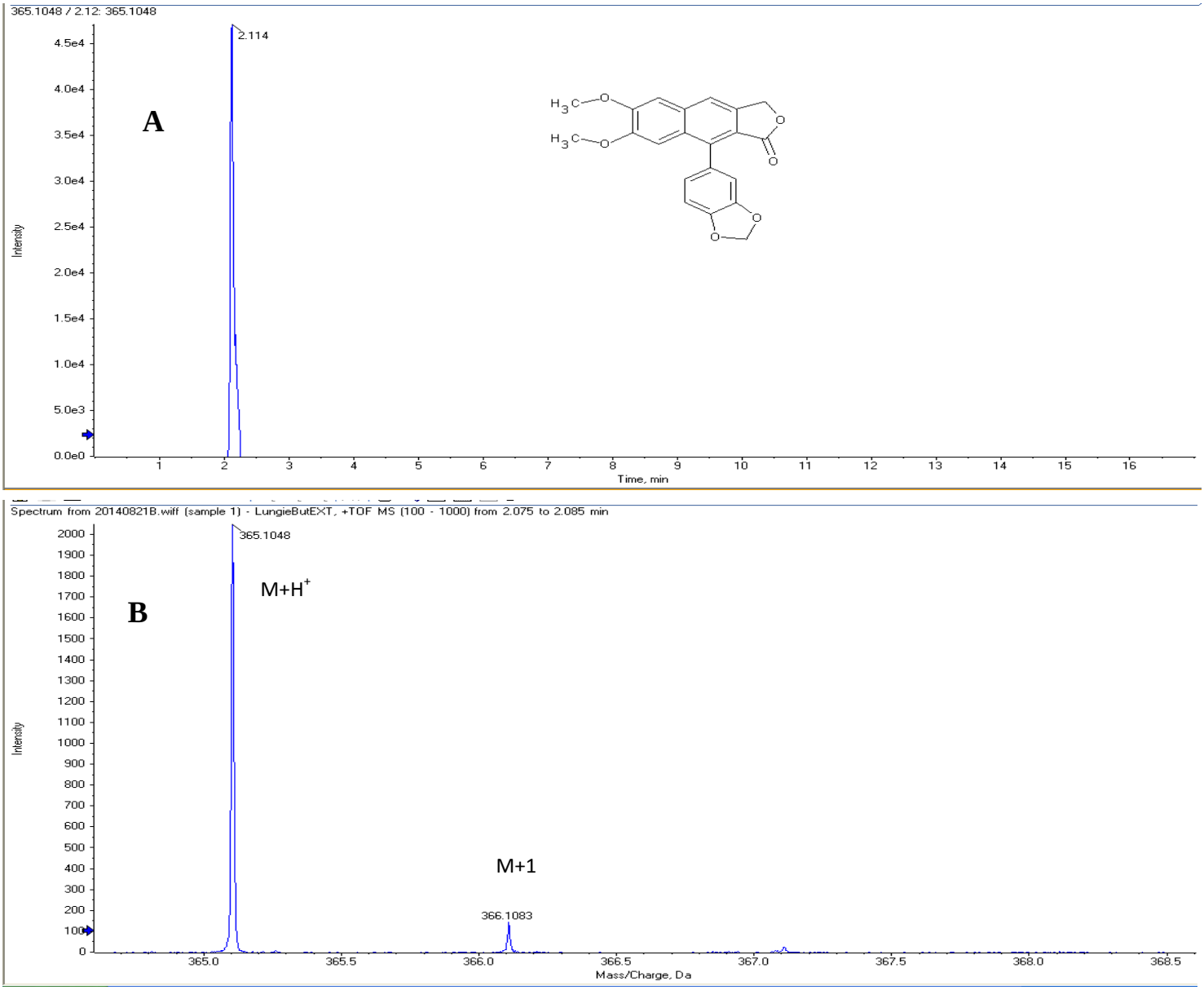

Figure 18: LC-MS chromatographic profiles of Justidin B. Spectrum at 211 min with the compound structure (A) displaying highlighted peaks at 365.1048 and 366.1083 m/z (B).

2. Tropine

Tropine ($C_8H_{15}NO$) is another compound that was identified in the butanol extract of *L. fruticosus*. The compound has a mass spectrum found at 2.14 min (Figure 19A), with peak highlighted at 142.1223 m/z f for the protiated compound ($M+H^+$) (Figure 19B). The compound belongs to a group of tropane alkaloids and its molecular mass is 141.21 Da.

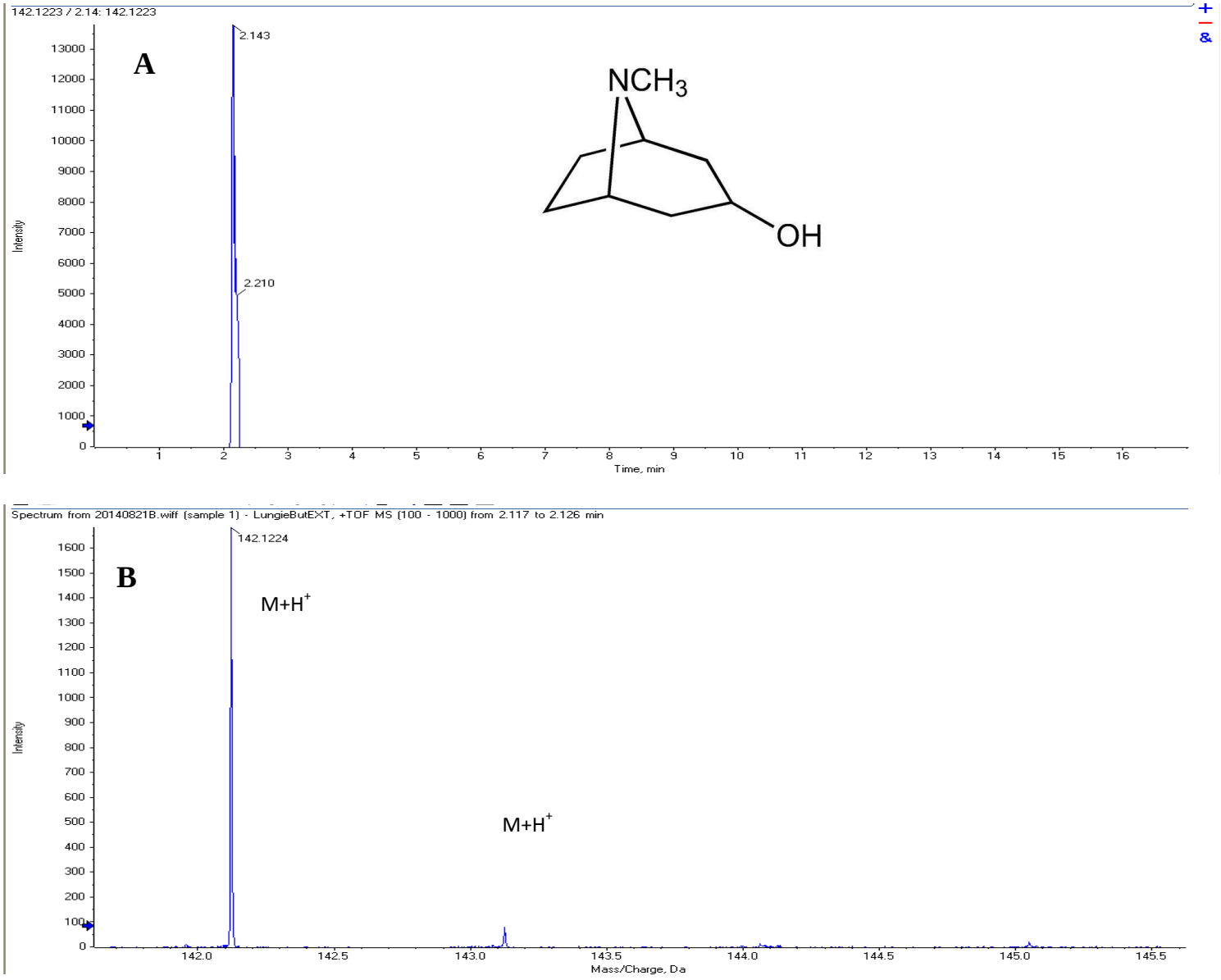

Figure 19: LC-MS chromatographic profiles of Tropine. peak 142.1223 M-1 at 2.14 min Spectrum at 2.14 min with the compound structure (A) displaying highlighted peaks at 142.1223 m/z (B).

3. Unidentified compound

The compound was isolated from the butanol extract of *L. fruticosus*. The compound has a mass spectrum found at 2.81 min (Figure 20A), with peaks highlighted at 300.1799 m/z for the protiated compound ($M+H^+$) (Figure 20B). The compound was no easily identified by the Mass bank library.

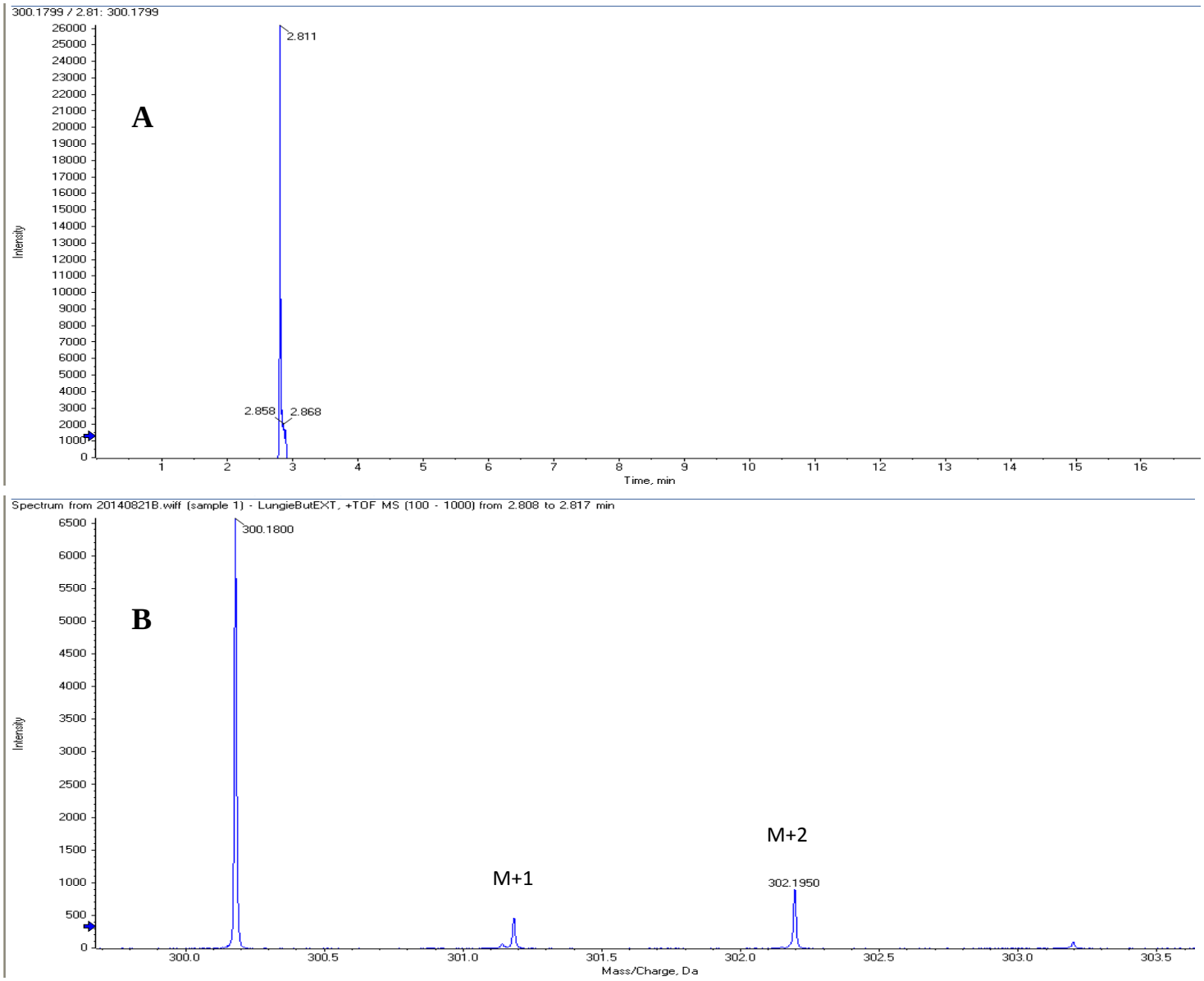

Figure 20: LC-MS chromatographic profiles unknown compound. Spectrum at 2.81 min with the compound structure (A) displaying highlighted peaks at 300.1799 m/z (B).

4. Flavocommelin

Flavocommelin ($C_{28}H_{32}O_{15)}$ was isolated from the butanol extract of *L. fruticosus*. The compound has a mass spectrum found at 2.83 min (Figure 21A), with peaks highlighted at 631.3403 m/z f for the protiated compound ($M+H^+$) and 632.3446 m/z its isotopic species (M+1) (Figure 21B). The compound belongs to a group of natural flavones of the flavonoid family and its molecular mass is 608.544 Da.

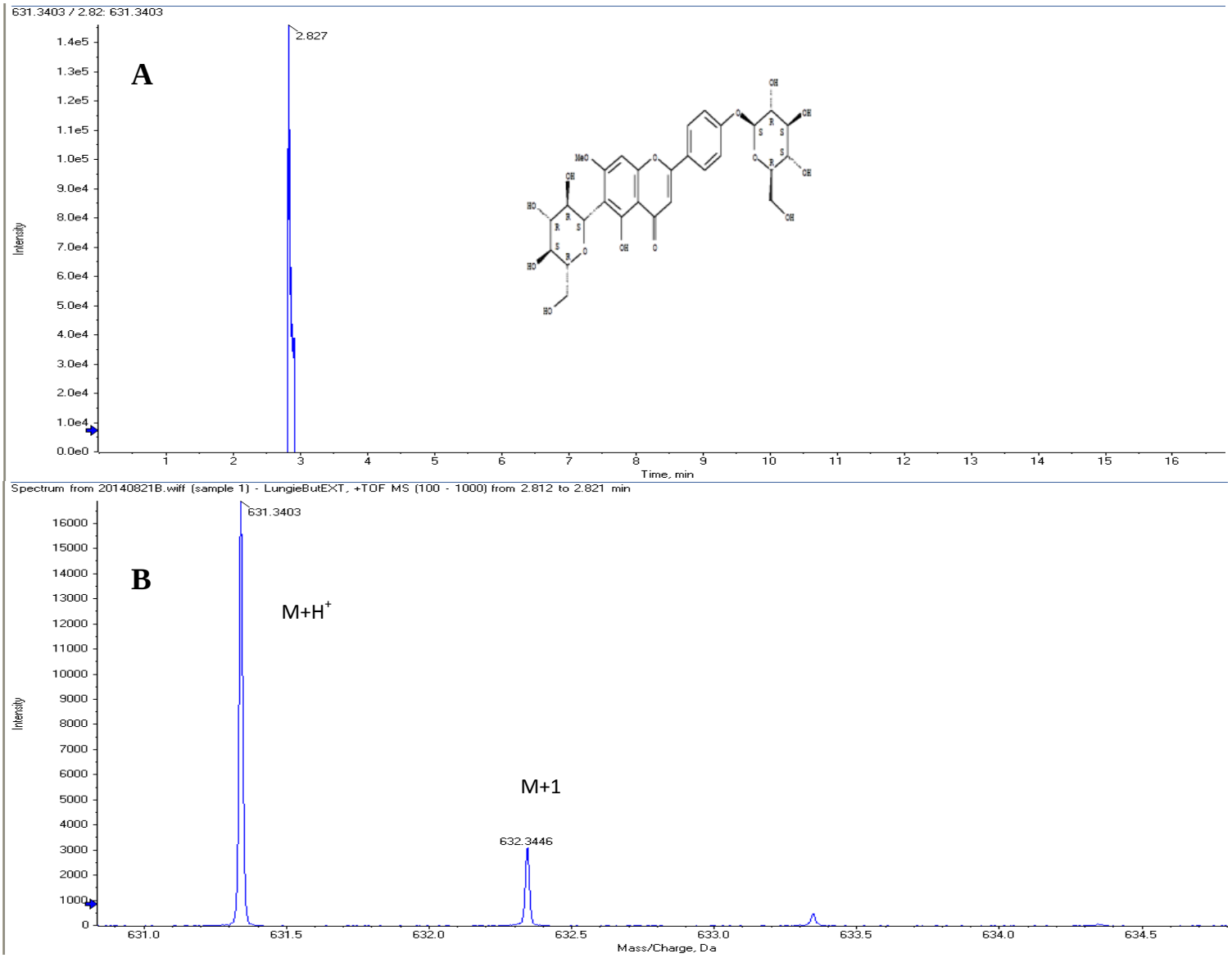

Figure 21: LC-MS chromatographic profiles Flavocommelin. Spectrum at 2.83 min with the compound structure (A) displaying highlighted peaks at 63.3403 and 3632.3446 m/z (B).

5. Fisetin

Fisetin ($C_{15}H_{10}O_6$) was isolated from the butanol extract of *L. fruticosus*. The compound has a mass spectrum found at 3.75 min (Figure 22A), with peaks highlighted at 157.083 m/z for the protiated compound ($M+H^+$) (Figure 22B). The compound belongs to a group of polyphenol flavonoids and its molecular mass is 286.236 Da.

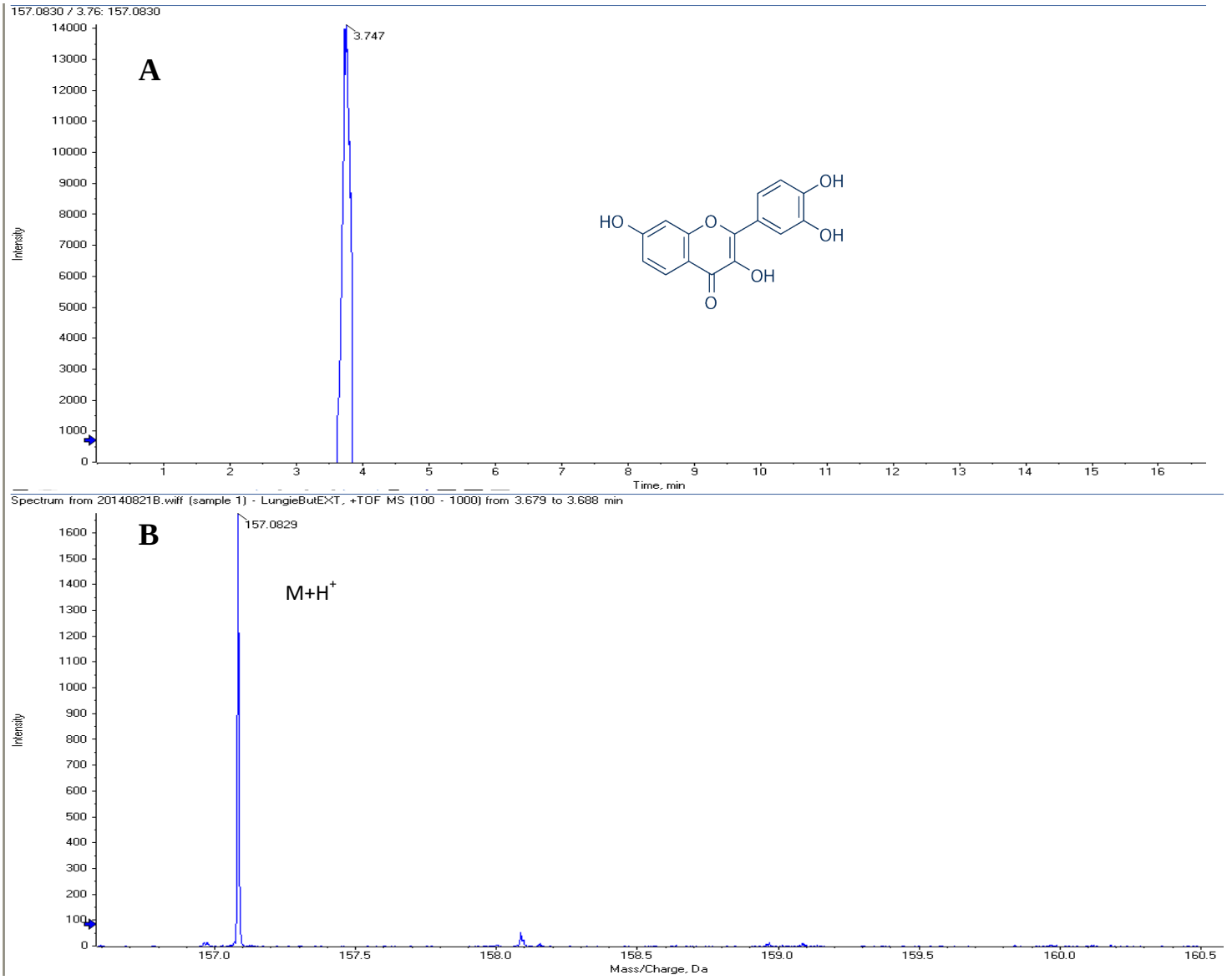

Figure 22: LC-MS chromatographic Fisetin. Spectrum at 3.75 min with the compound structure (A) displaying highlighted peaks at 157.083 m/z (B).

6. Unknown compound

The compound that was isolated from a butanol extract of *L. fruticosus*. The compound has a mass spectrum found at 8.38 min (Figure 23A), with peaks highlighted at 407.1564 m/z f for the protiated compound ($M+H^+$) and 408.1597 for its isotopic species (M+1) (Figure 23B).

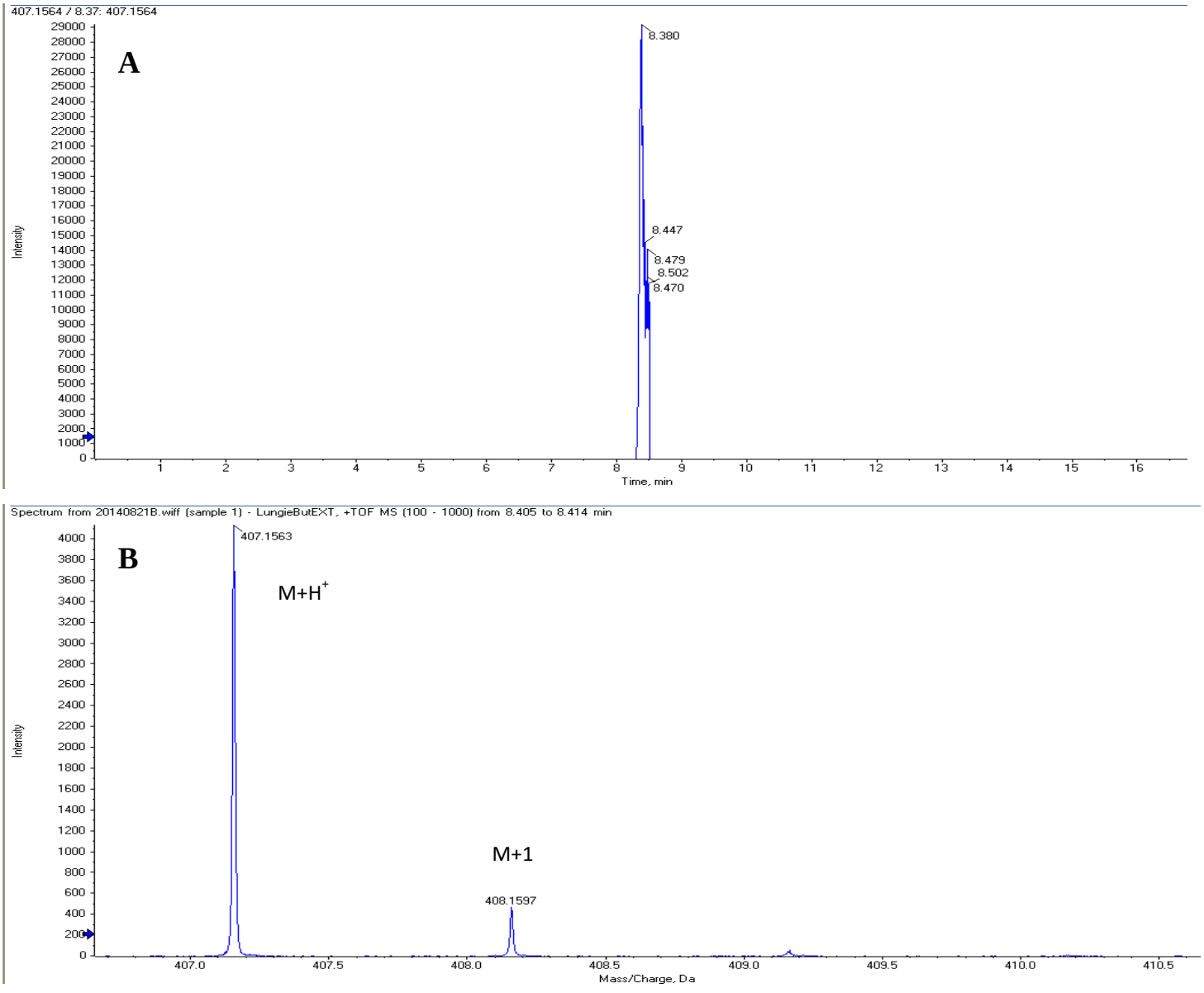

Figure 23: LC-MS chromatographic profiles unknown compound. Spectrum at 8.38 min with the compound structure (A) displaying highlighted peaks at 407.1564 and 408.1597 m/z (B).

7. Unknown

The unknown compound was isolated from the butanol extract of *L. fruticosus*. The compound has a mass spectrum found at 14.01 min (Figure 24A), with peaks highlighted at 387.1791 m/z f for the protiated compound ($M+H^+$) and 388.1826 m/z for its isotopic species (M+1) (Figure 24B).

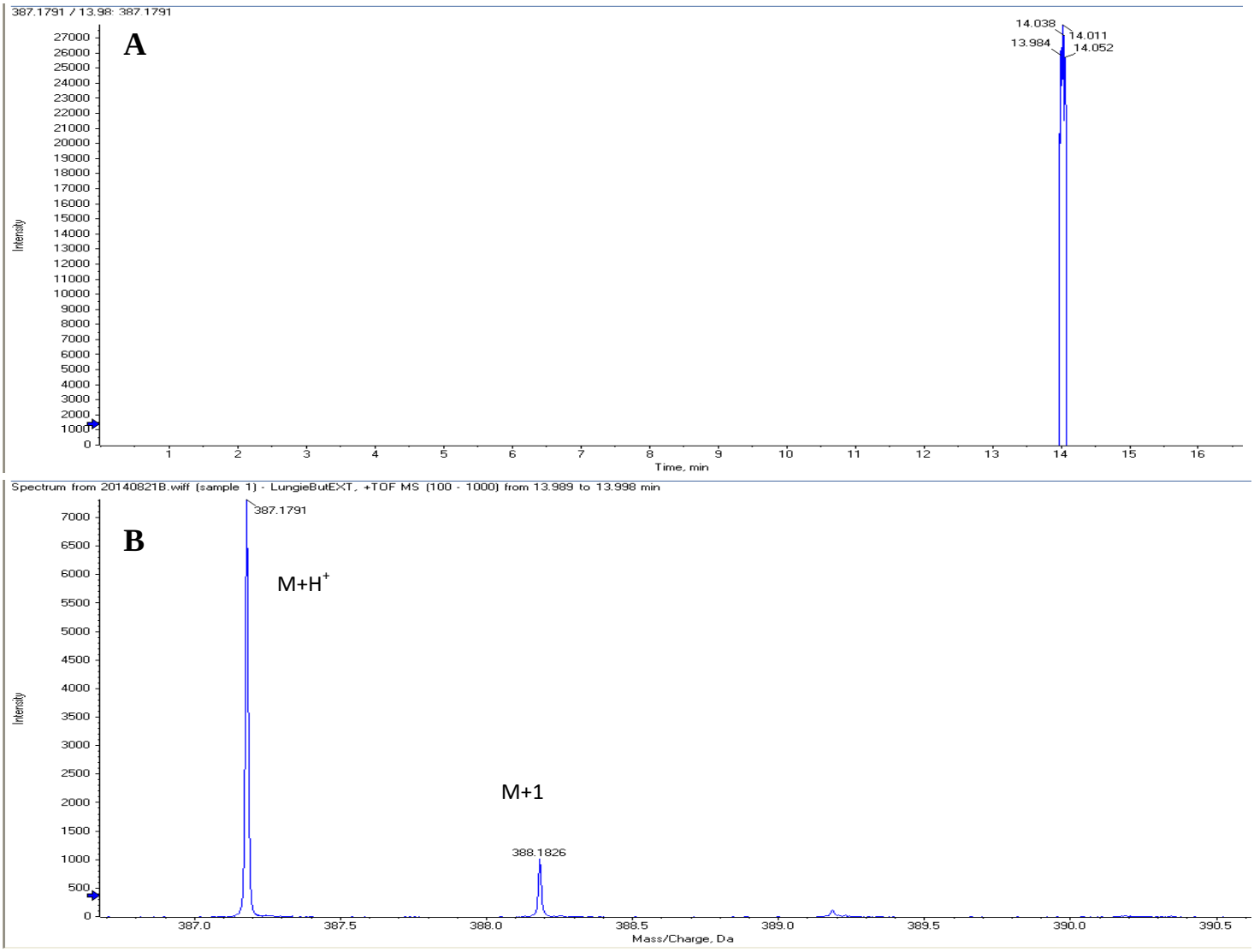

Figure24: LC-MS chromatographic profiles unknown compound. Spectrum at 14.01 min with the compound structure (A) displaying highlighted peaks at 387.179 and 388.1826 m/z (B).

8. Nodakenin

Nodakenin ($C_{20}H_{24}O_9$) was isolated from the butanol extract of *L. fruticosus*. The compound has a mass spectrum found at 14.02 min (Figure 25A), with peaks highlighted at 409.16 m/z for the protiated compound ($M+H^+$) and 410.16848 for its isotopic species (M+1) (Figure 25B). The compound belongs to the coumarin family and its molecular mass is 408.4 Da.

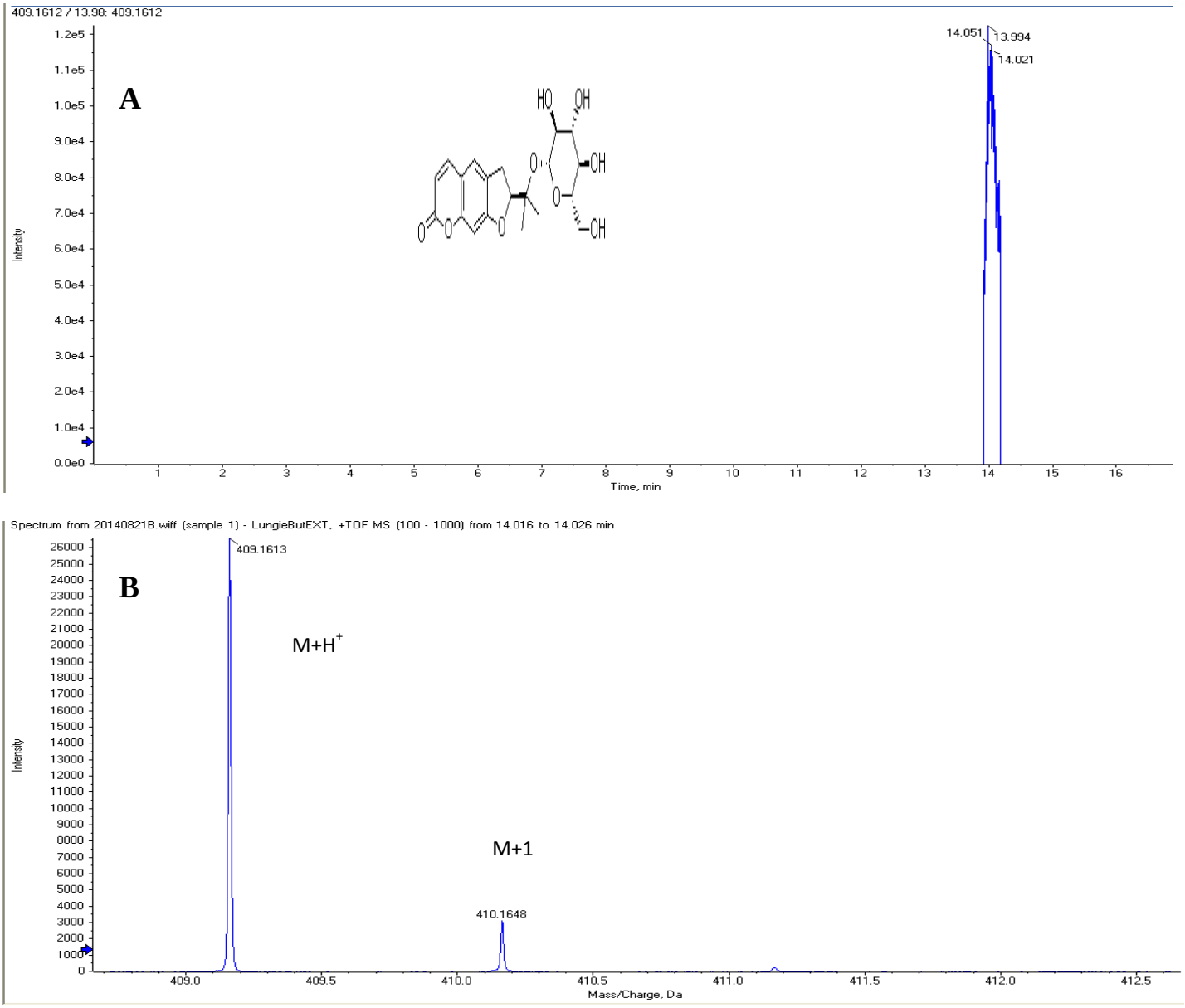

Figure 25: LC-MS chromatographic profiles nodakenin. Spectrum at 14.02 min with the compound structure (A) displaying highlighted peaks at 409.1613 and 410.1648 m/z (B).

Table 10. Structure and function of some of the compounds identified in L. *Fruticosus* through LC-MS of butanol extracts

Compound	Function	Reference
Justicidin B	Cytotoxic	(Vasilev *et al*., 2006)
Tropine	Unknown	
Unknown	Unknown	
Flavocommelin	Anti-inflammatory	(Oyama and Kondo, 2004, Panthong *et al*., 1994)
Fisetin	Anti-oxidant	(Sengupta *et al*., 2004)
Unknown	Unknown	
Unknown	Unknown	
Nodekenin	Anti-inflammatory	(Rim *et al*., 2012)

Chapter Four: Discussion and conclusion

4.1. Discussion

The focus of this study is to assess the cytotoxic effects of *Lobostemon fruticosus* on NSCLC cell line A549 and to elucidate the mode of cell death that the plant extract induces. Taxol and camptothecin were used as positive controls to compare the similarity in the method of cell death that is observed, either by cell arrest (TXL) (Scatena *et al*., 1998) or by DNA fragmentation (CPT) (Sane and Bertrand, 1998). The degree of cellular viability is measured not only by cell growth, but also by metabolic activity of the cell. Tetrazolium binds to NADH of healthy metabolic cells and it is reduced to formazan crystals during the assay (Wang *et al*., 2010). Cancer cells growing at an accelerated rate such as those in A549 are expected to result in high amounts of formazan crystals after treatment with tetrazolium salts (Wang *et al*., 2010). The experiment was set up to identify the concentration required to produce 50% cell death of cells that were treated with camptothecin, taxol and two aqueous extracts of *Lobostemon fruticosus.* The negative control, DMSO, displayed a low degree of cell death (Figure 2), thus confirming that cell death observed during the assay was not as a result of the dissolving solvent (DMSO). Camptothecin (CPT) binds to the topoisomerase I of DNA and forms a tight DNA-topoisomerase I-CPT complex, that leads to DNA breakage, thus initiating the onset of apoptosis (Hsiang *et al*., 1985). Taxol stabilises cellular microtubules, thus hindering any form of cellular functions that are important to the cell such as mitosis, cellular movement, cell cycle and spindle formation in DNA during these processes (Scatena *et al*., 1998). These two compounds were once widely used as effective chemotherapeutic drugs (Wall and Wani, 1995). *Lobostemon fruticosus* is a medicinal plant that is used in treating a vast range of ailments from treatments of skin diseases (eczema and ring worms) to treating STI (syphilis). The findings suggested that the extracts of *L. fruticosus* did display cytotoxic effects on A549 cells at relatively low concentrations,

40 µg/ml and 50 µg/ml for both methanol and butanol extracts, respectively (Figure 3). The cells treated with methanol extracts did not result in 50% cell death (cd), but could only induce 41.3% cd at 40 µg/ml. These findings seem to suggest that extracting the plant with crude methanol was not the most effective mode of extraction as opposed to those found in butanol.

The xCELLigence system is a technique that uses a variety of approaches to monitor cell viability without introducing any fixatives or poisons or invasive compounds to monitor cellular function. In the experiment the system was used in order to observe degree of cell viability at real-time. Cell adhesion and cell growth were indicative of cell viability and the data was plotted against a normalised cell index. The findings indicated that only cells treated with camptothecin displayed a significant decrease in cell viability marked by the decrease in CI. These findings did not corroborate with those of the previously conducted assay (Figure 3). During this experiment the xCELLigence system proved to be an imperfect system when monitoring the effects of *L. fruticosus* on A549 cell line, as it selectively recorded cells that were attached to the E-plates and not those that were detached.

DNA fragmentation is a spontaneous breaking down of the DNA into smaller pieces that tend to accumulate within the cell, this could be cause by external DNA stressors or induces with various laboratory techniques. The breaking down of DNA in the cell can often result in apoptosis, when no possible method of DNA repair can occur (Liu *et al.*, 1997). Thus DNA fragmentation is often used to determine degree of apoptosis in cancer studies. In the electrophoretograms (Figure 4), specific degrees of smearing in cells treated with either methanol or butanol extract were observed. DNA from CPT and TXL treated cells was relatively low which could indicate that smaller strands of DNA were lost during electrophoresis. The data seems to suggest that there was DNA fragmentation that was observed after 48 hour treatments of the A549 cells.

The AnnexinV-FITC assay measures the early onset of apoptosis by binding to exposed phosphatidylserine (PS), a phospholipid found in cell membranes. During the initial phases of apoptosis PS is translocated to the outer membrane where it can bind to Annexin-V during the assay (Bortner *et al*., 1995). Coupled with propidium iodide (PI), the assay can also measure late stages of apoptosis and other forms of cell death (Jayat and Ratinaud, 1993). The experiment was conducted to measure cell death of cells that were treated within a 24 hour period. Data indicate that the degree of apoptosis was extremely significant ($p \leq 0.001$) in TXL, methanol and butanol extracts of *L. fruticosus* (Figure 6F). CPT did display a very significant degree of apoptosis ($p \leq 0.01$) in relation to the untreated cells (Figure 6F). Most of the data seem to correlate with that observe with DNA fragmentation (Figure 5) which were denoted by smearing of gDNA-an indication of late apoptosis (Bortner *et al*., 1995, Liu *et al*., 1997, Zhang and Xu, 2000).

Propidium iodide is a stain used to bind to 4 base nucleotide of DNA thus identifying the stage that DNA is at different phases of the cell cycle (Jayat and Ratinaud, 1993). This is conducted after membrane has been permeabilised with the added fixative. RNase is coupled with the PI dye to ensure that no RNA affects DNA integrity at each phase of the cell cycle. The findings indicated a significant degree of cell cycle arrest ($p \leq 0.001$) in both camptothecin and taxol-treated cells as the cycle was inhibited at G_0/G_1 stage (Figure 7). There was, however, little evidence to suggest the same for *L. Fruticosus* extracts as most of the cells occurred in the sub-G_0 phase (Figure 7). This indicates that the extract caused a significant degree cell death during the cell cycle analysis.

This idea is also corroborated by the cell cycle analysis assay which indicated that an amount of cells treated with *L. fruticosus* after 48 h lead to cell death, even before entering the G_0/G_1 phase of cell cycle, evident by the apoptotic sub G_0/G_1 peak. This speaks to the idea that treatment with *L. fruticosus* is both dose and time-dependent. When comparing these finding

with CPT and TXL the results indicated that both the extracts of *L. fruticosus* induce apoptosis.

The findings indicate that the plant does exert induced cell death on A549 cells. The results observed from MTT- assay (Figure 3) and xCELLigence (Figure 4) indicate that the cytotoxic effects of both the plant extracts are time-dependent as cell death was below 50% after 24 hour treatment. Furthermore, the compound activity of the extracts did not take effect at the expected time. The research findings also indicated that the extracts induced late stages of apoptosis as there was evidence of the DNA degradation and large percent of the cells population being in the sub-G_0 phase, which is indicative of apoptosis (Delobel and Tesniere, 2014). The extracts of *L. fruticosus* indicate that the cytotoxic effect can be compared to that of camptothecin as there is indication of DNA degradation and most of the cells that were treated with extracts populated at the UR quadrant, which was an indication that those cells had undergone late stages of apoptosis. There is a growing interest in the cytotoxic effects of various medicinal plants and their application as chemotherapeutic treatments (Mthembu and Motadi, 2014; Assaf *et al*., 2013). This is due to the fact that plant approaches to cancer treatment are less harsh as compared to those found in current chemotherapeutic drugs (Chabner and Roberts, 2005). These findings suggest that *L. fruticosus* can be a very effective chemotherapeutic treatment of lung cancer.

Quantitative real-time polymerase chain reaction (qRT-PCR) monitors gene expression at real time. The target genes were expressed and quantified relative to the house keeping gene (GAPDH) and target genes from untreated cells. The target genes for this experiment; p53, p21, mdm-2, Bax and Bcl-2, were used to monitor the molecular pathway with-which *L. fruticosus* extracts would induce apoptosis in comparison to those of TXL and CPT. Data was extrapolated from the CP values that were computed by the Light Cycler 480™ software. The

box plots were set against an expression ratio of 1 (Figure 8 A-D). Statistical analysis was tabulated for each of the gene expression after various treatments (Tables 5-8).

The research findings demonstrated that the expression of p53 was significantly down-regulated ($p \leq 0.0001$) in all of the treatments (Figure 8, Tables 5-8). This seemed to suggest the apoptotic pathways were induced independent of the tumour suppressor gene (p53) in CPT, TXL and the *L. fruticosus* extracts. Mdm-2, a gene responsible for the ubiquitination of p53, was significantly up-regulated ($p \leq 0.0001$) in both TXL and the butanol extract of *L. fruticosus*, however, there was no significant changes in CPT and methanol extract of *L. fruticosus* ($p = 1$ and 0.834, respectively). Mdm2 is commonly up-regulated in various cancer cells (Tang *et al*., 2012; Wade *et al*., 2013); therefore, the up-regulation of mdm2 may not have been induced by any of the treatments. P21 (WAF1/CIP1), displayed a very significant up regulation ($p \leq 0.0001$) in all of the treatments of A549 cell line. The data (Table 5-8) suggested that these treatments initiated a p53 independent up-regulation of p21The findings imply that treatment of A549 cells with TXL, CPT and the extracts of *L. fruticosus* triggered cell cycle arrest, independent of p53. The finding also demonstrated a significant up-regulation of Bax ($p \leq 0.0001$) in cells that were treated with CPT, TXL and the butanol extract of *L. fruticosus* and significant down regulation in the expression on Bcl-2 in cells that were treated with CPT and both the extracts of *L. fruticosus*. These finding, therefore, speak to the idea that treatment with *L. fruticosus* extracts, of A549 cells induced an apoptotic pathway that was independent of p53.

Treating A549 cell with extracts of *L. fruticosus* and with positive controls CPT and TXL, resulted in induced Bax and p21 apoptotic pathway. Interestingly, these two genes have been vastly reported to be dependent on p53 induction (Kang and Reynolds, 2009; Michieli *et al*., 1994). There have been, however, reports of drug mediated apoptotic pathways that were p53 independent (Wang *et al*., 2004; Erdal *et al*., 2005). These reports corroborate with our

findings in that the compounds found in *L. fruticosus* could have induced a p53 independent apoptotic pathway. There have been studies that identified that the induction of p21 (WAF1/CAP1) pathway can occur in the absence of p53 (Michieli *et al*., 1994; Jeong *et al*., 2010), some of which were compound mediated (Jeong *et al*., 2010). This verifies our findings that, compounds such as those found in the *L. fruticosus* extracts can induce cell cycle arrest that is not mediated by p53. There have been various other molecule induced pathways that affect BCL-2 family (Kang and Reynolds, 2009; Abou-Nassar and Brown, 2010). These compounds inhibit Bcl-2 mRNA, directly thus in turn inducing Bax up-regulation that is p53-independent (Leone *et al*., 2003). There have been reports of natural compounds that mimic the Bcl-2 homology domain 3 (BH3) (Renault *et al*., 2014). BH3 is a domain found in pro-apoptotic proBH3 proteins of the Bcl-2 family, such as Bax and Bak (Suryani *et al*., 2014; Billard, 2013). The anti-apoptotic members of the Bcl-2 family, such as Bcl-2 and Bcl-X, prevent apoptosis by forming heterodimers with pro-apototic Bcl-2 proteins (van Delft *et al*., 2006). This heterodimer formation is achieved by binding the BH3 domain with the hydrophobic groove of the anti-apoptotic proteins (Suryani *et al*., 2014). The BH3 mimetics inhibit Bcl-2 anti-apoptotic proteins by binding to the protein's hydrophobic groove, thus resulting in a Bax dependent mitochondrial degradation pathway that leads to apoptosis (Billard, 2013). The results suggest that *L. fruticosus* extracts, CPT and TXL could have induced apoptosis through this pathway.

The method of extract identification Q-TOF LC-MS/MS is the most effective form of data analysis as it ensures that a wide range of compound identification is achieved. These include polar, non-polar, thermoliable and semi-volatile compound identification(Korfmacher, 2005). Compound identification was achieved through non-target screening of the extracts of *L. fruticosus*. Compound confidence was determined by mass accuracy, retention time and isotope pattern, this is done by matching the results with those found in the ABSciex library.

The results found using these methods are located in Appendix A and B for methanol and butanol extracts respectively. Retention time (RT) is the amount of time a compound spends in the column (Korfmacher, 2005). It is the sum of the time it takes a compound to move from the column to detector. A compound's RT will vary depending on the pressure used- as it affects flow rate of the solvent), the nature of the stationary phase (both the solvent and particle size), the exact composition of the solvent and the temperature of the column (Vipul *et al*., 2005). Most of the metabolic compounds have similar characteristics and size and tended to be identified at similar retention time. Compound confidence in both these extracts was satisfactory as displayed in the Appendix A and B.

Some of the compounds that were extracted from the plant such as hypoglycin b, a compound that inhibits the oxidation of acyl-CoA dehydrogenase and leads to a decrease in the oxidation of certain fatty acids, have had adverse effects on human health. There have been, however, studies that indicate that an addition of fatty acid reduce the effects of hypoglycin (Hassall and Reyle, 1955; Bressler *et al*., 1969). Ricinoleate is a fatty acid that was extracted from *L. fruticosus*; therefore, the presence of ricinoleate may antagonise hypoglycin b and its toxic effects. Coumarins such as 4- hydroxycoumarin (in methanol extract) and Nodakenin (in butanol extract) are a class of compounds that were first isolated in the 1820s from the tonka bean (Lacy and O'Kennedy, 2004). A vast majority of these compounds, which are found throughout the plant kingdom, have been identified to have anti-cancer proprieties, furthermore, these compounds were said to combat not only cancer activity but the effects of radiotherapy (Marshall *et al*., 1990). Interestingly, there has been a study that identified a curtain coumarin derivative (RKS262), which inhibited the progression of cell cycle analysis and induced a Bax dependent apoptotic pathway (Singh *et al*., 2011; Lopez-Gonzalez *et al*., 2004). These findings show that coumarins (such as, 4- hydroxycoumarin and nodakenin), found in both the extracts of the medicinal plant, *L. fruticosus* (Figure 11 and 25,

respectively), could have played a crucial role in the apoptotic cell death of the A549 cell line. Flavonoids such as flavocommelin, fistetin, and the glycoxyfalvones, are polyphenolic compound that are found in various plants and fruits (Panthong *et al*., 1994), which are known to have cytotoxic effect on cancer cells. Research has found that the various types of flavonoids exert a specific level of cytotoxicity on various cell lines (Kuntz *et al*., 1999). Other studies (Billard, 2014; Primikyri *et al*., 2014) have identified natural flavonoids as BH3 mimetics, which induce apoptosis. These studies confirm that the presence of certain flavonoids found in the plant extract could have brought about the p53-independent apoptotic pathway. Other compounds with cytotoxic and antioxidant characteristics are alkaloids such as tropine and sarpagines, which can be found in various plant extracts (Lu *et al*., 2012). Most of the compounds identified in both the extracts of *L. fruticosus*, have cytotoxic and anti-inflammatory effects and findings from various studies have noted that most of the compounds isolated from the medicinal plant have cytotoxic effects.

4.2. Conclusion

The up-regulation of genes in the absence of p53 suggests that treatments induce apoptosis using an alternative apoptotic pathway. The experimental findings described above have shown that the natural plant compounds of *Lobostemon fruticosus*, induces cell death in A549 cells. The plant extracts induced a p53-independent apoptotic mechanism, which was mediated by Bax and p21. In these findings the mode of cell death induced by the plant was compared to those of taxol and camptothecin, in order to elucidate how the extracts affected A549 cells. The results indicated that there was very little difference in the effects of TXL and CPT and therefore, the extracts of *L. fruticosus* were similar to both controls. The results suggest that the compounds extracted from *L. fruticosus* could exert the same mode of action as the BH3 mimetics. Most cancer cells have mutated p53 genes; this could result in chemotherapeutic drug resistance toward drugs/compounds that induce a p53 dependent

apoptotic pathway. The compounds that induce p53-independent apoptotic pathways would be very usefully as target therapeutic drugs in treating cancer cells. For future study it would be imperative to study the direct effect of the isolated compounds of *L. fruticosus* on lung cancer cells to observe their cytotoxic activity at a molecular level. Furthermore, it would be interesting to study the effects of *L. fruticosus* extracts on a normal cell line (MRC-5).

Chapter Five: References

ABOU-NASSAR, K. & BROWN, J. R. 2010. Novel agents for the treatment of chronic lymphocytic leukemia. *Clin Adv Hematol Oncol,* 8**,** 886-95.

ALBERG, A. J. & SAMET, J. M. 2003. Epidemiology of lung cancer. *Chest,* 123**,** 21S-49S.

AMES, B. N. 1983. Dietary carcinogens and anticarcinogens. Oxygen radicals and degenerative diseases. *Science,* 221**,** 1256-64.

AMES, B. N. & GOLD, L. S. 1990. Dietary carcinogens, environmental pollution, and cancer: some misconceptions. *Med Oncol Tumor Pharmacother,* 7**,** 69-85.

AMIRA, S., DADE, M., SCHINELLA, G. & RIOS, J. L. 2012. Anti-inflammatory, anti-oxidant, and apoptotic activities of four plant species used in folk medicine in the Mediterranean basin. *Pak J Pharm Sci,* 25**,** 65-72.

ARANGO, D., MOROHASHI, K., YILMAZ, A., KURAMOCHI, K., PARIHAR, A., BRAHIMAJ, B., GROTEWOLD, E. & DOSEFF, A. I. 2013. Molecular basis for the action of a dietary flavonoid revealed by the comprehensive identification of apigenin human targets. *Proc Natl Acad Sci U S A,* 110**,** E2153-62.

ARAP, W., PASQUALINI, R. & RUOSLAHTI, E. 1998. Cancer treatment by targeted drug delivery to tumor vasculature in a mouse model. *Science,* 279**,** 377-80.

ASSAF, A. M., HADDADIN, R. N., ALDOURI, N. A., ALABBASSI, R., MASHALLAH, S., MOHAMMAD, M. & BUSTANJI, Y. 2013. Anti-cancer, anti-inflammatory and anti-microbial activities of plant extracts used against hematological tumors in traditional medicine of Jordan. *J Ethnopharmacol,* 145**,** 728-36.

BASNAKIAN, A. G. & JAMES, S. J. 1994. A rapid and sensitive assay for the detection of DNA fragmentation during early phases of apoptosis. *Nucleic Acids Res,* 22**,** 2714-5.

BAUD, V. & KARIN, M. 2001. Signal transduction by tumor necrosis factor and its relatives. *Trends Cell Biol,* 11**,** 372-7.

BENLLOCH, S., GALBIS-CARAVAJAL, J. M., ALENDA, C., PEIRO, F. M., SANCHEZ-RONCO, M., RODRIGUEZ-PANIAGUA, J. M., BASCHWITZ, B., ROJAS, E. & MASSUTI, B. 2009. Expression of molecular markers in mediastinal nodes from resected stage I non-small-cell lung cancer (NSCLC): prognostic impact and potential role as markers of occult micrometastases. *Ann Oncol,* 20**,** 91-7.

BILLARD, C. 2013. BH3 mimetics: status of the field and new developments. *Mol Cancer Ther,* 12**,** 1691-700.

BILLARD, C. 2014. Apoptosis inducers in chronic lymphocytic leukemia. *Oncotarget,* 5**,** 309-25.

BORTNER, C. D., OLDENBURG, N. B. & CIDLOWSKI, J. A. 1995. The role of DNA fragmentation in apoptosis. *Trends Cell Biol,* 5**,** 21-6.

BRESSLER, R., CORREDOR, C. & BRENDEL, K. 1969. Hypoglycin and hypoglycin-like compounds. *Pharmacol Rev,* 21**,** 105-30.

BURGMANN, H., WIDMER, F., SIGLER, W. V. & ZEYER, J. 2003. mRNA extraction and reverse transcription-PCR protocol for detection of nifH gene expression by Azotobacter vinelandii in soil. *Appl Environ Microbiol,* 69**,** 1928-35.

BURRIS, H. A., 3RD 2009. Shortcomings of current therapies for non-small-cell lung cancer: unmet medical needs. *Oncogene,* 28 Suppl 1**,** S4-13.

BUSTIN, S. A., BENES, V., NOLAN, T. & PFAFFL, M. W. 2005. Quantitative real-time RT-PCR--a perspective. *J Mol Endocrinol,* 34**,** 597-601.

CAI, Y., LUO, Q., SUN, M. & CORKE, H. 2004. Antioxidant activity and phenolic compounds of 112 traditional Chinese medicinal plants associated with anticancer. *Life Sci,* 74**,** 2157-84.

CAMPBELL, N. A., REECE, J. B. & URRY, L. 2005. *Biology,* San Francisco, Calif. ; London, Pearson Benjamin Cummings.

CHABNER, B. A. & ROBERTS, T. G., JR. 2005. Timeline: Chemotherapy and the war on cancer. *Nat Rev Cancer,* 5**,** 65-72.

CUI, X. R., SAITO, R., KUBO, T., KON, D., HIRANO, Y. & SAITO, S. 2011. Preparations of anthraquinone and naphthoquinone derivatives and their cytotoxic effects. *Chem Pharm Bull (Tokyo),* 59**,** 302-14.

DELOBEL, P. & TESNIERE, C. 2014. A simple FCM method to avoid misinterpretation in Saccharomyces cerevisiae cell cycle assessment between G0 and sub-G1. *PLoS One,* 9**,** e84645.

DESAI, A. G., QAZI, G. N., GANJU, R. K., EL-TAMER, M., SINGH, J., SAXENA, A. K., BEDI, Y. S., TANEJA, S. C. & BHAT, H. K. 2008. Medicinal plants and cancer chemoprevention. *Curr Drug Metab,* 9**,** 581-91.

ENGELS, E. A. 2008. Inflammation in the development of lung cancer: epidemiological evidence. *Expert Rev Anticancer Ther,* 8**,** 605-15.

ERDAL, H., BERNDTSSON, M., CASTRO, J., BRUNK, U., SHOSHAN, M. C. & LINDER, S. 2005. Induction of lysosomal membrane permeabilization by compounds that activate p53-independent apoptosis. *Proc Natl Acad Sci U S A,* 102**,** 192-7.

ERENPREISA, J. & CRAGG, M. S. 2007. Cancer: a matter of life cycle? *Cell Biol Int,* 31**,** 1507-10.

ETTINGER, D. S., AKERLEY, W., BEPLER, G., BLUM, M. G., CHANG, A., CHENEY, R. T., CHIRIEAC, L. R., D'AMICO, T. A., DEMMY, T. L., GANTI, A. K., GOVINDAN, R., GRANNIS, F. W., JR., JAHAN, T., JAHANZEB, M., JOHNSON, D. H., KESSINGER, A., KOMAKI, R., KONG, F. M., KRIS, M. G., KRUG, L. M., LE, Q. T., LENNES, I. T., MARTINS, R., O'MALLEY, J., OSAROGIAGBON, R. U., OTTERSON, G. A., PATEL, J. D., PISTERS, K. M., RECKAMP, K., RIELY, G.

J., ROHREN, E., SIMON, G. R., SWANSON, S. J., WOOD, D. E. & YANG, S. C. 2010. Non-small cell lung cancer. *J Natl Compr Canc Netw,* 8**,** 740-801.

FABRICANT, D. S. & FARNSWORTH, N. R. 2001. The value of plants used in traditional medicine for drug discovery. *Environ Health Perspect,* 109 Suppl 1**,** 69-75.

FAVALORO, B., ALLOCATI, N., GRAZIANO, V., DI ILIO, C. & DE LAURENZI, V. 2012. Role of apoptosis in disease. *Aging (Albany NY),* 4**,** 330-49.

FENG, L., CHEN, Y., YUAN, L., LIU, X., GU, J. F., ZHANG, M. H. & WANG, Y. 2013. A combination of alkaloids and triterpenes of Alstonia scholaris (Linn.) R. Br. leaves enhances immunomodulatory activity in C57BL/6 mice and induces apoptosis in the A549 cell line. *Molecules,* 18**,** 13920-39.

FULDA, S. & DEBATIN, K. M. 2004. Targeting apoptosis pathways in cancer therapy. *Curr Cancer Drug Targets,* 4**,** 569-76.

GREENBLATT, M. S., BENNETT, W. P., HOLLSTEIN, M. & HARRIS, C. C. 1994. Mutations in the p53 tumor suppressor gene: clues to cancer etiology and molecular pathogenesis. *Cancer Res,* 54**,** 4855-78.

GROENEWALD, P., VOS, T., NORMAN, R., LAUBSCHER, R., VAN WALBEEK, C., SALOOJEE, Y., SITAS, F. & BRADSHAW, D. 2007. Estimating the burden of disease attributable to smoking in South Africa in 2000. *S Afr Med J,* 97**,** 674-81.

GROSS, A., MCDONNELL, J. M. & KORSMEYER, S. J. 1999. BCL-2 family members and the mitochondria in apoptosis. *Genes Dev,* 13**,** 1899-911.

HACKER, G. 2000. The morphology of apoptosis. *Cell Tissue Res,* 301**,** 5-17.

HALLIWELL, B. & CROSS, C. E. 1994. Oxygen-derived species: their relation to human disease and environmental stress. *Environ Health Perspect,* 102 Suppl 10**,** 5-12.

HARTWELL, L. H. & KASTAN, M. B. 1994. Cell cycle control and cancer. *Science,* 266**,** 1821-8.

HARTWELL, L. H. & WEINERT, T. A. 1989. Checkpoints: controls that ensure the order of cell cycle events. *Science,* 246**,** 629-34.

HASSALL, C. H. & REYLE, K. 1955. Hypoglycin A and B, two biologically active polypeptides from Blighia sapida. *Biochem J,* 60**,** 334-9.

HENDERSON, B. E. & FEIGELSON, H. S. 2000. Hormonal carcinogenesis. *Carcinogenesis,* 21**,** 427-33.

HILGER, H. H. & U. R. BÖHLE (2000) *Pontechium:* a new genus distincri from *Echium* and *Lobostemon* (Boraginaceae). *Taxon,* 49**,** 737-46.

HSIANG, Y. H., HERTZBERG, R., HECHT, S. & LIU, L. F. 1985. Camptothecin induces protein-linked DNA breaks via mammalian DNA topoisomerase I. *J Biol Chem,* 260**,** 14873-8.

HUANG, H. J., YEE, J. K., SHEW, J. Y., CHEN, P. L., BOOKSTEIN, R., FRIEDMANN, T., LEE, E. Y. & LEE, W. H. 1988. Suppression of the neoplastic phenotype by replacement of the RB gene in human cancer cells. *Science,* 242**,** 1563-6.

HUANG, W. & ZOU, K. 2011. Cytotoxicity of a plant steroidal saponin on human lung cancer cells. *Asian Pac J Cancer Prev,* 12**,** 513-7.

JASSEM, J. 2007. The role of radiotherapy in lung cancer: where is the evidence? *Radiother Oncol,* 83**,** 203-13.

JAYAT, C. & RATINAUD, M. H. 1993. Cell cycle analysis by flow cytometry: principles and applications. *Biol Cell,* 78**,** 15-25.

JEONG, J. H., KANG, S. S., PARK, K. K., CHANG, H. W., MAGAE, J. & CHANG, Y. C. 2010. p53-independent induction of G1 arrest and p21WAF1/CIP1 expression by ascofuranone, an isoprenoid antibiotic, through downregulation of c-Myc. *Mol Cancer Ther,* 9**,** 2102-13.

JUNG, J. C., LEE, J. H., OH, S., LEE, J. G. & PARK, O. S. 2004. Synthesis and antitumor activity of 4-hydroxycoumarin derivatives. *Bioorg Med Chem Lett,* 14**,** 5527-31.

KANG, M. H. & REYNOLDS, C. P. 2009. Bcl-2 inhibitors: targeting mitochondrial apoptotic pathways in cancer therapy. *Clin Cancer Res,* 15**,** 1126-32.

KASTAN, M. B., CANMAN, C. E. & LEONARD, C. J. 1995. P53, cell cycle control and apoptosis: implications for cancer. *Cancer Metastasis Rev,* 14**,** 3-15.

KELLERMANN, G., SHAW, C. R. & LUYTEN-KELLERMAN, M. 1973. Aryl hydrocarbon hydroxylase inducibility and bronchogenic carcinoma. *N Engl J Med,* 289**,** 934-7.

KELLY, K., CROWLEY, J., BUNN, P. A., JR., PRESANT, C. A., GREVSTAD, P. K., MOINPOUR, C. M., RAMSEY, S. D., WOZNIAK, A. J., WEISS, G. R., MOORE, D. F., ISRAEL, V. K., LIVINGSTON, R. B. & GANDARA, D. R. 2001. Randomized phase III trial of paclitaxel plus carboplatin versus vinorelbine plus cisplatin in the treatment of patients with advanced non--small-cell lung cancer: a Southwest Oncology Group trial. *J Clin Oncol,* 19**,** 3210-8.

KERR, J. F., WINTERFORD, C. M. & HARMON, B. V. 1994. Apoptosis. Its significance in cancer and cancer therapy. *Cancer,* 73**,** 2013-26.

KLASTERSKY, J. & AWADA, A. 2012. Milestones in the use of chemotherapy for the management of non-small cell lung cancer (NSCLC). *Crit Rev Oncol Hematol,* 81**,** 49-57.

KNOGGE, W. & WEISSENBOCK, G. 1984. Purification, characterization, and kinetic mechanism of S-adenosyl-L-methionine: vitexin 2"-O-rhamnoside 7-O-methyltransferase of Avena sativa L. *Eur J Biochem,* 140**,** 113-8.

KOMAROVA, E. A., CHRISTOV, K., FAERMAN, A. I. & GUDKOV, A. V. 2000. Different impact of p53 and p21 on the radiation response of mouse tissues. *Oncogene,* 19**,** 3791-8.

KORFMACHER, W. A. 2005. Principles and applications of LC-MS in new drug discovery. *Drug Discov Today,* 10**,** 1357-67.

KORSMEYER, S. J. 1999. BCL-2 gene family and the regulation of programmed cell death. *Cancer Res,* 59**,** 1693s-1700s.

KROEMER, G. 1999. Mitochondrial control of apoptosis: an overview. *Biochem Soc Symp,* 66**,** 1-15.

KUNTZ, S., WENZEL, U. & DANIEL, H. 1999. Comparative analysis of the effects of flavonoids on proliferation, cytotoxicity, and apoptosis in human colon cancer cell lines. *Eur J Nutr,* 38**,** 133-42.

LACY, A. & O'KENNEDY, R. 2004. Studies on coumarins and coumarin-related compounds to determine their therapeutic role in the treatment of cancer. *Curr Pharm Des,* 10**,** 3797-811.

LAM, W. K., WHITE, N. W. & CHAN-YEUNG, M. M. 2004. Lung cancer epidemiology and risk factors in Asia and Africa. *Int J Tuberc Lung Dis,* 8**,** 1045-57.

LEMMA, A. 1971. Present status of endod as a molluscicide for the control of schistosomiasis. *Ethiop Med J,* 9**,** 113-8.

LENGAUER, C., KINZLER, K. W. & VOGELSTEIN, B. 1998. Genetic instabilities in human cancers. *Nature,* 396**,** 643-9.

LEONE, M., ZHAI, D., SARETH, S., KITADA, S., REED, J. C. & PELLECCHIA, M. 2003. Cancer prevention by tea polyphenols is linked to their direct inhibition of antiapoptotic Bcl-2-family proteins. *Cancer Res,* 63**,** 8118-21.

LEVYNS, M. R. 1934 A revision of *Lobostemon* Lehm. and a discussion of the species problem. *Journ Linnean Soc Botany,* 49**,** 393-445.

LIU, X., ZOU, H., SLAUGHTER, C. & WANG, X. 1997. DFF, a heterodimeric protein that functions downstream of caspase-3 to trigger DNA fragmentation during apoptosis. *Cell,* 89**,** 175-84.

LOPEZ-GONZALEZ, J. S., PRADO-GARCIA, H., AGUILAR-CAZARES, D., MOLINA-GUARNEROS, J. A., MORALES-FUENTES, J. & MANDOKI, J. J. 2004. Apoptosis and cell cycle disturbances induced by coumarin and 7-hydroxycoumarin on human lung carcinoma cell lines. *Lung Cancer,* 43**,** 275-83.

LU, J. J., BAO, J. L., CHEN, X. P., HUANG, M. & WANG, Y. T. 2012. Alkaloids isolated from natural herbs as the anticancer agents. *Evid Based Complement Alternat Med,* 2012**,** 485042.

MANDY, F. F., BERGERON, M. & MINKUS, T. 1995. Principles of flow cytometry. *Transfus Sci,* 16**,** 303-14.

MARSHALL, M. E., BUTLER, K. & HERMANSEN, D. 1990. Treatment of hormone-refractory stage D carcinoma of prostate with coumarin (1,2-benzopyrone) and cimetidine: a pilot study. *Prostate,* 17**,** 95-9.

MATHEWS, C. K., VAN HOLDE, K. E. & AHERN, K. G. 2000. *Biochemistry,* San Francisco, Calif. ; Harlow, Benjamin Cummings.

MENG, X., ZHONG, J., LIU, S., MURRAY, M. & GONZALEZ-ANGULO, A. M. 2012. A new hypothesis for the cancer mechanism. *Cancer Metastasis Rev,* 31**,** 247-68.

MICHIELI, P., CHEDID, M., LIN, D., PIERCE, J. H., MERCER, W. E. & GIVOL, D. 1994. Induction of WAF1/CIP1 by a p53-independent pathway. *Cancer Res,* 54**,** 3391-5.

MOSMANN, T. 1983. Rapid colorimetric assay for cellular growth and survival: application to proliferation and cytotoxicity assays. *J Immunol Methods,* 65**,** 55-63.

MTHEMBU, N. N. & MOTADI, L. R. 2014. Apoptotic potential role of Agave palmeri and Tulbaghia violacea extracts in cervical cancer cells. *Mol Biol Rep,* 41**,** 6143-55.

MZILENI, O., SITAS, F., STEYN, K., CARRARA, H. & BEKKER, P. 1999. Lung cancer, tobacco, and environmental factors in the African population of the Northern Province, South Africa. *Tob Control,* 8**,** 398-401.

NANJI, A. A. & HILLER-STURMHOFEL, S. 1997. Apoptosis and necrosis: two types of cell death in alcoholic liver disease. *Alcohol Health Res World,* 21**,** 325-30.

OYAMA, K. & KONDO, T. 2004. Total synthesis of flavocommelin, a component of the blue supramolecular pigment from Commelina communis, on the basis of direct 6-C-glycosylation of flavan. *J Org Chem,* 69**,** 5240-6.

PANTHONG, A., KANJANAPOTHI, D., TUNTIWACHWUTTIKUL, P., PANCHAROEN, O. & REUTRAKUL, V. 1994. Antiinflammatory activity of flavonoids. *Phytomedicine,* 1**,** 141-4.

PARKIN, D. M. & MOSS, S. M. 2000. Lung cancer screening: improved survival but no reduction in deaths--the role of "overdiagnosis". *Cancer,* 89**,** 2369-76.

PRIMIKYRI, A., CHATZIATHANASIADOU, M. V., KARALI, E., KOSTARAS, E., MANTZARIS, M. D., HATZIMICHAEL, E., SHIN, J. S., CHI, S. W., BRIASOULIS, E., KOLETTAS, E., GEROTHANASSIS, I. P. & TZAKOS, A. G. 2014. Direct Binding of Bcl-2 Family Proteins by Quercetin Triggers Its Pro-Apoptotic Activity. *ACS Chem Biol*.

RAHMATULLAH, M. & BISWAS, K. R. 2012. Traditional medicinal practices of a Sardar healer of the Sardar (Dhangor) community of Bangladesh. *J Altern Complement Med,* 18**,** 10-9.

RENAULT, T. T., ELKHOLI, R., BHARTI, A. & CHIPUK, J. E. 2014. B cell lymphoma-2 (BCL-2) homology domain 3 (BH3) mimetics demonstrate differential activities

dependent upon the functional repertoire of pro- and anti-apoptotic BCL-2 family proteins. *J Biol Chem,* 289**,** 26481-91.

RIM, H. K., CHO, W., SUNG, S. H. & LEE, K. T. 2012. Nodakenin suppresses lipopolysaccharide-induced inflammatory responses in macrophage cells by inhibiting tumor necrosis factor receptor-associated factor 6 and nuclear factor-kappaB pathways and protects mice from lethal endotoxin shock. *J Pharmacol Exp Ther,* 342**,** 654-64.

RYAN, K. M., PHILLIPS, A. C. & VOUSDEN, K. H. 2001. Regulation and function of the p53 tumor suppressor protein. *Curr Opin Cell Biol,* 13**,** 332-7.

SAGER, R. 1989. Tumor suppressor genes: the puzzle and the promise. *Science,* 246**,** 1406-12.

SANE, A. T. & BERTRAND, R. 1998. Distinct steps in DNA fragmentation pathway during camptothecin-induced apoptosis involved caspase-, benzyloxycarbonyl- and N-tosyl-L-phenylalanylchloromethyl ketone-sensitive activities. *Cancer Res,* 58**,** 3066-72.

SCATENA, C. D., STEWART, Z. A., MAYS, D., TANG, L. J., KEEFER, C. J., LEACH, S. D. & PIETENPOL, J. A. 1998. Mitotic phosphorylation of Bcl-2 during normal cell cycle progression and Taxol-induced growth arrest. *J Biol Chem,* 273**,** 30777-84.

SECHLER, M., CIZMIC, A. D., AVASARALA, S., VAN SCOYK, M., BRZEZINSKI, C., KELLEY, N., BIKKAVILLI, R. K. & WINN, R. A. 2013. Non-small-cell lung cancer: molecular targeted therapy and personalized medicine - drug resistance, mechanisms, and strategies. *Pharmgenomics Pers Med,* 6**,** 25-36.

SENGUPTA, B., BANERJEE. A & SENGUPTA, P. K. 2004 Investigations on the binding and antioxidant propertiesof the plant flavonoid fisetin in model biomembranes. *FEBS Letters* ,570**,** 77–81.

SHERR, C. J. 1996. Cancer cell cycles. *Science,* 274**,** 1672-7.

SHIPLEY, W. U., THAMES, H. D., SANDLER, H. M., HANKS, G. E., ZIETMAN, A. L., PEREZ, C. A., KUBAN, D. A., HANCOCK, S. L. & SMITH, C. D. 1999. Radiation therapy for clinically localized prostate cancer: a multi-institutional pooled analysis. *JAMA,* 281**,** 1598-604.

SIGAL, A. & ROTTER, V. 2000. Oncogenic mutations of the p53 tumor suppressor: the demons of the guardian of the genome. *Cancer Res,* 60**,** 6788-93.

SINGH, R. K., LANGE, T. S., KIM, K. K. & BRARD, L. 2011. A coumarin derivative (RKS262) inhibits cell-cycle progression, causes pro-apoptotic signaling and cytotoxicity in ovarian cancer cells. *Invest New Drugs,* 29**,** 63-72.

SITAS, F., URBAN, M., BRADSHAW, D., KIELKOWSKI, D., BAH, S. & PETO, R. 2004. Tobacco attributable deaths in South Africa. *Tob Control,* 13**,** 396-9.

STANCHEV, S., MOMEKOV, G., JENSEN, F. & MANOLOV, I. 2008. Synthesis, computational study and cytotoxic activity of new 4-hydroxycoumarin derivatives. *Eur J Med Chem,* 43**,** 694-706.

SURYANI, S., CAROL, H., CHONGHAILE, T. N., FRISMANTAS, V., SARMAH, C., HIGH, L., BORNHAUSER, B., COWLEY, M. J., SZYMANSKA, B., EVANS, K., BOEHM, I., TONNA, E., JONES, L., MANESH, D. M., KURMASHEVA, R. T., BILLUPS, C., KAPLAN, W., LETAI, A., BOURQUIN, J. P., HOUGHTON, P. J., SMITH, M. A. & LOCK, R. B. 2014. Cell and molecular determinants of in vivo efficacy of the BH3 mimetic ABT-263 against pediatric acute lymphoblastic leukemia xenografts. *Clin Cancer Res,* 20**,** 4520-31.

TANG, Y. A., LIN, R. K., TSAI, Y. T., HSU, H. S., YANG, Y. C., CHEN, C. Y. & WANG, Y. C. 2012. MDM2 overexpression deregulates the transcriptional control of RB/E2F leading to DNA methyltransferase 3A overexpression in lung cancer. *Clin Cancer Res,* 18**,** 4325-33.

TAPSELL, L. C., HEMPHILL, I., COBIAC, L., PATCH, C. S., SULLIVAN, D. R., FENECH, M., ROODENRYS, S., KEOGH, J. B., CLIFTON, P. M., WILLIAMS, P. G., FAZIO, V. A. & INGE, K. E. 2006. Health benefits of herbs and spices: the past, the present, the future. *Med J Aust,* 185**,** S4-24.

THOR, A. D., MOORE, D. H., II, EDGERTON, S. M., KAWASAKI, E. S., REIHSAUS, E., LYNCH, H. T., MARCUS, J. N., SCHWARTZ, L., CHEN, L. C., MAYALL, B. H. & *ET AL*. 1992. Accumulation of p53 tumor suppressor gene protein: an independent marker of prognosis in breast cancers. *J Natl Cancer Inst,* 84**,** 845-55.

URCAN, E., HAERTEL, U., STYLLOU, M., HICKEL, R., SCHERTHAN, H. & REICHL, F. X. 2010. Real-time xCELLigence impedance analysis of the cytotoxicity of dental composite components on human gingival fibroblasts. *Dent Mater,* 26**,** 51-8.

VAN DELFT, M. F., WEI, A. H., MASON, K. D., VANDENBERG, C. J., CHEN, L., CZABOTAR, P. E., WILLIS, S. N., SCOTT, C. L., DAY, C. L., CORY, S., ADAMS, J. M., ROBERTS, A. W. & HUANG, D. C. 2006. The BH3 mimetic ABT-737 targets selective Bcl-2 proteins and efficiently induces apoptosis via Bak/Bax if Mcl-1 is neutralized. *Cancer Cell,* 10**,** 389-99.

VASILEV, N., ELFAHMI, BOS, R., KAYSER, O., MOMEKOV, G., KONSTANTINOV, S. & IONKOVA, I. 2006. Production of justicidin B, a cytotoxic arylnaphthalene lignan from genetically transformed root cultures of Linum leonii. *J Nat Prod,* 69**,** 1014-7.

VIEIRA, C., EVANGELISTA, S., CIRILLO, R., LIPPI, A., MAGGI, C. A. & MANZINI, S. 2000. Effect of ricinoleic acid in acute and subchronic experimental models of inflammation. *Mediators Inflamm,* 9**,** 223-8.

VIPUL, K., NITIN, M. & GUPTA, R. C. 2005. A sensitive and selective LC-MS-MS method for simultaneous determination of picroside-I and kutkoside (active principles of herbal preparation picroliv) using solid phase extraction in rabbit plasma: application

to pharmacokinetic study. *J Chromatogr B Analyt Technol Biomed Life Sci,* 820**,** 221-7.

WADE, M., LI, Y. C. & WAHL, G. M. 2013. MDM2, MDMX and p53 in oncogenesis and cancer therapy. *Nat Rev Cancer,* 13**,** 83-96.

WALL, M. E. & WANI, M. C. 1995. Camptothecin and taxol: discovery to clinic--thirteenth Bruce F. Cain Memorial Award Lecture. *Cancer Res,* 55**,** 753-60.

WANG, T., CHEN, F., CHEN, Z., WU, Y. F., XU, X. L., ZHENG, S. & HU, X. 2004. Honokiol induces apoptosis through p53-independent pathway in human colorectal cell line RKO. *World J Gastroenterol,* 10**,** 2205-8.

WANG, X., XIA, Y., LIU, L., LIU, M., GU, N., GUANG, H. & ZHANG, F. 2010. Comparison of MTT assay, flow cytometry, and RT-PCR in the evaluation of cytotoxicity of five prosthodontic materials. *J Biomed Mater Res B Appl Biomater,* 95**,** 357-64.

WEILL, D., MACK, M., ROTH, J., SWISHER, S., PROKSCH, S., MERRITT, J. & NEMUNAITIS, J. 2000. Adenoviral-mediated p53 gene transfer to non-small cell lung cancer through endobronchial injection. *Chest,* 118**,** 966-70.

WINKLER, V., OTT, J. J., COWAN, M. & BECHER, H. 2013. Smoking prevalence and its impacts on lung cancer mortality in Sub-Saharan Africa: An epidemiological study. *Prev Med*.

WISNIEWSKI, R. 1992. Principles of the design and operational considerations of large scale high performance liquid chromatography (HPLC) systems for proteins and peptides purification. *Bioseparation,* 3**,** 77-143.

WOGAN, G. N., HECHT, S. S., FELTON, J. S., CONNEY, A. H. & LOEB, L. A. 2004. Environmental and chemical carcinogenesis. *Semin Cancer Biol,* 14**,** 473-86.

WONG, R. S. 2011. Apoptosis in cancer: from pathogenesis to treatment. *J Exp Clin Cancer Res,* 30**,** 87.

YAGER, J. D. 2000. Endogenous estrogens as carcinogens through metabolic activation. *J Natl Cancer Inst Monogr***,** 67-73.

ZHANG, J., CHEN, Y. H. & LU, Q. 2010. Pro-oncogenic and anti-oncogenic pathways: opportunities and challenges of cancer therapy. *Future Oncol,* 6**,** 587-603.

ZHANG, J. H. & XU, M. 2000. DNA fragmentation in apoptosis. *Cell Res,* 10**,** 205-11.

ZHU, Z. J., SCHULTZ, A. W., WANG, J., JOHNSON, C. H., YANNONE, S. M., PATTI, G. J. & SIUZDAK, G. 2013. Liquid chromatography quadrupole time-of-flight mass spectrometry characterization of metabolites guided by the METLIN database. *Nat Protoc,* 8**,** 451-60.

http://www.plantzafrica.com/medmonographs/lobostemfrut.pdf

http://www.who.int/whosis/whostat/2009/en/

http://www.massbank.jp/?lang=en

Appendix

A. Methanol extract

#		Mass Error Retention Time Isotope Library	Name	Mass (Da)	Extraction Mass (Da)	Width (Da)	Found At Mass (Da)	Error (ppm)	Expected RT (min)	RT Width (min)	Found At RT (min)	Intensity	Library Hit	Purity Score
407	☑		2-hydroxylam	375.09139	376.09867	0.02	376.09908	1.1	0	2	10.27	21967		
669	☑		4-hydroxycou	375.09139	376.09867	0.02	376.09908	1.1	0	2	10.27	21967		
2589	☑		sarpagine	208.07356	209.08084	0.02	209.08017	-3.2	0	2	10.27	1757		
855	☑		7-O-methylvit	220.18272	221.18999	0.02	221.18886	-5.1	0	2	10.31	1320		
856	☑		7-O-ß-D-gluc	220.18272	221.18999	0.02	221.18509	-22.1	0	2	2.11	2510		
1793	☑		hypoglycin B	156.06875	157.07602	0.02	157.08237	40.4	0	2	2.95	1077		
2537	☑		ricinoleate	308.12284	309.13011	0.02	309.13356	11.1	0	2	10.97	4675		
2664	☑		sucrose-6-ph	153.89289	154.90016	0.02	0	0	0	2	2.11	5342		
2578	☑		S-tetrahydroc	192.99819	194.00547	0.02	0	0	0	2	0.09	4403		
1664	☑		germacrene (	306.07598	307.08326	0.02	0	0	0	2	7.35	3051		
1503	☑		dTDP-a-L-rha	274.26605	275.27333	0.02	0	0	0	2	12.96	2858		
2665	☑		sulfanilamide	410.13655	411.14383	0.02	0	0	0	2	11.89	2622		
668	☑		4-hydroxybut	213.03857	214.04585	0.02	0	0	0	2	10.01	2552		
406	☑		2-hydroxyisof	213.03857	214.04585	0.02	0	0	0	2	10.01	2552		
846	☑		7-methylthioh	166.04908	167.05635	0.02	0	0	0	2	8.59	2390		
1169	☑		cibacron blue	204.1878	205.19508	0.02	0	0	0	2	13.45	2259		
1109	☑		campest-4-er	584.42295	585.43022	0.02	0	0	0	2	15.29	1551		
765	☑		5-pentadecat	384.9127	385.91997	0.02	0	0	0	2	8.18	1478		
835	☑		7-hydroxy-2-(	300.06339	301.07066	0.02	0	0	0	2	8.65	1459		
483	☑		3'-adenosine	251.10184	252.10912	0.02	0	0	0	2	2.69	1424		
676	☑		4-methoxy-3-	177.10279	178.11006	0.02	0	0	0	2	14.2	1338		
971	☑		all-trans-hexa	410.1213	411.12857	0.02	0	0	0	2	6.34	1335		
1684	☑		glutaryl-CoA	546.22537	547.23264	0.02	0	0	0	2	7.88	1296		
666	☑		4-hydroxyber	103.03952	104.0468	0.02	0	0	0	2	11.72	1275		
1198	☑		CO	142.12319	143.13047	0.02	0	0	0	2	15.4	1229		
2224	☑		NO3-	426.38617	427.39344	0.02	0	0	0	2	13.95	1150		
1425	☑		difluororomet	327.12056	328.12784	0.02	0	0	0	2	3.08	1060		
1949	☑		L-glutamate-5	105.04259	106.04987	0.02	0	0	0	2	8.25	1012		
2447	☑		pratensein	165.11536	166.12264	0.02	0	0	0	2	14.57	1008		

B. Butanol extract

#		Mass Error Retention Time Isotope Library	Name	Mass (Da)	Extraction Mass (Da)	Width (Da)	Found At Mass (Da)	Error (ppm)	Expected RT (min)	RT Width (min)	Found At RT (min)	Intensity	Library Hit	Purity Score
1	☑		365.1048 / 2.7	365.10479	365.10479	0.026994346	365.1048	0	2.12	0.274133157	2.11	47061		
2	☑		142.1223 / 2.7	142.12234	142.12234	0.006736815	142.12237	0.2	2.14	0.223166656	2.14	13792		
3	☑		118.0862 / 2.7	118.08622	118.08622	0.009211165	118.08622	0	2.16	0.260233354	2.16	21843		
4	☑		300.1799 / 2.8	300.17994	300.17994	0.009790680	300.18001	0.2	2.81	0.213900041	2.81	26178		
5	☑		631.3403 / 2.8	631.34033	631.34033	0.021298309	631.34034	0	2.82	0.204633188	2.83	145965		
6	☑		316.1747 / 2.8	316.17475	316.17475	0.045216674	316.17482	0.2	2.83	0.376066875	2.84	406767		
7	☑		316.1751 / 2.9	316.17513	316.17513	0.010048146	316.17512	0	2.99	0.204633426	3.03	67247		
8	☑		157.0830 / 3.7	157.08298	157.08298	0.015935676	157.08292	-0.4	3.76	0.283416700	3.75	14115		
9	☑		438.2374 / 6.9	438.23744	438.23744	0.056191154	438.23742	-0.1	6.98	0.408517074	6.97	61499		
10	☑		438.2374 / 7.0	438.2374	438.2374	0.005914890	438.23731	-0.2	7.09	0.204633426	7.01	35175		
11	☑		407.1564 / 8.3	407.15635	407.15635	0.028506322	407.15628	-0.2	8.37	0.288032722	8.38	29184		
12	☑		387.1791 / 13	387.17914	387.17914	0.008339494	387.17913	0	13.98	0.204633903	14.01	27867		
13	☑		409.1612 / 13	409.1612	409.1612	0.054295478	409.16128	0.2	13.98	0.413132858	14.02	122473		
	☐													